Modeling the effectiveness of control measures from the within-host dynamics to the population dynamics of sleeping sickness

Mulalo Makhuvha

Student number: 220082266

A thesis submitted in fulfilment of the requirements for the degree of

DOCTOR OF PHILOSOPHY

in

APPLIED MATHEMATICS

School of Mathematics, Statistics & Computer Science University of KwaZulu-Natal, Durban, South Africa.

Thesis Supervisor: Dr Hermane Mambili-Mamboundou

August 2024

Declaration of Authorship - Plagiarism

I, **Mulalo Makhuvha**, declare that the thesis titled “Modeling the effectiveness of control measures from the within-host dynamics to the population dynamics of sleeping sickness" is my own work.

I declare that:

1. The research reported in this thesis is my original research, except where otherwise indicated.
2. This thesis has not been submitted for any degree or examination at any other university.
3. This thesis does not contain other persons’ data, pictures, graphs or other information, unless specifically acknowledged as being sourced from other persons.
4. This thesis does not contain other persons’ writing, unless specifically acknowledged as being sourced from other researchers. Where other written sources have been quoted, then:
    a. their words have been re-written but the general information attributed to them have been referenced, and
    b. where their exact words have been used, then their writing has been placed in italics and inside quotation marks, and referenced.
5. This thesis does not contain text, graphics or tables copied and pasted from the Internet, unless specifically acknowledged, and the source being detailed in the thesis and in the References section/s.

Signature: .....

Mulalo Makhuvha

Date: **19 August 2024**

Declaration- Supervisor

This thesis has been prepared according to Format 2 as outlined in the Information for the guidance of examiners of Higher degrees, which states:
Format 2: As a set of papers which are published, in press, submitted, or intended for submission.

This is to confirm that this research discussed in this thesis was done under my supervision, and it is the candidate's original work. The research was carried out in the College of Agriculture, Engineering and Science of the University of KwaZulu-Natal, from January 2020 until December 2023 by Mulalo Makhuvha. As the candidate's supervisor, I have approved this thesis for submission.

[redacted] 19/08/2024

Signature (Student) Date

..... [redacted] 19/08/2024

or) Date

School of Mathematics, Statistics & Computer Science
University of KwaZulu-Natal, Durban, South Africa.

Dedication

This work is dedicated to my two beautiful kids, Phathutshedzo Denzhe Nemavhola and Mpho Makhuvha. The strength, quality, and fulfillment you have given me have exceeded my expectations. Until the end of time, I will always love you.

Acknowledgements

The first thing I want to say is how grateful I am for the love, support, encouragement, and prayers that my parents (Ragimana T.D and Ragimana N) have given me throughout this journey to achieve my goal of becoming a Ph.D. holder. A special thanks goes out to my siblings, Makhuvha Khetho, Ragimana Ronewa, Monyai Tshamano, and Ragimana Gundo, who have supported my thesis and taken care of my children while I was focused on it. My sincere appreciation goes to my future husband for being patient with me when I decided to take a sabbatical leave from work so that I could focus on the completion of this dissertation.

I owe my supervisor a great deal of gratitude for his steadfast support, care, mentorship, and patience, Dr. Hermane Mambili-Mamboundou, in making every effort to ensure the completion of the doctoral program. I want to extend my most tremendous appreciation to my supervisor's family; they were my extended family outside home. I will miss the African food not forgetting the great times we shared.

The support of the DSI-NRF Centre of Excellence in Mathematical and Statistical Sciences (CoE-MaSS) towards this research is hereby acknowledged. I am grateful to the College of Engineering, Agriculture and Science, University of KwaZulu-Natal, for granting me fee remission throughout my studies and a conducive working environment at Galileo for this research". I also wish to thank Christel Barnard, the administrative assistant in the Department of Computer Science, Asandile Tshijila, and Jothimala Manickum, the CAES: Higher degree academic administrative officer. I cannot forget everyone at Galileo: Nzama, Nkosi, Zuma, and Mohammed; you made the sleepless nights fun and motivating.

Finally, my profound gratitude also goes to Nelson Mandela University, my current employer, for granting me a six-month sabbatical leave to focus on my submission. I want to thank the University Capacity Development Programme(UCDP) for funding my teacher replacement at my workplace. I was able to complete this research because UCDP sponsored my teacher replacement.

Declaration-Publications

DETAILS OF CONTRIBUTION TO PUBLICATIONS that form part and/or include research presented in this thesis (include publications in preparation, submitted, in press and published and give details of the contributions of each author to the experimental work and writing of each publication).

Details of publications:
The student whose thesis is under examination assumes the primary authorship role in all publications derived from said thesis. In my case, I was responsible for conducting all experimental work and played a significant role in the composition of the publications alongside my supervisor. When other authors were involved in specific experimental/practical aspects, my involvement primarily revolved around interpreting the data or consulting with them to ensure a comprehensive understanding. Additionally, co-authors contributed editorial oversight, providing the scientific integrity within their respective fields and verifying the accuracy of my data interpretation within those domains. Their expertise occasionally led to the inclusion of minor segments within the manuscripts, reflecting their specialized knowledge.

Signature 

Mulalo Makhuvha

Date: **19 August 2024**

List of Publications

The following journal articles emerge from this work have either published or under review:

1. Makhuvha, M., and Mambili-Mamboundou, H. (2023). Studying the Effect of Parasite Switching in Optimal Control Analysis of Sleeping Sickness. *Letters in Biomathematics*, 10(1), 207-233. (Published)

2. Makhuvha, M., and Mambili-mamboundou, H. (2024). Human African Trypanosomiasis multiscale model. *Journal of Mathematical Biology*. (under review)

Proceedings:

1. Makhuvha, M. (2021). Mathematicians are wide awake in the fight against sleeping sickness, Heart of Research. Published on the DST-NRF Centre of Exellence booklet.

2. Makhuvha, M. (2022). Studying the effect of parasite switching in optimal control analysis of sleeping sickness. [Presentation]. University of Kwazulu-Natal at the Postgraduate Research and Innovative Symposium. (Third prize and most impactful research prize).

3. Makhuvha, M., and Mambili-mamboundou, H. (2023). Studying the Control Analysis Of Sleeping Sickness Under the Implementation of Specific Treatment, and Vector Trapping. In 9^{th} International conference on Infectious Disease Dynamics P (Vol. 3). (Poster presentation)

Abstract

This study addresses the persistent health challenge of sleeping sickness in sub-Saharan Africa by comprehensively exploring its transmission dynamics. The primary focus is on developing, studying, and analyzing mathematical models spanning from within-host dynamics to multiscale interactions of sleeping sickness. The thesis begins by investigating the dynamics within a single sleeping sickness-infected human host. The model considers the interplay between parasite types, macrophages, and cytokines within the human host. Findings suggest that the immune response play a pivotal part in regulating parasite growth, and the absence of switching enables effective immune system intervention. Two distinct optimal control problems emerge, emphasizing the need to identify the disease stage for effective drug application, thereby preventing parasite persistence and reducing drug toxicity. The study's second phase focuses on developing an epidemiological model of sleeping sickness transmission among humans, non-human hosts, and tsetse flies. Sensitivity analysis reveals that parameters such as biting rate and death rate are particularly influential. The examination of bifurcation concerning the effective reproductive number (R_e) indicates the presence of a backward bifurcation within the system which signifies that the traditional condition of $R_e < 1$ is no longer adequate for achieving effective disease elimination. Disease dynamics are strongly scale dependent, so we propose a multi-temporal scale model that incorporates within-host and between-host disease dynamics. Results are compared with the single-scaled models. Furthermore, the numerical solutions for susceptible humans in both the between-host and multiscale models demonstrated a similar pattern: a rapid reduction in susceptible human populations within the first 50 days in the absence of intervention. The vector profiles in both the multiscale and between-host models showed similar trends, with intervention initially applied at maximum intensity and rapidly reduced within the first 50 days of use. However, a notable distinction arose regarding treatment profiles: whereas within-host results indicated that drugs needed to be administered at maximum dosage to reduce the burden of infection effectively, the opposite was observed in the between-host model. In conclusion, this thesis offers valuable insights into the disease transmission

dynamics of sleeping sickness, highlighting the significance of comprehending both within-host and between-host interactions. Essentially, our models proved to be more mathematically, numerically, and biologically tractable compared to most standard models used for projecting sleeping sickness.

Table of contents

Declaration of Authorship - Plagiarism i

Declaration- Supervisor ii

Dedication iii

Acknowledgements iv

Declaration - Publications v

List of Publications vi

Abstract vii

1 Introduction 1

1.1 Background on sleeping sickness 1

1.2 Within-host dynamics 3

1.2.1 Trypanosome parasite 4

1.2.2 Immune responses 5

1.3 Cytokines 5

1.4 Between-host dynamics 6

1.5 Available interventions 7

1.6 Review of mathematical models 8

1.6.1 Background 8

1.6.2 Review of mathematical models for sleeping sickness 9
1.6.3 The role of optimal control in epidemiology 10
1.7 Problem statement 12
1.8 Aim and objectives 13
1.9 Methodology 14
1.9.1 The existence and uniqueness theorem 14
1.9.2 Positivity and boundedness of solutions 15
1.9.3 Equilibrium points 15
1.9.4 Reproductive number (R_0) 15
1.9.5 Stability analysis 17
1.10 Sensitivity analysis 20
1.11 Optimal control 20
1.12 Significance of the study 21
1.13 Outline of the thesis 22

2 Studying the effect of parasite switching in optimal control analysis of sleeping sickness 24

3 Control analysis of sleeping sickness under the implementation of specific treatment and vector trapping 52

4 Multiscle modeling of Sleeping sickness 83

5 Discussion and conclusion 115

References 119

Chapter 1

Introduction

1.1 Background on sleeping sickness

Sleeping sickness, also known as Human African Trypanosomiasis (HAT), is a vector-borne neglected tropical disease. Several neglected tropical diseases are listed in the second World Health Organization report [1]. These diseases include Dengue, Chagas disease, Rabies, Trachoma, and HAT. Sleeping sickness is a parasitic disease predominantly found in sub-Saharan Africa. HAT remains a significant public health concern in this region, caused by the protozoan parasites *Trypanosoma brucei gambiense* and *Trypanosoma brucei rhodesiense*, transmitted through tsetse fly bites [2]. The disease manifests with various symptoms and presents two distinct forms based on the parasite species involved.

Symptoms of sleeping sickness vary depending on the species of the parasite and the form of the disease. There is a variable period between the bite of an infective tsetse fly and the onset of symptoms, ranging from a few days to several weeks. *T.b. gambiense* causes the chronic form, which progresses more slowly and accounts for the majority of cases. This form can persist for months or even years, often leading to neurological complications. In contrast, the acute form, caused by *T.b. rhodesiense*, progresses rapidly and can lead to severe neurological symptoms within weeks.

The disease is clinically classified into two distinct stages: Hemolymphatic stage and Meningoencephalitic stage [2]. During the initial stage, parasites are present in the bloodstream and

lymphatic system, leading to symptoms such as fever, headaches, joint pains, and swelling of the lymph nodes. If untreated, the disease progresses to chronic or acute sleeping sickness, exhibiting increased severity and specific symptoms that make detection challenging. In the second stage, the parasites invade the central nervous system by crossing the blood-brain barrier, leading to symptoms such as sleep disturbances, mood changes, difficulties in motor coordination, and severe neurological and psychiatric manifestations. Additionally, early symptoms may be nonspecific and could be attributed to other illnesses, making the diagnosis challenging during the initial stages.

A favorable outcome depends on early detection and prompt treatment, as the disease becomes more challenging to manage once it reaches the neurological stage. Regular surveillance and improvements in healthcare infrastructure are essential in affected regions to enhance early diagnosis and intervention. However, historically, detection relied solely on analyzing the symptoms presented by patients due to limited knowledge about the disease. One of the earliest documented records on human trypanosomiasis comes from the renowned Arabian geographer Abu Abdallah Yaqut, who lived between 1179-1229 [3]. Most of these reports originated from the Arab world, with case discoveries made based on symptoms dating back centuries, particularly in West African regions such as Mali, Benin, Songhai, and Ghana. Back in 1852, the Scottish missionary David Livingston reported that the bite of tsetse flies causes nagana (animal trypanosomiasis). It took another 40-50 years before the trypanosome was identified as the culprit behind sleeping sickness and nagana. In 1895, the Scottish pathologist and microbiologist David Bruce discovered that the trypanosome parasite *T. Brucei* causes cattle trypanosomiasis.

In the 20th century, Africa experienced three severe epidemics: one between 1896 and 1906, the next in the 1920s, and the last between 1970 and the late 1990s. The first epidemic occurred mostly in Uganda and the Congo Basin, and the latter epidemic occurred in several countries. The Democratic Republic of Congo (DRC) reported 61% of the cases, which is 522 cases per year. According to WHO, Angola, the Central African Republic, Chad, Congo, Gabon, Guinea, Malawi, and South Sudan declared 10–100 cases, while Cameroon, Côte d'Ivoire, Equatorial Guinea, Uganda, Tanzania, Ethiopia, and Zambia declared 1–10 cases per year [2]. Historically, sleeping sickness faced periods of neglect, particularly in the early century due to various factors, including limited awareness of the disease, its prevalence in remote and economically disadvantaged regions, and the challenging nature of conducting research in these areas. According to WHO, in the 2000s that is when sleeping sickness was coined as a Neglected Tropical Disease (NTD) to draw attention to a group of diseases that historically received inadequate attention and research funding despite their impact on

affected communities. The NTD list consists of diseases that historically receive low levels of attention, research, and funding compared to other prominent global health issues.

Tsetse flies are commonly found in dense forests, water sources, and places with moderate temperatures. The transmission of this disease is heavily influenced by ecological factors, such as tsetse fly distribution and density, however human activities that expose individuals to these vectors play an important role in contact that is exposing themselves to tsetse flies when they are working in agricultural fields, fishing, herding livestock, and hunting. Cases have been reported in non-endemic areas due to travelers and immigrants from endemic regions. A comprehensive understanding of the dynamics, significance, and implications of modeling the effectiveness of control measures requires an exploration of the impact of this disease on different host populations.

1.2 Within-host dynamics

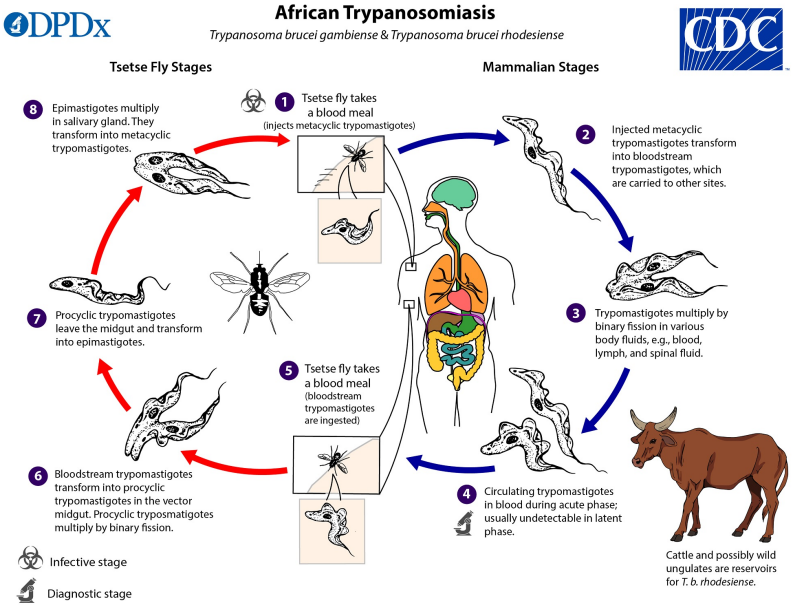

Fig. 1.1 The life cycle for sleeping sickness [4]

Figure 1.1 delineates the life cycle of sleeping sickness, drawing on information from the Centers for Disease Control and Prevention [4]. The intricacies of this cycle commence with the tsetse fly's ingestion of bloodstream trypanosomes by biting an infected human or other mammals.

Within the tsetse fly midgut, the parasites traverse developmental stages, transitioning from the bloodstream to procyclic and epimastigote forms, pivotal for their maturation. Following these developmental stages, an infected tsetse fly, in turn, bites an uninfected human or another mammal. During the subsequent blood meal, the parasites from the tsetse fly are deposited into the human bloodstream [4].

Upon injection into the human skin, the trypanosome undergoes rapid proliferation at the bite site, inducing inflammation that culminates in the development of a chancre on the skin. Subsequently, waves of parasites invade the bloodstream, differentiating into slender forms. The transmission to other organs occurs through the bloodstream.

Recognition of the parasite by the human immune system triggers a response against the foreign invader. This response involves the production of various antibodies aimed at combating the parasites. In the initial stage, minor symptoms manifest, encompassing common signs such as headache, fever, and other mild manifestations[5].

The second stage of sleeping sickness is initiated when the parasite traverses the brain-blood barrier, entering the central nervous system. At this juncture, neurological disorders begin to manifest in the affected individual. If left untreated, the disease progresses inexorably towards a fatal outcome[10].

1.2.1 Trypanosome parasite

A critical factor in understanding sleeping sickness dynamics is that the trypanosome parasite targets brain organs, inducing inflammation in hypothalamic structures that can lead to sleep-regulatory system dysfunction. The intricate life cycle of trypanosomes plays a pivotal role in describing disease dynamics, involving a series of transformations within the tsetse fly, ultimately preparing the parasite to infect the human host upon a tsetse bite. Remarkably, extracellular trypanosome parasites can manipulate the host's humoral immune system [5],[6],[7]. As illustrated in Figure 1.1, a crucial phase involves the invasion of the human host by the metacyclic form, developing into the blood form. Each parasite is covered in a Variant Surface Glycoprotein (VSG) coat, a glycoprotein coat exhibiting continuous variation, enabling them to escape immune surveillance. As a result of the VSG, the parasite alters its coat in response to the immune response. This survival mechanism results in the emergence of a diverse array of new parasites within the host.

Concurrently, as the parasite engages in this survival mechanism, the human host activates innate and adaptive immune responses to eliminate the parasite. This defensive process involves cytokine stimulation and chemokine secretion. Furthermore, the parasite undergoes

binary fusion during its life cycle, adding another layer of complexity. Despite considerable efforts to control African trypanosomiasis, these efforts have been hindered by the parasite's constant modification of its VSG [8]. The intricate interplay between the parasite's survival strategies and the host's immune responses highlights the inherent challenges in devising effective methods for controlling African trypanosomiasis.

1.2.2 Immune responses

The impact of sleeping sickness on host health is also influenced by the interplay between the immune system and sleep, as sleep loss impairs immune function, and sleep is altered during infection [9]. The immune system serves as an intricate network comprising various cell types and proteins with the primary goal of recognizing and responding to foreign materials or germs. This crucial defense mechanism is distributed throughout the human host to guard against infections and is divided into innate and adaptive immune responses. The innate response acts as the initial line of defense, while the adaptive response functions as the secondary line.

In countering the trypanosome parasite, macrophages assume a pivotal role, adapting their functions based on the host's needs, either engulfing foreign substances or secreting cytokines [10]. A macrophage can be classified into naive, classical, and alternative activated macrophages, with the latter two forming part of the responsive immune response activated in response to the parasite's presence in the host [11]. Effective communication within the immune system necessitates cytokines, which are chemical messengers, proteins that bind to receptors and promote cell activation.

Several mathematical models have been developed to study the dynamics of Human African Trypanosomiasis (HAT) disease, incorporating immune responses [5], [48], [49], [50]. In this study, our focus goes beyond incorporating the immune system; we emphasize the significance of cytokines [15] in the progression of the disease within an infected human host.

1.3 Cytokines

Cytokines are communication mediators that play a pivotal role in modulating immune responses by binding to specific receptors. The cytokines are proteins produced by various immune cells such as macrophages, dendritic cells, lymphocytes, monocytes, and neutrophils,

serve as key regulators of inflammation. Inflammation occurs as results of exposure of tissues and organs to harmful stimuli [16].

Two distinct categories of cytokines exist: pro-inflammatory cytokines and anti-inflammatory cytokines. Pro-inflammatory cytokines, including IL-1, IL-6, and TNF, are generated by activated macrophages, contributing to the up-regulation of inflammatory reactions and the promotion of inflammation. These cytokines, such as IL-1, IL-6, and TNF, are integral components stimulating early innate responses. On the other hand, anti-inflammatory cytokines represent a series of immuno-regulatory molecules that exert control over pro-inflammatory cytokine responses. Examples of anti-inflammatory cytokines encompass IL-1 receptor antagonist, IL-4, IL-10, and IL-13.

Certain cells release cytokines, while others possess cytokine receptors. When a cytokine, acting as the key, binds to its corresponding receptor, resembling a lock, the receiving cell receives a message, instructing it on how to respond. This cellular response can vary; for instance, an immune cell detecting a harmful substance in the body, or may release cytokines in response. These cytokines can traverse the bloodstream or directly enter tissues, reaching cells with matching receptors. Once bound, the cytokine imparts instructions to the recipient cell, prompting specific actions.

1.4 Between-host dynamics

The vector-borne nature of sleeping sickness underlines the reliance of the infection on the presence of a vector for the transmission of the causative pathogen. Sleeping sickness is often transmitted by the tsetse fly, a blood-sucking insect. This vector becomes a crucial intermediary in the life cycle of the infectious pathogen. Transmission begins when the blood-sucking insect feeds on an infected host, whether human or animal, during a blood meal. At this stage, the vector ingests the microorganisms responsible for causing the disease [2]. These microorganisms may include trypanosomes, the parasites responsible for sleeping sickness. Following the ingestion of the infectious agent, a critical phase evolves within the vector. The pathogen undergoes replication and development within the vector's body. Pathogens replicate to prepare for transmission to new hosts, essential for their life cycle [5].

After the vector takes another blood meal, the infectious pathogen is transmitted to a new host. The vector introduces replicated and now infectious microorganisms into the new host's bloodstream during this feeding process [54]. This transmission event establishes a new infection, continuing the disease cycle. It is important to note that the specific mechanisms of

transmission and the types of pathogens involved may vary based on vector and geographical factors. The vector-borne nature of sleeping sickness accentuates the significance of studying both within-host and between-host dynamics to comprehensively address the complexities of disease transmission.

1.5 Available interventions

The absence of a vaccine against African Trypanosomiasis persists, likely attributed to the adaptive nature of the parasite, which exhibits a capacity to switch between various strains. Interventions for sleeping sickness are multifaceted and encompass prevention, disease surveillance, treatment, and control strategies [17],[18].

Preventive measures for human populations primarily hinge on minimizing exposure to tsetse fly bites. This objective can be achieved through various means, including avoiding regions known to be infested by tsetse flies, such as areas with dense bushes. Furthermore, individuals can mitigate risk by adopting practices such as wearing long-sleeved and knee-length clothing, inspecting vehicles for the presence of tsetse flies before entry, and employing insect repellents.

Disease surveillance entails the process of screening, diagnosis, and staging. There are two types of screening; active screening and passive screening [19], [20], [21], [22], [23], [24]. Active screening takes place as in mobile teams regularly travel to remote villages to test the population, important for early case detection mostly conducted in at-risk villages. Unlike active screening, passive screening entails testing at a fixed health sites. Passive screening is mostly insufficient due to the fact that health facilities are remotely located, resource-poor, and insecure settings. The advantage to active screening is that it reduces mortality and reduces disease transmission. Diagnosis is the process of confirming the infection through confirmatory test conducted using card arggluti onation test (CATT) conducted on serum, capillary blood obtained from a prick [18], [25]. Ounce the case has been confirmed positive for HAT, a lumbar puncture is done to determine the stage of the disease. The differentiation of the stages are classified by examining the cerebrospinal fluid (CSF), more than 5 white blood cells per μL or increased protein content ($> 370 mg/L$) defines the second-stage of the disease, otherwise it is the first stage [17].

The treatment is in the form of drugs and is based on the stage of each individual case identified. The first effective drug for treating sleeping sickness was discovered in 1916 after a number of attempts by Wilhelm Roehl with the help of a team of chemists. Drugs

effective during the initial stage are *Suramin* and *Pentamidine* which are inefficient in the second stage of the disease since they are unable to cross the blood-brain barrier [26], [27], [28], [29]. Drugs effective against the second stage are *Melarsopol* and *Elflornithine*. The difference between them is that *Melarsopol* is less expensive but more toxic as compared to *Elflornithine*.

1.6 Review of mathematical models

1.6.1 Background

The modeling of infectious diseases serves as a crucial tool for comprehending the mechanisms governing disease spread, predicting future outcomes, and assessing strategies for disease control. Deterministic models, renowned for their versatility, predictive capabilities, ease of setup, assumption of exact relationships between variables, and repeatability of results for the same input values, have been pivotal in the field of infectious disease epidemiology. This approach eliminates randomness, allowing for precise prediction of future events.

The inception of mathematical modeling in the study of disease spread can be traced back to 1760 when Daniel Bernoulli explored inoculation against smallpox during its endemic phase [31]. Bernoulli's mathematical model argued that smallpox inoculation would increase life expectancy with a marginal risk of infection and death. His work not only garnered favorable reception but has also permeated actuarial literature.

In 1855, John Snow made a significant contribution by studying the temporal and spatial patterns of cholera cases. His investigation successfully identified the Broad Street water pump as the source of infection. Subsequent to Snow's work, researchers such as William Hamer and Ronald Ross applied the law of mass action to elucidate epidemic behavior. The advent of compartmental models in 1927 by Kermack-Mckendrick furthered the understanding of disease transmission dynamics, providing a framework to predict outbreak behaviors similar to those observed in many epidemics [32].

A pivotal shift occurred in 1991 when Anderson's research marked the integration of control measures into mathematical models of infectious disease transmission, guiding public health policy [33], [34], [35], [36], [37]. However, deterministic models have limitations in capturing stochastic effects prevalent in real-world scenarios, prompting the exploration of more robust deterministic approximations of stochastic models to enhance prediction accuracy.

Traditionally, mathematical models have treated the epidemic process (disease transmission between hosts) and the immunological process (virus-cell interaction within a host) as separate entities, referred to as single-scale models [38]. Over time, modelers have recognized the need to couple these processes to better understand the integration of different infection scales. This coupling results in a multiscale model, which integrates both within-host and between-host scales of infectious disease systems. Five identified categories of multiscale models include individual-based multiscale models (IMSMs), nested multiscale models (NMSMs), embedded multiscale models (EMSMs), hybrid multiscale models (HMSMs), and coupled multiscale models (CMSMs) [30]. Each category exhibits unique characteristics and employs distinct integration frameworks

1.6.2 Review of mathematical models for sleeping sickness

Sleeping sickness, a prominent health threat in sub-Saharan Africa, has not been receiving substantial attention from mathematical and theoretical biologists hence it is part of the neglected tropical disease list. Mathematical modeling proves to be a highly effective tool for comprehending the dynamics of various vector-borne infectious diseases, including Malaria [39], [40], [41], [42].

Over the years, several mathematical model structures have been developed and employed as the foundation of knowledge for modeling sleeping sickness, as evidenced by works such as [43], [44], and [45]. In 1988, Rogers proposed a model with two hosts and one vector for sleeping sickness. This model relied on interactions among humans, cattle or domestic animals, and the tsetse fly. In Rogers' study, it was argued that domestic animals are essential in maintaining *T.b Gambiense*. Artzrouni and Gouteux [44] proposed a different approach, suggesting a model that only humans serve as reservoirs for the parasite and presented a compartmental model for the spread of Gambian sleeping sickness.

The studies reviewed in the discussion have laid the groundwork for the current investigation, providing essential concepts and findings that serve as foundational elements. Notably, an observation emerged regarding the existing within-host models of sleeping sickness, as evidenced by studies such as [48], [49], and [50]. These studies, while valuable, tended to overlook certain critical aspects, namely the explicit inclusion of various parasite types, the dynamics of different immune cells, and the effects of cytokines, all of which play pivotal roles in the progression of sleeping sickness infection.

It is noticeable that prior models often neglected the intricate interplay between parasite diversity, immune response dynamics, and the influence of cytokines, thus potentially lim-

iting the predictions regarding within-host disease dynamics. Although some models did incorporate antigenic variants to account for parasite switching, the inclusion of immune response dynamics and cytokine effects in this study offers a more comprehensive and realistic portrayal of the disease dynamics within the host. By integrating these elements, the current study aims to enhance the predictive capabilities of the model and provide deeper insights into the interplay between the immune system and the infectious agent in sleeping sickness. In subsequent years, models examining the dynamics of sleeping sickness introduced the evaluation of different interventions, as exemplified by models in [45], [46], [47]. Despite this progress, further work is needed to fully understand the infection dynamics of Human African Trypanosomiasis (HAT) across different scales. Notably, a limited number of studies have investigated within-host dynamics using mathematical models, as found in [5], [48], [49], [50]. Conversely, plenty of studies have focused on between-host dynamics, utilizing mathematical models to study sleeping sickness, as seen in [51], [52], [53], [54], [55], [56], [57].

Furthermore, the reviewed within-host studies predominantly focused on modeling sleeping sickness in the absence of therapeutic interventions, which presented an opportunity for the current investigation to explore the effects of therapeutic drugs on disease dynamics. This shift in focus towards assessing the impact of intervention strategies is crucial for informing public health initiatives and guiding the development of effective treatment protocols for sleeping sickness. In addition to within-host dynamics, this study also touched upon between-host dynamics, where varying approaches were observed regarding the inclusion of animal populations (wild or domesticated) in modeling the spread of sleeping sickness. This divergence in modeling strategies underscores the complexity of the disease epidemiology and highlights the importance of considering diverse host populations and transmission dynamics in understanding and controlling sleeping sickness. The third component of this study was proposed following the studies that was focused on multiscale model that investigated the multiscale approach in modeling infectious disease in [59], [60], [61], [62], [63], [64], [65], [66], [67], [68], [69] to name a few. To the best of our knowledge we have not seen a study that focuses on using the concepts of multiscale to explore the disease dynamics for sleeping sickness.

1.6.3 The role of optimal control in epidemiology

The late 1950s marked the initiation of a concerted effort by public health officials to address infectious diseases by targeting the organisms responsible [70]. A pivotal development in this pursuit is the application of optimal control theory, an extension of the calculus of

variations, which has found widespread use, notably in epidemiology for disease prevention and intervention. Optimal control theory furnishes a mathematical framework to optimize resource allocation and interventions, with the overarching objective of minimizing or maximizing a specified criterion [71], [72]. In the realm of infectious diseases, this theory proves indispensable for formulating strategies that effectively limit pathogen spread within the constraints of available resources.

In summary, optimal control strategies in epidemiology present a refined and systematic approach to tackling infectious diseases. By leveraging mathematical models and optimization techniques, these strategies offer insights into the most effective interventions to mitigate the impact of epidemics. Ongoing collaboration among mathematicians, epidemiologists, and policymakers is imperative for refining models and enhancing our ability to respond to infectious disease threats.

The attention on optimal control for infectious diseases has grown significantly in recent years. Numerous studies have explored optimal control theory in mathematical models for various infectious diseases, encompassing vector-borne diseases [79], cholera [73], [74], HIV [75], [76], malaria [78], and tuberculosis [77]. Although the control of Human African Trypanosomiasis (HAT) began in the 1960s, intensive efforts to describe it gained momentum in the 20th century.

Apollinaire et al. [80] formulated a control model to derive optimal prevention and treatment strategies with minimal costs. They proposed optimal strategies for preventing, treating, and controlling vectors for both humans and animals. Another study by Gervas and Hugo [81] presented a model analyzing cost-effectiveness to identify the best control strategy involving education, treatment, and insecticides. The results indicated that a combined strategy of education, treatment, and insecticides was more effective in eliminating both infectious humans and tsetse flies. However, the most cost-effective approach for eliminating HAT disease was found to be education and treatment. Liana et al. [82] implemented control efforts aiming to minimize the number of infected humans, cattle, and tsetse fly populations using education, human and cattle treatment, and tsetse fly trapping. Their findings revealed that a strategy involving education, human and cattle treatment, and vector trapping was most effective in reducing the number of infected individuals in respective populations. Cost-effectiveness analysis suggested that tsetse fly trapping was the most effective strategy in resource-limited settings.

In our study, we incorporated two interventions, namely treatment and vector trapping, drawing inspiration from previous works [80], [81], and [82]. These interventions were selected for their effectiveness and cost-efficiency. The spread of sleeping sickness is a

complex process, and mathematical models of transmission dynamics play a crucial role in simulating the prevalence of HAT and evaluating treatment strategies across different scales. Our model integrated a within-host component involving two different drugs for treatment, a between-host component with specific stage drugs and vector trapping, and a multiscale model extending the framework with treatment and vector trapping.

1.7 Problem statement

Sleeping sickness, caused by Trypanosoma brucei parasites transmitted through tsetse flies, remains a significant public health concern in sub-Saharan Africa. Current treatment strategies involve the administration of drugs, yet their efficacy is limited due to factors such as drug resistance and complex host-parasite interactions. To enhance treatment outcomes and address the dynamic nature of the disease, there is a critical need for a comprehensive and adaptive approach to therapeutic interventions. Existing mathematical models have primarily focused on single-scale representations of the disease dynamics, often oversimplifying the complex interactions within the host and the parasite population. A more realistic portrayal of the disease necessitates the incorporation of multiscale modelling, considering the intricate interplay between molecular, cellular, and organismal levels. By bridging the gap between microscopic and macroscopic dynamics, a multiscale modelling approach can provide a more nuanced understanding of the disease progression and treatment response. This thesis aims to develop a novel framework for the optimal control of treatments in sleeping sickness, integrating both single-scale and multiscale mathematical models. The objective is to identify optimal drug administration strategies that maximize treatment efficacy while minimizing adverse effects and the emergence of drug resistance. The research will involve the construction of detailed single-scale models capturing the essential biological processes at play within the host and the parasites. Subsequently, these models will be integrated into a multiscale framework, allowing for a more comprehensive exploration of the complex interactions influencing disease dynamics. The proposed research will not only contribute to advancing our fundamental understanding of sleeping sickness dynamics but will also have practical implications for the design of improved treatment protocols. The developed models will serve as a predictive tool for optimizing drug dosages, administration schedules, and combination therapies. Ultimately, this thesis seeks to provide a holistic and adaptive approach to the control of sleeping sickness, offering a valuable contribution to the global efforts aimed at eliminating this debilitating tropical disease.

1.8 Aim and objectives

The aim of the study is to develop a general multiscale model for sleeping sickness to illustrate disease dynamics from the within-host scale to the between-host scale. The complex interplay between between-host transmission and within-host interactions for sleeping sickness needs to be more adequately explained, due to the lack of a cohesive representation of their mutual influence on each other.

The study will focus on:

1. Comprehensive modeling- develop detailed mathematical models that capture single-scale disease dynamics. Within-host models will focus on molecular, cellular, and immune responses whereas the between-host model will focus on multi-host infection dynamics.
2. Multiscale integration- integrate the single-scale models into a multiscale framework to represent the complex interactions of HAT disease dynamics.
3. Optimal Control Strategies- identify optimal control strategies to control disease dynamics incorporating mathematical optimization techniques. To maximize treatment efficacy while minimizing adverse effects, the emergence of drug resistance, and overall treatment burden.
4. Quantitative assessment- quantitatively assess the impact of different treatment strategies on key disease metrics, including parasitemia levels, host immune responses, and overall treatment success, to provide insights into the most effective intervention approaches.

The objective of the study is:

- To develop a mathematical model that depicts the immune system's and cytokine's role in sleeping sickness dynamics within a single infected human individual.
- To apply optimal control theory to the within-host model to identify the treatment strategy that maximises therapeutic impact.
- To develop and analyze a mathematical model that illustrates HAT disease dynamics among humans, animals, and vectors.

- To investigate the benefits of incorporating treatment and vector control as intervention strategies in the between-host model.
- To develop a multiscale model by integrating the single-scale mathematical models ensuring interactions between scales.
- To investigate the effects of certain within-host parameters on between-host variables as well as the effects of certain between-host parameters on within-host variables.
- To analyse the effects of incorporating interventions on the multiscale model assessing optimal control conditions.

1.9 Methodology

This section presents the mathematical concepts, theories, theorems, lemmas, definitions, and all methodologies used in the model analysis of Chapters 2, 3, and 4. There will be a detailed discussion of the methods, including how they are derived and used.

1.9.1 The existence and uniqueness theorem

This Theorem is used to conclude that given a first order differential equations, we can show the solutions exist and are unique under certain conditions.

Theorem 1.9.1 *Let $\mathbb{R}^n_+ = [0,\infty)^n$ be the cone of non-negative vector in $\mathbb{R}^n_+$. Let H: $\mathbb{R}^{n+1}_+ \to \mathbb{R}^n_+$ be a Lipschitz function, $H(t,x) = (H_1(t,x), H_2(t,x), \ldots, H_n(t,x))$ satisfying $H_i(t,x) \geq 0$ whenever $t \geq 0$, $x \in \mathbb{R}^n_+$, $x_i = 0$. Then, for every $x^0 \in \mathbb{R}^n_+$, there exists a unique solution of $x^{'} = H(t,x)$, $x(0) = x^0$, with values in $\mathbb{R}^n_+$, which is defined on some time interval $[0,b); b > 0$ [83].*

The Lipschitz function $H(t,x) = H(t_+, x_+)$ where $t_+ = max\{t,0\}$, and $x_+ = (x_1, x_2, x_3, \ldots, x_n)$ are positive parts of the scalar t and vector x. We can check that $\|x_+ - y_+\| \leq \|x - y\|$ for any of the usual norms on $\mathbb{R}^n$. Hence H is a locally Lipschitz continuous vector field on $\mathbb{R}^n$ satisfies $H_i(t,x) \geq 0$ for all $t \in \mathbb{R}, x \in \mathbb{R}^n_+, x_i = 0$.

Proof can be found in [83].

1.9.2 Positivity and boundedness of solutions

When analyzing mathematical models, it is necessary to prove that all the solutions of any system of first-order differential equations remain non-negative given non-negative initial for all $t > 0$, and the solutions occupy a feasible region defined by Ω.

Consider a first order system of differential equations in the form

$$\frac{dx}{dt} = f(x), \quad \text{given,} \quad x(t_0) = x_0, \quad x(t_0) > 0 \tag{1.9.1}$$

where $x = (x_1, x_2, \ldots, x_n)$. Then the solution $x(t)$ for the system of equation are non-negative for all $t > 0$. The region Ω defined by $\Omega = \{x(t) \in \mathbb{R}^n_+\}$ is bounded, biologically meaningful.

1.9.3 Equilibrium points

An equilibrium point of the system (1.9.1) is the solution x^* such that $f(x^*) = 0$.

When a dynamical system reaches an equilibrium point, its state variables do not change over time. The equilibrium points determine how the dynamical system will behave. In epidemiology, we are interested in two kinds of equilibrium points:

- Disease Free Equilibrium (DFE) point,
- Endemic Equilibrium (EE) point .

Disease free equilibrium point
The DFE point refers to when there are no diseases in a population. At this point, the infective and infected classes are zero [84], [85].

Endemic equilibrium point The EE point is a state when the disease persists in the population [84], [85].

1.9.4 Reproductive number (R_0)

The basic reproductive number (R_0) is the most important parameter in epidemiology, it is defined in [85] as the average number of secondary infections emanating from a single infective person in a completely vulnerable population. The following two approaches are often to calculate R_0.

First approach: the next generation matrix
We first decompose the system (1.9.1) in the form

$$\frac{dx}{dt} = f(x) = \mathscr{F}(x) - \mathscr{V}(x), \quad x \in \mathbb{R}^n \tag{1.9.2}$$

where $\mathscr{F}(x) = \begin{bmatrix} \mathscr{F}_1(x) \\ \mathscr{F}_2(x) \\ \vdots \\ \mathscr{F}_n(x) \end{bmatrix}$ the transmission matrix, containing terms in (1.9.1) that produce new infections and $\mathscr{V}(x) = \begin{bmatrix} \mathscr{V}_1(x) \\ \mathscr{V}_2(x) \\ \vdots \\ \mathscr{V}_n(x) \end{bmatrix}$ is the transition matrix, describing transfers between compartments.
If we let $F = \left[\frac{\partial \mathscr{F}_i(x^*)}{\partial x_j}\right]_{1\leq i,j\leq n}$ and $V = \left[\frac{\partial \mathscr{V}_i(x^*)}{\partial x_j}\right]_{1\leq i,j\leq n}$ where x^* is the DFE solution of (1.9.1) the basic reproduction ratio is the dominant eigenvalue of FV^{-1} that is,

$$R_0 = \rho(FV^{-1}).$$

Second approach: the next generation operator
From [86], it is said that for any epidemiological model that can described in the form

$$\begin{cases} \dfrac{dX}{dt} = f(X,Y,Z), \\ \dfrac{dY}{dt} = g(X,Y,Z), \\ \dfrac{dZ}{dt} = h(X,Y,Z), \end{cases} \tag{1.9.3}$$

where $X \in \mathbb{R}^r, Y \in \mathbb{R}^s, Z \in \mathbb{R}^n, r,s,n \geq 0$, and $h(X,0,0) = 0$, the components are defined as follows

(i) X represents all individuals who are not infected, including susceptible, recovered, and other non-infected individuals,

(ii) Y represents all individuals who are infected who are not capable of infecting other individuals, including latent or non-infectious stage,

(iii) Z represents all individuals who are infected who are capable of infecting others, including infectious and non-quarantined individuals.

Let the DFE be denoted by $E_0 = (X^*, 0, 0) \in \mathbb{R}^{r+s+n}$, that is,

$$f(X^*, 0, 0) = g(X^*, 0, 0) = h(X, 0, 0) = 0.$$

Assume that the equation $g(X^*, Y, Z) = 0$ implicitly determines a function $Y = \tilde{g}(X^*, Z)$. Let the diagonal matrix A, be expressed as $A = D_Z h(X^*, \tilde{g}(X^*, 0), 0)$, assuming that A can be written in the form $A = M - D$, with $M \geq 0$ (that is, $m_{ij} \geq 0$) and $D > 0$. Similarly to the first approach the reproductive number is defined as the spectral radius, the largest eigenvalue of the matrix MD^{-1}, that is

$$R_0 = \rho(MD^{-1}).$$

One calculated the value of R_0 is interpreted as follows:

- If $R_0 > 1$, the disease is more likely to spread in the population.
- If $R_0 < 1$, the disease is likely to die out.

1.9.5 Stability analysis

The stability analysis of dynamical systems is crucial in analysing and predicting the long term behavior of a system. It provides valuable insight in behavior of the system even in the absense of analysis solutions [88].

Local stability of equilibrium

An equilibrium point x^* of the model system (1.9.1) is said to be locally stable [89] provided that the initial values x_0 are close to the equilibrium point and the solution $x(t)$ remains close to x^* for all $t > 0$. We will make use of the Jacobian matrix to determine the local stability of an equilibrium point.

The Jacobian matrix can be thought of as matrices of all first-order partial derivatives of vector-valued functions [90]. Assume $F : \mathbb{R}^n \to \mathbb{R}^m$ is a function, where F is given by $m-$real valued component functions $F_1(x_1, \ldots, x_n), \ldots, F_m(x_1, \ldots, x_n)$. If the partial derivatives of all

these functions exist, they can be organised in an $m \times m$ matrix with respect to the variables $x_1, \ldots, x_n$. Therefore, the Jacobian matrix of the function F is derived as

$$J = \begin{pmatrix} \frac{\partial F_1}{\partial x_1} & \cdots & \frac{\partial F_1}{\partial x_n} \\ \vdots & \vdots & \vdots \\ \frac{\partial F_m}{\partial x_1} & \cdots & \frac{\partial F_m}{\partial x_n} \end{pmatrix}. \tag{1.9.4}$$

There were two approaches used to ensure negative eigenvalues. One approach uses the Routh-Hurwitz criteria, and the other uses the Gershgorian Circle Theorem. Routh-Hurwitz criteria require us to find the characteristic equation for the Jacobian matrix (1.9.4) in one variable λ, which is found using $|J - \lambda I| = 0$, where I is the $m \times m$ identity matrix and J is the Jacobian matrix. Then, the eigenvalues will be the solution to the characteristic equation, and the conditions should satisfy the Routh-Hurwitz criteria.

Theorem 1.9.2 *(Routh-Hurwitz Criteria)[91]. Given the polynomial,*

$$p(\lambda) = \lambda^n + a_1\lambda^{n-1} + \ldots + a_{n-1}\lambda + a_n,$$

where the coefficient a_i are real constants , $i = 1, 2, \ldots n$ define the n Hurwitz matrices using the coefficient a_i of the characteristics polynomial:

$$H_1 = \begin{pmatrix} a_1 \end{pmatrix}, \qquad H_2 = \begin{pmatrix} a_1 & 1 \\ a_3 & a_2 \end{pmatrix}, \qquad H_3 = \begin{pmatrix} a_1 & 1 & 0 \\ a_3 & a_2 & a_1 \\ a_5 & a_4 & a_3 \end{pmatrix},$$

$$H_n = \begin{pmatrix} a_1 & 1 & 0 & 0 & \cdots & 0 \\ a_3 & a_2 & a_1 & 1 & \cdots & 0 \\ a_5 & a_4 & a_3 & a_2 & \cdots & 0 \\ \vdots & \vdots & \vdots & \vdots & \cdots & 0 \\ 0 & 0 & 0 & 0 & \cdots & a_n \end{pmatrix},$$

where $a_j = 0$ if $j > n$. All of the roots of the polynomial $P(\lambda)$ are negative or have negative real parts if and only if the determinants of all Hurwitz matrices are positive:

$$|H_j| > 0, \quad j = 1, 2, \ldots, n.$$

The other approach we find the eigenvalues of the Jacobian matrix (1.9.4) by using the Gershgorian Circle Theorem from [92].

Lemma 1.9.3 (Gershgorian theorem) *[92]. Let M be a size $n \times n$ with real entries M_{ij}. If the diagonal elements of that matrix satisfy $m_{ij} < -r_i$ where $r_i = \sum_{i=1, j \neq i}^{n} |m_{ij}|$ for $i, j = 1, \ldots, n$, the eigenvalues of M are negative or have negative real parts .*

Thus, any equilibrium point x^* for the model system (1.9.1) is said to be locally stable when its Jacobian matrix has negative eigenvalues and is unstable otherwise.

Global stability of equilibrium

The next generation operator was used to determine the global stability of the model system (1.9.1). An equilibrium point x^* is said to be globally stable provided the equilibrium point and the solution $x(t)$ remains close to x^* for all $t > 0$.

Lemma 1.9.4 *[93] Consider a model written in the form*

$$\begin{aligned} \frac{dX_1}{dt} &= F(X_1, X_2), \\ \frac{dX_2}{dt} &= G(X_1, X_2), \qquad\qquad G(X_1, 0) = 0, \end{aligned} \tag{1.9.5}$$

where $X_1 \in \mathbb{R}^m$ denotes (its components) the number of uninfected individuals and $X_2 \in \mathbb{R}^n$ denotes (its components) the number of infected individuals including latent, infectious, etc; $X_0 = (X_1^*, 0)$ denotes the disease-free equilibrium of the system.

Also assume the conditions (H_1) and (H_2) below:

(H_1) *For $\frac{dX_1}{dt} = F(X_1, 0)$, X_1^* is globally asymptotically stable;*

(H_2) *$G(X_1, X_2) = AX_2 - \hat{G}(X_1, X_2) \geq 0$ for $(X_1, X_2) \in \Omega$, where the Jacobian $A = \frac{\partial G}{\partial X_2}(X_1^*, 0)$ is the M matrix (the off diagonal elements of A are nonnegative) and Ω is the region where the model makes biological sense.*

Then the DFE $X_0 = (X_1^*, 0)$ *is globally asymptotically stable provided that* $R_0 < 1$.

1.10 Sensitivity analysis

Sensitivity analysis plays a crucial role in identifying which parameters have the most significant impact on the output of a system. It enhances our understanding of feedback mechanisms, stability properties, bifurcation analysis.

1.11 Optimal control

Optimal control theory plays a vital role in disease dynamics by guiding the design, implementation, and evaluation of intervention strategies to mitigate the impact of infectious diseases, enhance public health outcomes, and inform evidence-based policy decisions. It facilitates the integration of mathematical modelling and quantitative analysis into public health policy development and decision-making processes. By providing policymakers with evidence-based recommendations grounded in rigorous mathematical analysis and epidemiological evidence, optimal control methods help bridge the gap between scientific research and policy implementation, ultimately improving the effectiveness and efficiency of disease control efforts.

The general form of an optimal control problem is to maximise or minimise a performance measure (objective function)

$$J(x,u) = \int_{t_0}^{t_f} F(t,x,u)dt, \tag{1.11.6}$$

where $x \in \mathbb{R}^n$ is the state variable, $u \in A \subset \mathbb{R}^m$ is the control variable. The state variable is often subjected to satisfying the state system

$$\begin{cases} \dfrac{dx}{dt} = g(t,x,u), \\ \\ x(t_0) = x_0. \end{cases} \tag{1.11.7}$$

The objective is to determine the optimal pair (x^*, u^*) that maximises or minimises the objective function $J(x,y)$ among all admissible pairs $(x,u) \in \mathbb{R}^n \times \mathbb{R}^m$.

Pontryagin's maximum principle

To determine the optimal pair (x^*, u^*), several techniques can be used. In this study Pontryagin's maximum principle is used to solve all our optimal control problems. The method goes as follows:

1. Determine the Hamiltonian of the system (1.11.6)-(1.11.7)
   $H(t,x,u,\lambda) = F(t,x,u) + \lambda g(t,x,u)$, where $\lambda \in \mathbb{R}^n$ are the co-states or adjoint functions. Then the maximum principle provides the necessary conditions for a pair (x^*, u^*) to be optimal.

2. u^* maximises/minimises the Hamiltonian H, that is :

   (a) $\dfrac{\partial H}{\partial u}(t,x^*,u^*) = 0$, and

   (b) $\dfrac{\partial^2 H}{\partial u^2}(t,x^*,u^*) < 0$, maximisation

   $\dfrac{\partial^2 H}{\partial u^2}(t,x^*,u^*) > 0$, minimisation

3. The co-state satisfy

$$\begin{cases} \dfrac{d\lambda}{dt} = -\dfrac{\partial H}{\partial x}(t,x^*,u^*), \\ \lambda(t_f) = 0. \end{cases} \tag{1.11.8}$$

The solution of the optimal control problem is solved numerically using the forward-backward sweep method, with equation (1.11.7) solved forward in time and equation (1.11.8) solved backward in time.

1.12 Significance of the study

Sleeping sickness, also known as human African trypanosomiasis (HAT), remains a major threat to human well-being in sub-Saharan Africa and has profound socioeconomic consequences. The landscape of infectious diseases challenges global health, necessitating a comprehensive approach for effective mitigation. This study elucidates the pivotal role of such research, especially in finding the best way to control sleeping sickness disease.

HAT is a complex and often neglected tropical disease with significant health implications. This essay delineates the crucial significance of studying sleeping sickness, emphasizing the unique insights of multiscale modeling that contribute to understanding and managing this infection.

Mathematical models can simulate the interactions between humans, tsetse flies (the vectors transmitting the causative parasites), and reservoir hosts. Mathematical modeling allows for the evaluation of the impact of different interventions, such as vector control measures or treatment strategies. This optimization ensures that resources are directed towards the most effective and efficient methods for curbing the prevalence of sleeping sickness.

As with any infectious disease, the insights gained from studies on sleeping sickness are instrumental in informing public health policies. Decision-makers can use quantitative data on disease dynamics and intervention outcomes to formulate evidence-based policies. This ensures that interventions align with the specific challenges posed by sleeping sickness, considering factors such as regional variations and the involvement of multiple hosts.

The significance of studying sleeping sickness is profound, from unraveling transmission dynamics to optimizing control strategies, predictive modeling, informing policies, and managing this complex tropical disease. As we navigate the intricate landscape of sleeping sickness, integrating mathematical modeling ensures that our strategies are both evidence-based and adaptive, offering hope for effective control and eradication.

By developing mathematical models based on immunological and epidemiological dynamics, we can understand the transmission patterns, population dynamics, and impact of various control measures on different scales. This information forms the foundation for evidence-based decision-making by public health authorities and policymakers.

1.13 Outline of the thesis

In this thesis, five chapters are presented, namely Chapter 2, Chapter 3, Chapter 4, and Chapter 5. The first chapter provides background information on infectious diseases, specifically focusing on sleeping sickness, and outlines the motivation behind the study. This chapter delivers an overview of the disease, covering transmission dynamics, treatment, and existing research. Additionally, a detailed description of multiscale mathematical model is presented.

Chapter 2 is dedicated to developing and analyzing a within-host mathematical model for sleeping sickness within a single infected human. The model incorporates the dynamics of Type 1 and Type 2 parasites, naive macrophages, classical macrophages, alternative activated

macrophages, and cytokines through the use of first-order ordinary differential equations. Furthermore, introducing two therapeutic drugs to the model is discussed, and an analysis of the two optimal control problems is conducted.

In Chapter 3, we formulate and analyze a three-species mathematical model that explains the transmission of sleeping sickness. We consider the effects of three controls: stage 1 treatment drug, stage 2 treatment drug, and vector control. Additionally, we solve and analyze the associated optimal control problem.

Chapter 4 serves as a crucial link between Chapter 2 and Chapter 3. In Chapter 4, an embedded multiscale model is developed and analyzed to understand the influence of the within-host model on the population-scale model. The multiscale model is modified to incorporate the treatment drug and vector control, resulting in the formulation of an optimal control problem, which is also subjected to analysis. Lastly, Chapter 5 summarizes a conclusion and discussion of the findings presented in this thesis, along with suggestions for future studies, which one can explore further.

Chapter 2

Studying the effect of parasite switching in optimal control analysis of sleeping sickness

---

This chapter introduces the initial mathematical model that integrates the immune response to parasite invasion in a single infected host with sleeping sickness. The mathematical model considers the interaction among cells, the response to fluctuation of immune cells, and the reaction to parasite growth. The model emphasizes parameters critical in the context of parasite invasion, thereby identifying characteristics of the invasion that can be targeted to mitigate parasite growth. We determine numerical solutions for the model, both with and without switching. Additionally, we formulate and analyze an optimal control problem, incorporating therapeutic drugs. Lastly, we present numerical solutions for the optimal control of the model.

LETTERS IN BIOMATHEMATICS
An International Journal

RESEARCH ARTICLE OPEN ACCESS

Studying the Effect of Parasite Switching in Optimal Control Analysis of Sleeping Sickness

Mulalo Makhuvha[a,b] Hermane Mambili-Mamboundou[a]

[a]University of Kwazulu-Natal, South Africa; [b]DSI-NRF Centre of Excellence in Mathematical and Statistical Sciences (CoE-MaSS), South Africa

ABSTRACT

We construct and analyze an immunological mathematical model to explore within-host dynamics of a neglected tropical vector disease called human African trypanosomiasis (HAT). The disease, caused by a parasite with immune-evading strategies, is represented by six differential equations encompassing type 1 and type 2 parasites, naive macrophages, classical macrophages, alternative activated macrophages, and cytokines. Initial analysis without control measures reveals a disease-free equilibrium and two endemic equilibria, one with co-existing type 1 and type 2 parasites and the other with only one parasite type. Additionally, we explore the impact of control measures on parasite persistence and extinction. Two optimal control models assess the effect of two therapeutic drugs; one focuses on the parasite's invasion, and the other targets the parasite growth rate. Findings indicate that the first drug shifts the system from co-existence to a type 2 parasite endemic state, while the growth inhibitor drug eliminates the parasite from the host.

ARTICLE HISTORY
Received September 6, 2022
Accepted August 30, 2023

KEYWORDS
Immunology, Cytokines, Macrophages, Parasite Infection, Switching, Optimal Control

1 Introduction

Human African trypanosomiasis (HAT) also known as the sleeping sickness is one of the neglected tropical diseases transmitted by tsetse flies. The HAT disease is caused by a parasite named Trypanosoma brucei. There are two types of Trypanosoma brucei that cause the HAT disease, namely Trypanosoma Brucei Gambiense (TBG) and Trypanosoma Brucei Rhodesience (TBR) (WHO, 2019). TBG causes the chronic form of the HAT disease, and TBR causes the acute form.

The World Health Organisation (WHO) had targets to have HAT disease eliminated by 2020, unfortunately, that has not been achieved because at the moment HAT is not of high importance to the WHO as compared to other diseases (WHO, 2019). HAT affects people in 36 countries in sub-Saharan Africa with 62% of the reported cases most predominately in Democratic Republic of Congo (Uniting to Combat NTD, 2019). In addition, TBG accounts for 80% of the reported cases.

HAT is complex to diagnose, and surveillance is difficult due to the fact that most of the people affected reside in remote rural places. The HAT disease harbour itself in both human and nonhuman hosts like cattle and wild animals, making it difficult to control as it requires different host to maintain itself into the community (Wamwiri et al., 2007). The disease being mostly chronic adds more strain to diagnoses, the infected individuals show mild symptoms in the first stage making it difficult to detect from case to case which can lead to the disease being fatal if not diagnosed early. The common symptoms in the first stage entail fever, headache, enlarged lymph nodes, joint pains, and itching (WHO, 2019). The more obvious signs and symptoms appear in the second stage when the parasite crosses the blood-brain barrier, affecting the central nervous system which causes changes in behavior, confusion, sensory disturbances, poor coordination, and sleeping disorder.

HAT is transmitted to humans by a bite from tsetse flies. During the biting, metacyclic trypomastigotes larvae get injected into the human host and later evolve into bloodstream trypomastigotes to easily be transported from the bloodstream to other organs. Once in the bloodstream, the parasites invade the immune system by antigenic variations of the glycoproteins surface coating (Rogers, 1988). Antigenic variation is the ability to switch periodically to thousands more parasite types. The HAT parasite is known to display extreme adaptation to their environment, therefore, the immune cells fail to identify the parasite ounce it has gone through that variation. The more they switch, the less the immune cells is able to keep up with the parasite leading to an increase in the parasite load.

CONTACT Mulalo M. Public makhubamulalo@gmail.com

The first line of defense against the trypomastigotes are macrophages. Macrophages are an important part of the immune system for its function to engulf foreign substances, they are also responsible for the secretion of cytokines which plays an important role in the communication between immune cells during infections. In this study, we will consider three types of macrophages: the naive macrophages, the classical activated macrophages, and the alternative activated macrophages. Naive macrophages are made in the bone marrow and mature either into classical macrophages to form part of the innate immune system or, later on, into alternative activated macrophages to be part of the adaptive immune response. Innate immune response is initiated when a foreign substance enters the body, and it's mostly dealt with in a matter of a few hours. On the other hand, adaptive immune response takes over when the innate immune system is not able to destroy the invader.

For effective immune response, communication between various immune cells type is capital. At the center of that communication are chemical messengers called cytokines. Cytokines are proteins that bind to specific receptors to promote and activate immune cells (Turner et al., 2014). Their role is modulation of inflammation with TNF, NO, IL-1, IL-6, and IFN being pro-inflammatory signaling cytokines, IL-4 and IL-10 being the anti-inflammatory signaling cytokines. The pro-inflammation cytokines are responsible for enhancing and stimulating inflammatory responses whereas anti-inflammatory control the pro-inflammatory cytokine responses (Zhang and An, 2007). Cytokines are communication mediators. They alert the immune system when a response is needed. For the purposes of this study, cytokines will be considered collectively as part of their communication function in the human host.

The infection dynamics of HAT is still not well understood. Only a few noticeable mathematical models have been dedicated to studying this neglected tropical disease. This is mostly due to the fact that HAT has not enjoyed the attention given to more widespread disease like Cancer, HIV/AIDS, and Ebola. With those few noticeable HAT models most of them are population models (see, for example, Rogers, 1988; Ndondo et al., 2016; Artzrouni and Gouteux, 1996; Gervas et al., 2018; Rock et al., 2015, to mention a few). Modeling African tyrpanosomisais goes back to Rogers (1988) who presented a two-vertebrate-host species and one-vector species to simulate how the disease cannot be maintained by the human hosts alone. He had modified a model describing Maleria to allow for incubation and temporary immunity periods for both host species. Rogers also looked at the probability of transmission with a susceptible vector bites an infectious host. Results show that the disease prevalence can be influenced by fly density and seasonal changes in fly numbers. Unlike Rogers, Artzrouni and Gouteux (1996) considered modeling the disease with only the human as the main host for the parasite. From that paper we gather that the human host cannot be neglected since it plays a vital role in the HAT disease dynamics, and it is important to explicitly understand how the disease manifest in the human host.

With HAT being a vector borne disease, a study done by Ndondo et al. (2016) models the transmission dynamics, taking into account the growth of the tsetse fly population at the different stages of its life cycle. That gave motivation to this study to take into account the different stages of the parasite life cycle and the different components involved in the disease transmission within the human host. Some studies modeled HAT by incorporating control theory in implementing measures like education, treatment, and insecticides to mathematical models (Gervas et al., 2018; Rock et al., 2015).

With population models being enhanced, less attention is paid to within-host models. It is imperative to focus attention on how within-host dynamics influence disease progression because diseases succeed when host mechanisms fail. Studying those mechanisms will lead to targeted control measures that can be implemented at the correct level of disease progression. An interesting study by Navarrete (2019) constructed a within-host mathematical model that associated host rhythms in temperature and immunity with parasite replication and immune evasion. Their findings show that temperature and immunity play an important role in mammal host transmission. Another within host model done by Frank (1999) developed a mathematical model that integrate parasite and host immunity, the results show that the minor modifications of switch rates by natural selection are required to develop a sequence of ordered parasites. The study does acknowledge that the switching rate can lead to a series of outbreaks that enable the parasite to escape immune surveillance.

There is little to no knowledge on the effect of antigenic variations by the parasite in evading the immune system within the human host. To our knowledge, there is no study that incorporate cytokines into the modeling of HAT. It is unrealistic to have immune cells singly working without incorporating the role of cytokines. This study seeks to investigate the effect of parasite switching in the evolution of the disease and how the immune system responds to the evasion. Our study differentiates the parasite types and acknowledges the specific immune response to the new parasite type. We later introduce treatment dynamics of different therapeutic drugs to capture the desirable effects of the drugs and expose the effects of drug toxicity. We employ optimal control theory to the improved models in order to get a desired outcome by optimising the duration of the infection while minimising the parasite in the system.

The paper is organised as follows: In Section 2, we introduce our immunological model. In Section 3, we present the mathematical analysis of the immunological model, which includes the positivity and uniqueness of solutions, model equilibria, and the stability of the model equilibria. In Section 4, we present the numerical solutions for the model; whereas, in Section 5, the optimal control models are analysed by incorporating effects of two different therapeutic drugs to the previous model. Moreover, the numerical simulations for the optimal control models are also presented in this section together with the optimality conditions solutions. Lastly, we provide the conclusion in Section 6.

2 Model Formulation

In this section, the basic immunological mathematical model that captures explicitly how the trypanosomiasis parasite interact with the immune system is developed. The within-host transmission is modeled using six variables: Parasite type 1 P_1, Naive macrophages M_n, Classical activated macrophages M_c, Cytokine C, Alternative activation macrophages M_{aa}, and Parasite type 2 P_2. The parameters and variables are explained in Tables 1 and 2, respectively.

From the model diagram in Figure 1, the following system of differential equations are derived:

$$\frac{dP_1}{dt} = \alpha_1 P_1 - s_1 P_1 - k_1 P_1 M_c - \mu_1 P_1, \tag{1}$$

$$\frac{dM_n}{dt} = \Lambda_n - \alpha_n M_n P_1 + (1-k_1) P_1 M_c + (1-k_2) P_2 M_{aa} - \alpha_c M_n - \alpha_{aa} M_n P_2 + \alpha_I M_n C - \mu_n M_n, \tag{2}$$

$$\frac{dM_c}{dt} = \alpha_n M_n P_1 + \alpha_c M_n + \gamma_c M_c C - (1-k_1) P_1 M_c - \mu_c M_c, \tag{3}$$

$$\frac{dM_{aa}}{dt} = \alpha_{aa} M_n P_2 + \gamma_{aa} M_{aa} C - (1-k_2) P_2 M_{aa} - \mu_{aa} M_{aa}, \tag{4}$$

$$\frac{dC}{dt} = \alpha_{p1} P_1 M_c + \alpha_{p2} P_2 M_{aa} - \alpha_I M_n C - \gamma_{aa} M_{aa} C - \gamma_c M_c C - \mu_s C, \tag{5}$$

$$\frac{dP_2}{dt} = s_1 P_1 + \alpha_2 P_2 - k_2 P_2 M_{aa} - \mu_2 P_2. \tag{6}$$

Equation (1) describes the rate of change of parasite type 1 over time, the equation was developed considering the different mechanism in the parasite population growth, switching to another type and removal. The recruited parasites multiply through binary fusion that follows exponential growth with the growth rate given by α_1. The second term in Equation (1) models the parasite switches at a switch rate s_1 (Frank, 1999). Switching to more parasite types can be easily incorporated despite our restriction on parasite types. The third term models the parasite being engulfed by classical macrophages at a rate k_1. It is assumed that parasite type 1 population decays at a natural rate μ_1.

Equation (2) describes the rate of change of the naive macrophages over time. In addition to the immune system, this population is affected by deactivated macrophages and macrophage activation. The first term of the Equation (2) models the recruitment of the naive macrophages at a rate Λ_n. The second term of the Equation (2) represents naive macrophages being activated by dead parasite by a process called classical activation (Baral, 2010). The third and fourth term models the deactivation of the classical and alternative activated macrophages when they interact with the parasites. The fifth and sixth terms describe the differentiation of the naive macrophages into classical and alternative activated macrophages, respectively (Rőszer, 2015). When cytokines bind to then naive macrophages more of the macrophages are produced at a rate α_I. It is assumed that this population decays naturally at a μ_n.

Equation (3) describe the rate of change of the classical activated macrophages over time. The naive macrophages activated by dead parasites increase the classical macrophages population, this is modeled by the first term of Equation (3). As a result of differentiation of naive macrophages, the classical macrophage population is supplied with more classical macrophages at an activation rate α_c. Similarly to naive macrophages, more classical macrophages are produced at the rate γ_c when they bind to the cytokines. When classical activated macrophages come into contact with parasites, they deactivate to naive macrophages at a rate of $(1-k_1)$, reducing the population of this macrophage. It is assumed that the classical macrophages decay naturally at a rate μ_c.

Equation (4) describe the rate of change of the alternative activated macrophages with respect to time. In the presence of parasite type 2, these macrophages activate in order to combat infection (Rőszer, 2015). The alternative activated macrophages are produced when naive macrophages differentiate, at an activation rate of γ_{aa}. In the third term model the deactivated M_{aa} macrophages when they interact with the parasite type 2 . The population of alternative activation macrophages is assumed to decay naturally at a rate μ_{aa}.

Equation (5) describe the rate of change of the concentration of a group of cytokines over time. Macrophages secrete cytokines, which are represented by the parameters α_{p1}, α_{p2}. The cytokines are responsible for the activation of the three types of macrophages which in turn reduces the concentration of the C at a rate α_c, γ_{aa}, and γ_c. With the disease progressing, the concentration of cytokine is assumed to decay naturally at a rate μ_s.

Equation (6) describes the rate of change of parasite type 2 with respect to time. Equation (6) is developed following the parasite switch, growth, and removal. The first term of the equation (6) models the parasite switch from first type to the second type of parasite. Similarly to type 1 parasite, the second type grow exponentially. The third term represents the killing effect of alternative activated macrophages on type 2 parasite at a rate k_2. It is assumed that parasite type 2 decay naturally at a rate μ_2.

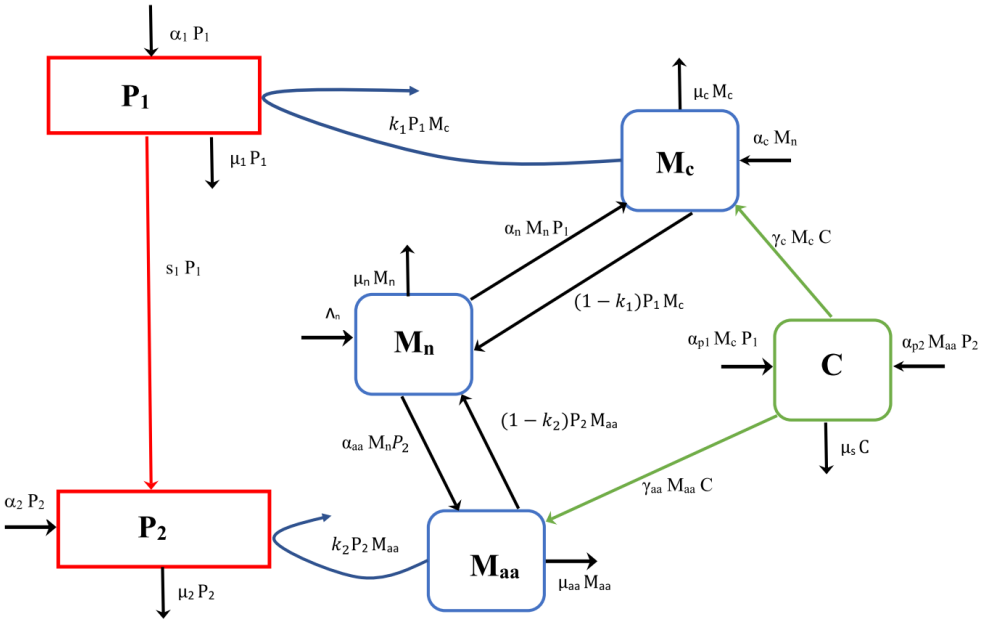

Figure 1: HAT immunological transmission dynamics.

Table 1: Description of the parameters of the model.

Parameter	Description
α_1	Growth rate of parasite type 1
s_1	Switching rate of the parasite type 1 to parasite type 2
k_1	Killing rate of parasite type 1 by classical macrophages
μ_1	Natural death rate of the parasite type 1
Λ_n	Supply of naive macrophages
α_n	Activation rate of naive macrophages by dead parasite
α_c	Activation rate of the classical macrophages from the naive macrophages
α_{aa}	Activation rate of the alternative activated macrophages from naive macrophages
α_I	Activation rate of naive macrophages by cytokine
μ_n	Natural death rate of naive macrophages
γ_c	Production rate for classical macrophages in the presence of cytokine
μ_c	Natural death rate of classical macrophages
γ_{aa}	Activation of alternative activated macrophages by the presence of cytokines
μ_s	Natural decay of cytokines
α_{p1}	Secretion rate of cytokine by classical macrophages
α_{p2}	Secretion rate of cytokine by the alternative activated macrophages
k_2	Killing rate of parasite type 2 by alternative activated macrophages
μ_{aa}	Natural death rate of the alternative activated macrophages
α_2	Growth rate of parasite type 2
μ_2	Natural death rate of parasite type 2

Table 2: Description of the state variables of the model.

Variables	Description	Initial Value
$P_1(t)$	Parasite type 1 population size	1000
$M_n(t)$	Naive macrophage population size	800
$M_c(t)$	Classical macrophage population size	500
$M_{aa}(t)$	Alternative activated macrophage population size	0
C	Cytokine population size	3.8
$P_2(t)$	Parasite type 2 population size	0

3 Mathematical Analysis

In this section, we show that the solutions to the system of equations (1)–(6) exist and are unique, and that the solutions remain positive for all time $t \geq 0$. In addition, the system's equilibria is given together with the stability analysis of both the disease-free equilibrium and endemic equilibrium.

3.1 Existence and uniqueness of solutions

We need to prove existence and uniqueness of the solutions for the system of equations (1)–(6). To show uniqueness, the system of equations can be written in the form $x' = H(x)$ with $x = (P_1, M_n, M_c, M_{aa}, C, P_2)$ and re-indexing $x = (x_1, x_2, x_3, x_4, x_5, x_6)$. Therefore, we define

$$
\begin{aligned}
H_1(x) &= \alpha_1 x_1 - s_1 x_1 - k_1 x_1 x_2 - \mu_1 x_1,\\
H_2(x) &= \Lambda_n - \alpha_n x_2 x_1 + (1-k_1) x_1 x_3 + (1-k_2) x_6 x_4 - \alpha_c x_2 - \alpha_{aa} x_2 x_6 + \alpha_I x_2 x_5 - \mu_n x_2,\\
H_3(x) &= \alpha_n x_2 x_1 + \alpha_c x_2 + \gamma_c x_3 x_5 - (1-k_1) x_1 x_3 - \mu_c x_3,\\
H_4(x) &= \alpha_{aa} x_2 x_6 + \gamma_{aa} x_4 x_5 - (1-k_2) x_6 x_4 - \mu_{aa} x_4,\\
H_5(x) &= \alpha_{p1} x_1 x_3 + \alpha_{p2} x_6 x_4 - \alpha_I x_2 x_5 - \gamma_{aa} x_4 x_5 - \gamma_c x_3 x_5 - \mu_s x_5,\\
H_6(x) &= s_1 x_1 + \alpha_2 x_6 - k_2 x_6 x_4 - \mu_2 x_6.
\end{aligned}
$$

Theorem 3.1 (see Thieme, 1948, Theorem A.4). *Let $\mathbb{R}^n_+ = [0,\infty)^n$ be the cone of non-negative vector in $\mathbb{R}^n_+$. Let $H\colon \mathbb{R}^{n+1}_+ \to \mathbb{R}^n_+$ be a Lipschitz function, $H(t,x) = \big(H_1(t,x), H_2(t,x), \ldots, H_6(t,x)\big)$ satisfying $H_i(t,x) \geq 0$ whenever $t \geq 0$, $x \in \mathbb{R}^n_+$, $x_i = 0$. Then, for every $x^0 \in \mathbb{R}^n_+$, there exists a unique solution of $x' = H(t,x)$, $x(0) = x^0$, with values in $\mathbb{R}^n_+$, which is defined on some time interval $[0, b)$; $b > 0$.*

Using Theorem 3.1 we then check for $i = 1, 2, 3, 4, 5, 6$, $H_i(x) \geq 0$ if $x \in \mathbb{R}^6_+$ and $x_i = 0$; therefore,

$$
\begin{aligned}
H_1(0, M_n, M_c, M_{aa}, C, P_2) &= 0,\\
H_2(P_1, 0, M_c, M_{aa}, C, P_2) &= \Lambda_n + (1-k_1) P_1 M_c + (1-k_2) P_2 M_{aa} \geq 0,\\
H_3(P_1, M_n, 0, M_{aa}, C, P_2) &= \alpha_n M_n P_1 + \alpha_c M_n \geq 0,\\
H_4(P_1, M_n, M_c, 0, C, P_2) &= \alpha_{aa} M_n P_2 \geq 0,\\
H_5(P_1, M_n, M_c, M_{aa}, 0, P_2) &= \alpha_{p1} P_1 M_c + \alpha_{p2} P_2 M_{aa} \geq 0,\\
H_6(P_1, M_n, M_c, M_{aa}, C, 0) &= 0.
\end{aligned}
$$

We can further define $H(t,x) = H(t_+, x_+)$ where $t_+ = max\{t, 0\}$ and $x_+ = (x_1, x_2, x_3, x_4, x_5, x_6)$ are positive parts of the scalar t and vector x. We can check that $\|x_+ - y_+\| \leq \|x - y\|$ for any of the usual norms on $\mathbb{R}^n$. Hence H is a locally Lipschitz continuous vector field on $\mathbb{R}^6$ satisfies $H_i(t,x) \geq 0$ for all $t \in \mathbb{R}, x \in \mathbb{R}^6_+, x_i = 0$.

3.2 Positivity of solutions

We need to prove that all the variables remain non-negative given positive initial conditions for all time $t \geq 0$.

Lemma 3.2. *Let the non-negative initial conditions be $\big(P_1(0) \geq 0, M_n(0) \geq 0, M_c(0) \geq 0, M_{aa}(0) \geq 0, C(0) \geq 0, P_2(0) \geq 0\big) \in \mathbb{R}^6_+$, then all solutions of the system of equations (1)–(6) are positive for all $t > 0$ and non-negative for all t such that all positive solution satisfy $\big(P_1(t) > 0, M_n(t) > 0, M_c(t) > 0, M_{aa}(t) > 0, C(t) > 0, P_2(t) > 0\big)$ for all large t.*

Proof. From the system of equations (1)–(6) we have the first equation as

$$\frac{dP_1}{dt} = \alpha_1 P_1 - s_1 P_1 - k_1 P_1 M_c - \mu_1 P_1.$$

We then obtain the inequality to be

$$\frac{dP_1}{dt} \geq -s_1 P_1 - k_1 P_1 M_c - \mu_1 P_1.$$

Then it follows that

$$\frac{dP_1}{dt} \geq (-s_1 - k_1 M_c - \mu_1) P_1 \qquad \Rightarrow \qquad \frac{dP_1}{P_1} \geq (-s_1 - k_1 M_c - \mu_1) dt.$$

Integrate the above expression

$$P_1(t) \geq P_1(0) \exp\left(-\left((s_1 + \mu_c)t + \int_0^t k_1 M_c(s) ds\right)\right).$$

Similarly, we have

$$M_n(t) \geq M_n(0) \exp\left(-\left(\mu_n t + \int_0^t (\alpha_c P_1(s) ds + \alpha_{aa} P_2(s) ds)\right)\right),$$

$$M_c(t) \geq M_c(0) \exp\left(-\left(\mu_c t + \int_0^t (1 - k_1) P_1(s) ds\right)\right),$$

$$C(t) \geq C(0) \exp\left(-\left(\mu_s t + \int_0^t (\alpha_I M(s) ds + \gamma_c M_c(s) ds + \gamma_{aa} M_{aa}(s) ds)\right)\right),$$

$$M_{aa}(t) \geq M_{aa}(0) \exp\left(-\left(\mu_{aa} t + \int_0^t (1 - k_2) P_2(s) ds\right)\right),$$

$$P_2(t) \geq P_2(0) \exp\left(-\left(\mu_2 t + \int_0^t k_2 M_{aa}(s) ds\right)\right).$$

It then follows that

$$\lim_{t\to\infty} P_1(t) > 0, \qquad \lim_{t\to\infty} M_n(t) > 0, \qquad \lim_{t\to\infty} M_c(t) > 0,$$
$$\lim_{t\to\infty} C(t) > 0, \qquad \lim_{t\to\infty} M_{aa}(t) > 0, \qquad \lim_{t\to\infty} P_2(t) > 0.$$

Therefore, we can conclude that $P_1(t), M_n(t), M_c(t), M_{aa}(t), C(t), P_2(t)$ are positive for all $t > 0$ □

3.3 Model equilibria

In this subsection we give the model equilibrium states and the stability analysis of both the disease-free equilibrium and endemic equilibrium.

3.3.1 Disease-free equilibrium (DFE)

The disease-free equilibrium is when there is no HAT disease in the human host. The equilibrium point is found by equating the right hand side of the system of equations (1)–(6) to zero, thus the DFE point is given by

$$E_0 = \left(0, \frac{\Lambda_n}{\alpha_c + \mu_n}, \frac{\alpha_c \Lambda_n}{\mu_c (\alpha_c + \mu_n)}, 0, 0, 0\right).$$

The DFE describes the natural immune response in the absence of parasites. Only naive macrophages and classsical macrophages are present. Moreover, alternative activated macrophages are non-existant at the DFE, due to the fact that the adaptative immune response is not yet required.

3.3.2 Endemic equilibrium (EE)

The endemic equilibrium point represents the state at which the disease persists in the human host. The solutions to the system of equations (1)–(6) reach the solution curves given by

$$E^* = (P_1^*, M_n^*, M_c^*, M_{aa}^*, C^*, P_2^*).$$

We found that there exist two endemic equilibrium points for the system of equations (1)–(6), which are as follows:

Case 1: There is no parasite P_1; only parasite P_2 exists. That is, $P_1 = 0$ and only parasite P_2 exists; therefore, the disease continues. In this scenario, the endemic point is given by

$$E_1^* = \left(0, M_n^*, M_c^*, M_{aa}^*, C^*, P_2^*\right)$$

where

$$\begin{aligned}
P_1^* &= 0,\\
M_n^* &= -\frac{\alpha_2(\mu_{aa} - C^*\gamma_{aa}) + \mu_2(C^*\gamma_{aa} - \mu_{aa}) - k_2\Lambda_n}{k_2\,(\alpha_c - \alpha_i C^* + \mu_n)},\\
M_c^* &= -\frac{\alpha_c\left(\alpha_2(C^*\gamma_{aa} - \mu_{aa}) + \mu_2(\mu_{aa} - C^*\gamma_{aa}) + k_2\Lambda_n\right)}{k_2(C^*\gamma_c - \mu_c)(\alpha_c - \alpha_i C^* + \mu_n)},\\
M_{aa}^* &= \frac{\alpha_2 - \mu_2}{k_2},\\
C^* &= \frac{P_2^* M_{aa}^* \alpha_{p2}}{\gamma_{aa} M_{aa}^* + \gamma_c M_c^* + \alpha_i M_n^* + \mu_s},\\
P_2^* &= \frac{(\alpha_2 - \mu_2)(C^*\gamma_{aa} - \mu_{aa})(-\alpha_c + \alpha_i C^* - \mu_n)}{\mu_2\alpha_{aa}\mu_{aa} + \alpha_2\left(\alpha_{aa}(C^*\gamma_{aa} - \mu_{aa}) + (k_2 - 1)\alpha_c + (k_2 - 1)\mu_n\right) - C^*\mu_2\alpha_{aa}\gamma_{aa} + k_2\alpha_{aa}\Lambda_n + e_0},
\end{aligned}$$

and where

$$e_0 = \mu_2\alpha_c - k_2\mu_2\alpha_c - \alpha_i C^*\,(k_2 - 1)\,(\alpha_2 - \mu_2) - k_2\mu_2\mu_n + \mu_2\mu_n.$$

Case 2: Both parasites P_1 and P_2 co-exist. In this scenario, the endemic point is given by

$$E_2^* = \left(P_1^{**}, M_n^{**}, M_c^{**}, M_{aa}^{**}, C^{**}, P_2^{**}\right)$$

where

$$\begin{aligned}
P_1^{**} &= \frac{(\mu_{aa} - C^{**}\gamma_{aa})(b_3) + P_2(b_1)}{(C^{**}\gamma_{aa} - \mu_{aa})(b_4) + P_2(b_2)},\\
M_n^{**} &= \frac{\left((k_2 - 1)P_2^{**} + C^{**}\gamma_{aa} - \mu_{aa}\right)\left(-k_1\Lambda_n + C^{**}\gamma_c\mu_1 + s_1(C^{**}\gamma_c - \mu_c) - \mu_1\mu_c + \alpha_1(\mu_c - C^{**}\gamma_c)\right)}{k_1\left((C^{**}\gamma_{aa} - \mu_{aa})(C^{**}\alpha_i - \mu_n) + P_2^{**}\left(C^{**}(k_2 - 1)\alpha_i + \alpha_{aa}(\mu_{aa} - C^{**}\gamma_{aa}) - (k_2 - 1)\mu_n\right)\right)},\\
M_c^{**} &= \frac{\alpha_1 - s_1 - \mu_1}{k_1},\\
M_{aa}^{**} &= \frac{P_2^{**}\alpha_{aa}\left(k_1\Lambda_n - C^{**}\gamma_c\mu_1 + \alpha_1(C^{**}\gamma_c - \mu_c) + \mu_1\mu_c + s_1(\mu_c - C^{**}\gamma_c)\right)}{k_1\left((C^{**}\gamma_{aa} - \mu_{aa})(C^{**}\alpha_i - \mu_n) + P_2^{**}\left(C^{**}(k_2 - 1)\alpha_i + \alpha_{aa}(\mu_{aa} - C^{**}\gamma_{aa}) - (k_2 - 1)\mu_n\right)\right)},\\
C^{**} &= \frac{P_2^{**}M_{aa}^{**}\alpha_{p2} + P_1^{**}M_c^{**}\alpha_{p1}}{\gamma_{aa}M_{aa}^{**} + \gamma_c M_c^{**} + \alpha_i M_n^{**} + \mu_s},\\
P_2^{**} &= \frac{P_1^{**}s_1}{k_2 M_{aa}^{**} - \alpha_2 - \mu_2},
\end{aligned}$$

and where

$$\begin{aligned}
b_1 = {} & -\alpha_1\alpha_{aa}\gamma_{aa}\gamma_c(C^{**})^2 + \alpha_{aa}\gamma_{aa}\gamma_c\mu_1(C^{**})^2 - k_2\alpha_1\alpha_c\gamma_c C^{**} + \alpha_1\alpha_c\gamma_c C^{**} + k_2\alpha_c\gamma_c\mu_1 C^{**} - \alpha_c\gamma_c\mu_1 C^{**}\\
& + \alpha_1\alpha_{aa}\gamma_c\mu_{aa}C^{**} - \alpha_{aa}\gamma_c\mu_1\mu_{aa}C^{**} + (k_2 - 1)\alpha_i(\alpha_1 - \mu_1)(C^{**}\gamma_c - \mu_c)C^{**} + \alpha_1\alpha_{aa}\gamma_{aa}\mu_c C^{**}\\
& - k_2\alpha_1\gamma_c\mu_n C^{**} + \alpha_1\gamma_c\mu_n C^{**} + k_2\gamma_c\mu_1\mu_n C^{**} - \gamma_c\mu_1\mu_n C^{**} + k_1\alpha_c\Lambda_n - k_1k_2\alpha_c\Lambda_n + k_2\alpha_1\alpha_c\mu_c - \alpha_1\alpha_c\mu_c\\
& - k_2\alpha_c\mu_1\mu_c + \alpha_c\mu_1\mu_c - \alpha_1\alpha_{aa}\mu_{aa}\mu_c + \alpha_{aa}\mu_1\mu_{aa}\mu_c + k_2\alpha_1\mu_c\mu_n - \alpha_1\mu_c\mu_n - k_2\mu_1\mu_c\mu_n + \mu_1\mu_c\mu_n\\
& - s_1(C^{**}\gamma_c - \mu_c)\left(C^{**}(k_2 - 1)\alpha_i - k_2\alpha_c + \alpha_c - C^{**}\alpha_{aa}\gamma_{aa} + \alpha_{aa}\mu_{aa} - k_2\mu_n + \mu_n\right) - \alpha_{aa}\gamma_{aa}\mu_1\mu_c C^{**},\\
b_2 = {} & -C^{**}\alpha_1\alpha_{aa}\gamma_{aa} + C^{**}k_1\alpha_1\alpha_{aa}\gamma_{aa} + C^{**}\alpha_{aa}\mu_1\gamma_{aa} - C^{**}k_1\alpha_{aa}\mu_1\gamma_{aa} - C^{**}\alpha_1\alpha_n\gamma_c + C^{**}k_2\alpha_1\alpha_n\gamma_c - k_1\alpha_n\Lambda_n\\
& + k_1k_2\alpha_n\Lambda_n - C^{**}(k_1 - 1)(k_2 - 1)\alpha_i(\alpha_1 - \mu_1) + C\alpha_n\gamma_c\mu_1 - C^{**}k_2\alpha_n\gamma_c\mu_1 - k_1\alpha_1\alpha_{aa}\mu_{aa} + \alpha_1\alpha_{aa}\mu_{aa}\\
& + k_1\alpha_{aa}\mu_1\mu_{aa} - \alpha_{aa}\mu_1\mu_{aa} - k_2\alpha_1\alpha_n\mu_c + \alpha_1\alpha_n\mu_c + k_2\alpha_n\mu_1\mu_c - \alpha_n\mu_1\mu_c - k_1\alpha_1\mu_n + k_1k_2\alpha_1\mu_n - k_2\alpha_1\mu_n\\
& + k_1\mu_1\mu_n - k_1k_2\mu_1\mu_n + k_2\mu_1\mu_n - \mu_1\mu_n + \alpha_1\mu_n\\
& + s_1\left(C^{**}(k_1 - 1)(k_2 - 1)\alpha_i - (k_1 - 1)\alpha_{aa}(C^{**}\gamma_{aa} - \mu_{aa}) - (k_2 - 1)\left(\alpha_n(C^{**}\gamma_c - \mu_c) + (k_1 - 1)\mu_n\right)\right),
\end{aligned}$$

$$b_3 = C^{**}\alpha_1\alpha_c\gamma_c - C^{**}\alpha_c\mu_1\gamma_c + C^{**}\alpha_1\mu_n\gamma_c - C^{**}\mu_1\mu_n\gamma_c + k_1\alpha_c\Lambda_n - C^{**}\alpha_i(\alpha_1-\mu_1)(C^{**}\gamma_c-\mu_c) - \alpha_1\alpha_c\mu_c + \alpha_c\mu_1\mu_c + s_1(C^{**}\gamma_c-\mu_c)(C^{**}\alpha_i-\alpha_c-\mu_n) - \alpha_1\mu_c\mu_n + \mu_1\mu_c\mu_n,$$

$$b_4 = C^{**}\alpha_1\alpha_n\gamma_c - C^{**}\alpha_n\mu_1\gamma_c + k_1\alpha_n\Lambda_n - C^{**}(k_1-1)\alpha_i(\alpha_1-\mu_1) - \alpha_1\alpha_n\mu_c + \alpha_n\mu_1\mu_c + k_1\alpha_1\mu_n - \alpha_1\mu_n - k_1\mu_1\mu_n + \mu_1\mu_n + s_1\big(C(k_1-1)\alpha_i + \alpha_n(\mu_c - C^{**}\gamma_c) - (k_1-1)\mu_n\big).$$

3.4 Stability analysis of model equilibria

In this subsection, we focus on the stability analysis of the model equilibrium points of the system of equations (1)–(6).

3.4.1 Local stability of the DFE

The stability of the disease free equilibrium point E_0, is determined by solving $|J(E_0) - \lambda I| = 0$ where λ is the eigenvalue. According to van den Driessche and Watmough, if the eigenvalue of the Jacobian have negative real parts, then the point E_0 is a locally asymptomatic stable. The Jacobian matrix associated with the system of equations (1)–(6) at E_0 is given by

$$J(E_0) = \begin{pmatrix} \alpha_1 - k_1M_c - \mu_1 - s_1 & 0 & 0 & 0 & 0 & 0 \\ (1-k_1)M_c - M_n\alpha_n & -\alpha_c-\mu_n & 0 & 0 & \alpha_I M_n & -\alpha_{aa}M_n \\ M_n\alpha_n - (1-k_1)M_c & \alpha_c & -\mu_c & 0 & \gamma_c M_c & 0 \\ 0 & 0 & 0 & -\mu_{aa} & 0 & \alpha_{aa}M_n \\ M_c\alpha_{pl} & 0 & 0 & 0 & -\gamma_c M_c - \alpha_I M_n - \mu_s & 0 \\ s_1 & 0 & 0 & 0 & 0 & \alpha_2 - \mu_2 \end{pmatrix}$$

where

$$M_n = \frac{\Lambda_n}{\alpha_c+\mu_n}, \qquad M_c = \frac{\alpha_c\Lambda_n}{\mu_c(\alpha_c+\mu_n)}.$$

The eigenvalues for the above Jacobian matrix are given by

$$\lambda_1 = \alpha_2 - \mu_2,$$
$$\lambda_2 = -\mu_{aa},$$
$$\lambda_3 = -\mu_c,$$
$$\lambda_4 = -\alpha_c - \mu_n,$$
$$\lambda_5 = \frac{-(\mu_1\alpha_c\mu_c - \alpha_1\alpha_c\mu_c + k_1\alpha_c\Lambda_n - \alpha_1\mu_c\mu_n + \mu_1\mu_c\mu_n + s_1\mu_c\mu_n + s_1\alpha_c\mu_c)}{\mu_c(\alpha_c+\mu_n)},$$
$$\lambda_6 = \frac{-\alpha_c\gamma_c\Lambda_n - \alpha_i\mu_c\Lambda_n - \mu_c\mu_n\mu_s - \alpha_c\mu_c\mu_s}{\mu_c(\alpha_c+\mu_n)}.$$

The eigenvalues λ_2, λ_3, λ_4, and λ_6 have negative real parts. For λ_1 and λ_5 to have negative real parts, the following conditions have to hold:

$$\frac{\alpha_2}{\mu_2} < 1, \qquad \frac{\alpha_1\alpha_c\mu_c + \alpha_1\mu_c\mu_n}{\mu_1\alpha_c\mu_c + k_1\alpha_c\Lambda_n + \mu_1\mu_c\mu_n + s_1\mu_c\mu_n + s_1\alpha_c\mu_c} < 1. \tag{7}$$

To understand the biological meaning of these conditions, we observe that from Equation (6), when $P_1 = 0$ at the DFE, P_2 tends to be zero only when $\alpha_2 < k_2M_{aa} + \mu_2$ because $k_2M_{aa} + \mu_2$ is the rate at which P_2 decreases overall and α_2 is P_2's reproductive rate. Hence

$$\frac{\alpha_2}{\alpha_2 + k_2M_{aa} + \mu_2} < 1.$$

This means that the reproductive rate of P_2 should be less than the rate at which P_2 is being washed out of the host. Since $M_{aa} = 0$ at DFE, the condition reduces to $\frac{\alpha_2}{\mu_2} < 1$. The second condition on Equation (7) can be written as

$$\frac{\alpha_1}{\mu_1 + \frac{k_1\alpha_c\Lambda_n}{\mu_c(\alpha_c+\mu_n)} + s_1}$$

where M_c^* is the value of M_c at the DFE. Using the same reasoning, for P_1 in Equation (1), P_1 tends to zero only if $\alpha_1 < \mu_1 + k_1M_c^* + s_1$, where $\mu_c + K_1M_c^* + s_1$ is the overall decreasing rate of P_1. Hence for the DFE to be stable, the reproduction rates of all parasite types should be less than their overall flashing rates.

3.4.2 Local stability of endemic equilibrium

The stability of the endemic point E_1^* depends on the stability of the Jacobian matrix $J(E_1^*)$ given by

$$J(E_1^*) = \begin{pmatrix} L_0 & 0 & 0 & 0 & 0 & 0 \\ (1-k_1)M_c^* - M_n^*\alpha_n & L_6 & 0 & (1-k_2)P_2^* & \alpha_I M_n^* & (1-k_2)M_{aa}^* - \alpha_{\mathrm{aa}}M_n^* \\ M_n^*\alpha_n - (1-k_1)M_c^* & \alpha_c & L_7 & 0 & \gamma_c M_c^* & 0 \\ 0 & \alpha_{aa}P_2^* & 0 & L_3 & \gamma_{aa}M_{aa}^* & \alpha_{\mathrm{aa}}M_n^* - (1-k_2)M_{aa}^* \\ \alpha_{\mathrm{p1}}M_c^* & -\alpha_I C^* & -\gamma_c C^* & \alpha_{\mathrm{p2}}P_2^* - \gamma_{aa}C^* & L_4 & \alpha_{p2}M_{aa}^* \\ s_1 & 0 & 0 & -k_2P_2^* & 0 & L_5 \end{pmatrix}$$

where

$$L_0 = \alpha_1 - k_1M_c^* - \mu_1 - s_1, \qquad L_3 = \gamma_{aa}C^* - (1-k_2)P_2^* - \mu_{\mathrm{aa}}, \qquad L_4 = -\alpha_I M_n^* - \gamma_{aa}M_{aa}^* - \gamma_c M_c^* - \mu_s,$$
$$L_5 = \alpha_2 - k_2M_{aa}^* - \mu_2, \qquad L_6 = \alpha_I C^* - \alpha_c - \alpha_{aa}P_2^* - \mu_n, \qquad L_7 = \gamma_c C^* - \mu_c.$$

We find the sign of eigenvalues using the Gershgorian Circle Theorem below, where $n = 6$.

Theorem 3.3 (Gershgorian theorem from Bejarano et al., 2018). *Let $\bar{x}$ be an equilibrium point of a dynamical system in the form $\frac{dx}{dt} = f(x)$,*

$$D_{f(\bar{x})} = \begin{pmatrix} J_{11} & J_{12} & \cdots & J_{1n} \\ J_{21} & J_{22} & \cdots & J_{2n} \\ \vdots & \vdots & \ddots & \vdots \\ J_{n1} & J_{n2} & \cdots & J_{nn} \end{pmatrix}$$

the Jacobian matrix of the dynamical system evaluated in $\bar{x}$, and $R_i = \sum_{j=1, j\neq i}^{n} |J_{ij}|$ for $i = 1, \ldots, n$. If $J_{ii} < 0$ and $R_i < |J_{ii}|$ for $i = 1, \ldots, n$, then $\bar{x}$ is locally asymptotically stable.

Using Theorem 3.3, the first condition $J_{ii} < 0$ for $i = 1, \ldots, 6$ leads to

$$\alpha_1 < k_1M_c^* + \mu_1 + s_1, \quad \gamma_{aa}C^* < (1-k_2)P_2^* + \mu_{\mathrm{aa}}, \quad \alpha_2 < k_2M_{aa}^* + \mu_2, \quad \alpha_I C^* < \alpha_c + \alpha_{aa}P_2^* + \mu_n, \quad \gamma_c C^* < \mu_c.$$

The second condition, $R_i < |J_{ii}|$ for $i = 1, \ldots, 6$ leads to

$$\frac{2|(1-k_1)M_c^* - M_n^*\alpha_n| + \alpha_{\mathrm{p1}}M_c^* + s_1}{L_0} < 1, \quad \frac{\alpha_c + \alpha_{aa}P_2^* + \alpha_I C^*}{L_6} < 1, \quad \frac{(1-k_2)P_2^* + \alpha_{\mathrm{p2}}P_2^* - \gamma_{aa}C^* + k_2P_2^*}{L_3} < 1,$$
$$\frac{\gamma_c C^*}{L_7} < 1, \quad \frac{\alpha_I M_n^* + \gamma_c M_c^* + \gamma_{aa}M_{aa}^*}{\alpha_I M_n^* + \gamma_{aa}M_{aa}^* + \gamma_c M_c^* + \mu_s} < 1, \quad \frac{2|(1-k_2)M_{aa}^* - \alpha_{aa}M_n^*| + \alpha_{\mathrm{p2}}M_{aa}^*}{L_5} < 1.$$

The stability of the endemic point E_2^* depends on the stability of the Jacobian matrix $J(E_2^*)$ given by

$$J(E_2^*) = \begin{pmatrix} L_0 & 0 & -k_1P_1^{**} & 0 & 0 & 0 \\ (1-k_1)M_c^{**} - M_n^{**}\alpha_n & L_1 & (1-k_1)P_1^{**} & (1-k_2)P_2^{**} & \alpha_I M_n^{**} & (1-k_2)M_{aa}^{**} - \alpha_{\mathrm{aa}}M_n^{**} \\ M_n^{**}\alpha_n - (1-k_1)M_c^{**} & \alpha_n P_1^{**} + \alpha_c & L_2 & 0 & \gamma_c M_c^{**} & 0 \\ 0 & \alpha_{aa}P_2^{**} & 0 & L_3 & \gamma_{aa}M_{aa}^{**} & \alpha_{\mathrm{aa}}M_n^{**} - (1-k_2)M_{aa}^{**} \\ \alpha_{\mathrm{p1}}M_c^{**} & -\alpha_I C^{**} & \alpha_{\mathrm{p1}}P_1^{**} - \gamma_c C^{**} & \alpha_{\mathrm{p2}}P_2^{**} - \gamma_{aa}C^{**} & L_4 & \alpha_{p2}M_{aa}^{**} \\ s_1 & 0 & 0 & -k_2P_2^{**} & 0 & L_5 \end{pmatrix}$$

where

$$L_0 = \alpha_1 - k_1M_c^{**} - \mu_1 - s_1, \qquad L_1 = \alpha_I C^{**} - \alpha_c P_1^{**} - \alpha_c - \alpha_{aa}P_2^{**} - \mu_n, \qquad L_2 = \gamma_c C^{**} - (1-k_1)P_1^{**} - \mu_c,$$
$$L_3 = \gamma_{aa}C^{**} - (1-k_2)P_2^{**} - \mu_{\mathrm{aa}}, \qquad L_4 = -\alpha_I M_n^{**} - \gamma_{aa}M_{aa}^{**} - \gamma_c M_c^{**} - \mu_s, \qquad L_5 = \alpha_2 - k_2M_{aa}^{**} - \mu_2.$$

Similarly, applying Theorem 3.3 to $J(E_2^*)$ with size 6×6 we get the following inequalities:

$$\alpha_1 < k_1M_c^{**} + \mu_1 + s_1, \qquad \alpha_I C^{**} < \alpha_c P_1^{**} + \alpha_c + \alpha_{aa}P_2^{**} + \mu_n, \qquad \gamma_c C^{**} < (1-k_1)P_1^{**} + \mu_c,$$
$$\gamma_{aa}C^{**} < (1-k_2)P_2^{**} + \mu_{\mathrm{aa}}, \qquad \alpha_2 < k_2M_{aa}^{**} + \mu_2.$$

According to the Gershgorian theorem, $R_i < |J_{ii}|$ for $i = 1,\dots,6$ is equivalent to $R_j < |J_{jj}|$ for $j = 1,\dots,6$. Using Theorem 3.3 on matrix $J(E_2^*)$ with size 6×6 we get the following inequalities:

$$\frac{2|(1-k_1)M_c^{**} - M_n^{**}\alpha_n| + \alpha_{p1}M_c^{**} + s_1}{L_0} < 1, \qquad \frac{\alpha_n P_1^{**} + \alpha_c + \alpha_{aa}P_2^{**} + \alpha_I C^{**}}{L_1} < 1, \tag{8}$$

$$\frac{(1-k_1)P_1^{**} + |\alpha_{p1}P_1^{**} - \gamma_c C^{**}| + k_1 P_1^{**}}{L_2} < 1, \qquad \frac{(1-k_2)P_2^{**} + |\alpha_{p2}P_2^{**} - \gamma_{aa}C^{**}| + k_2 P_2^{**}}{L_3} < 1, \tag{9}$$

$$\frac{\alpha_I M_n^{**} + \gamma_c M_c^{**} + \gamma_{aa}M_{aa}^{**}}{\alpha_I M_n^{**} + \gamma_{aa}M_{aa}^{**} + \gamma_c M_c^{**} + \mu_s} < 1, \qquad \frac{2|(1-k_2)M_{aa}^{**} - \alpha_{aa}M_n^{**}| + \alpha_{p2}M_{aa}^{**}}{L_5} < 1. \tag{10}$$

Therefore, we conclude that the equilibrium point E_2^* is locally stable only provided the conditions given in Equation (8)–(10) hold.

4 Numerical Solutions

This section presents numerical simulations of the system of equations (1)–(6). The model simulations were carried out using the MATLAB software, using the parameter values in Table 3 and initial values in Table 2. Due to lack of information on the immunological dynamics for the sleeping sickness disease obtaining the parameter values presented some challenges. Few parameter values were obtained from published literature, while others were assumed based on assumptions made in the model formulation and in comparison with the dynamics of other tropical diseases like malaria, whose parasite exhibit similar characteristics as the HAT parasite (Mhlanga et al., 1997). Therefore our results are purely theoretical but qualitatively sound.

The model simulations gave us an insight into the effects of parasite switching on the evolution of HAT and how the disease progresses over time in the human host. In order to investigate the effects of parasite switching, we first simulate the model when the switch parameter is zero. Figures 2–4 illustrate the evolution of various populations in this scenario. From Figures 2 and 3, it can be seen that with no switching of the parasite, the innate immune response is adequate to deal with the pathogen. The parasite is cleared within a week of infection. During that same period, there is a rise in the levels of naive and classical macrophages (Figure 3) as well as cytokines levels (Figure 4) in the host. It can be noted that the levels of macrophages and cytokines decrease after the pathogen has been dealt with. This highlights the significant role played by both macrophages and cytokines in the innate immune response, immediately after infection, to limit the spread of the pathogen. Moreover, it can be noted that when the innate response is effective against the infection, adaptive response is not required.

In the second scenario, we allow the parasite to switch to another parasite type. The response of various populations to the switch is shown in Figures 5–8, when the value of the switching parameter is $s_1 = 0.0001$. The way at which the parasite evades the immune response by switching type to different parasite type, can be depicted in Figure 5. This is illustrated by exponential rise of the type 2 parasite, two weeks after infection. Figure 7 show cases the host adaptative immune response to the resurgent parasite, characterise by the activation of alternative activated macrophages, whose role is to deal with the new rise in the type 2 pathogen. Figure 8 show cases the cytokine concentration which justifies the behaviour of alternative activated macrophages.

5 Optimal Control Strategies

In this section, we formulate two optimal control models by modifying the system of equations (1)–(6), to incorporate the effect of different drug strategies. Often the treatment of HAT patients depends on the stage of the disease at which the patient is diagnosed. Drugs can be categorized into two types:

- Initial stage drug and
- Second stage drug.

5.1 Initial stage drug

These are drugs that are administered in the early stage of the disease, due to their inability to cross the blood brain barrier. This for instance is the case of Pentamidine, Suramin (Etchegorry et al., 2001). The main function of these drugs is to reduce the parasite load in the host. Our performance measure is to minimize the parasites load in a finite time t_f. The corresponding optimal control problem is

$$\text{minimise}\{J = P_1(t_f) + P_2(t_f)\}.$$

Table 3: Parameter values.

Parameter	Value	Units	References
α_1	0.75	day^{-1}	Wockner et al., 2020
s_1	0.0001	day^{-1}	Frank, 1999
k_1	0.00045	day^{-1}	Assumed
μ_1	0.45	day^{-1}	Assumed
Λ_n	100	$cells/ml/day^{-1}$	Assumed
α_n	0.5	day^{-1}	Assumed
α_c	0.00304	day^{-1}	Assumed
α_{aa}	0.0045	day^{-1}	Assumed
α_I	0.4	day^{-1}	Mohamed et al., 2018
μ_n	0.02	day^{-1}	Pienaar and Lerm, 2014
γ_c	0.4	day^{-1}	Mohamed et al., 2018
μ_c	0.02	day^{-1}	Pienaar and Lerm, 2014
γ_{aa}	0.4	day^{-1}	Assumed
μ_s	0.0154	day^{-1}	Assumed
α_{p1}	0.0015	day^{-1}	Assumed
α_{p2}	0.006	day^{-1}	Assumed
k_2	0.0006	day^{-1}	Assumed
μ_{aa}	0.02	day^{-1}	Pienaar and Lerm, 2014
α_2	0.8	day^{-1}	Assumed
μ_2	0.45	day^{-1}	Assumed
d_0	0.2	day^{-1}	Assumed
d_1	0.02	day^{-1}	Assumed
μ_u	0.00045	day^{-1}	Assumed

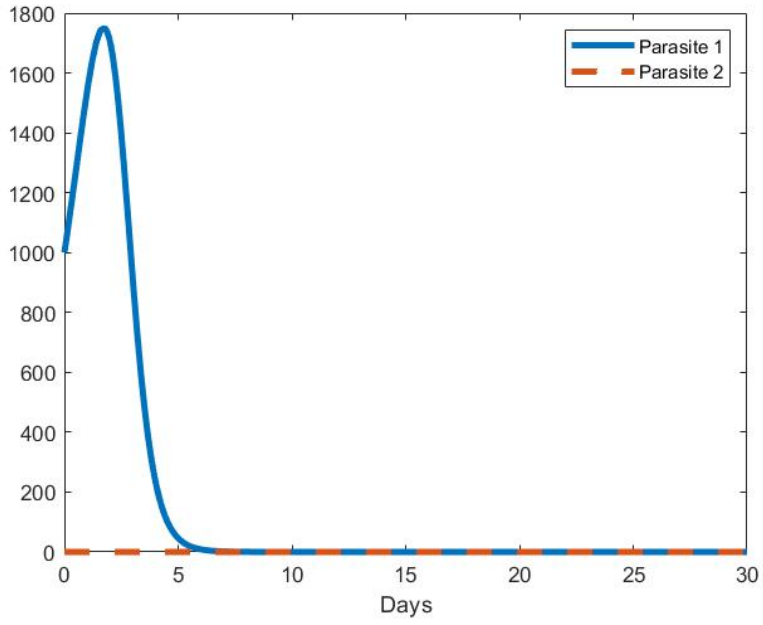

Figure 2: Numerical solution showing progression of the parasite types with no parasite switching.

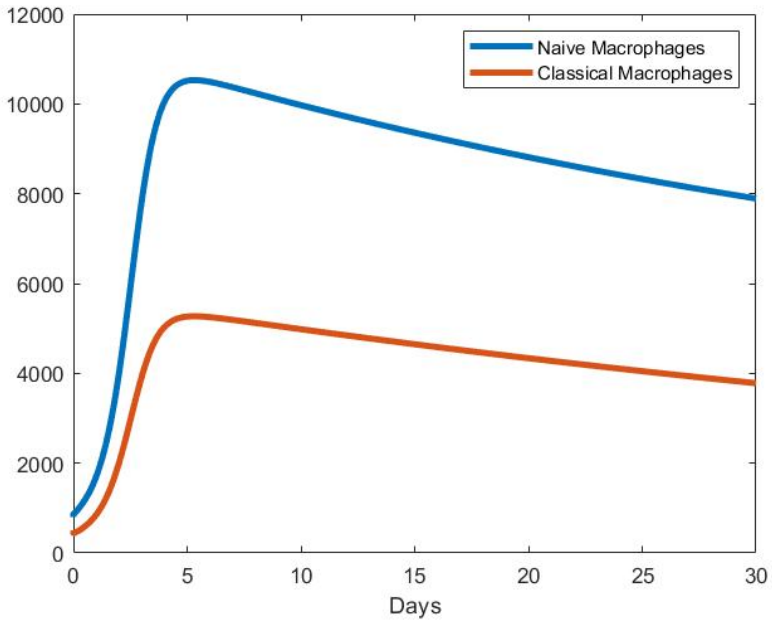

Figure 3: Numerical solution showing progression of the naive and classical macrophages with no parasite switching.

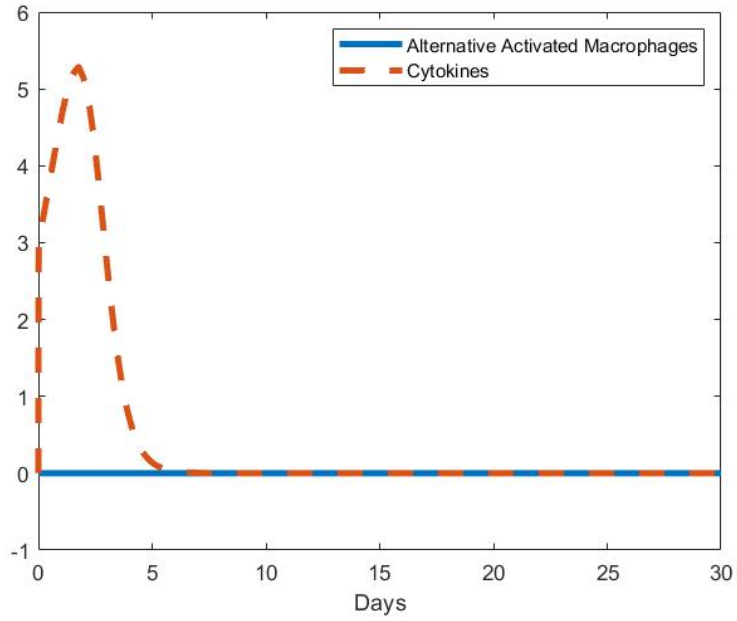

Figure 4: Numerical solution showing progression of the alternative activated macrophages and the cytokines levels with no parasite switching.

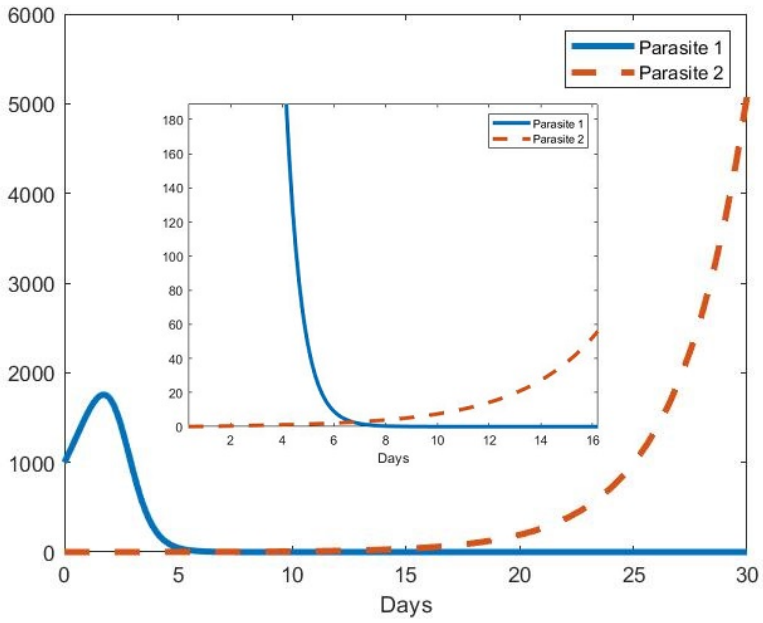

Figure 5: Numerical solution showing progression of the parasite types with parasite switching.

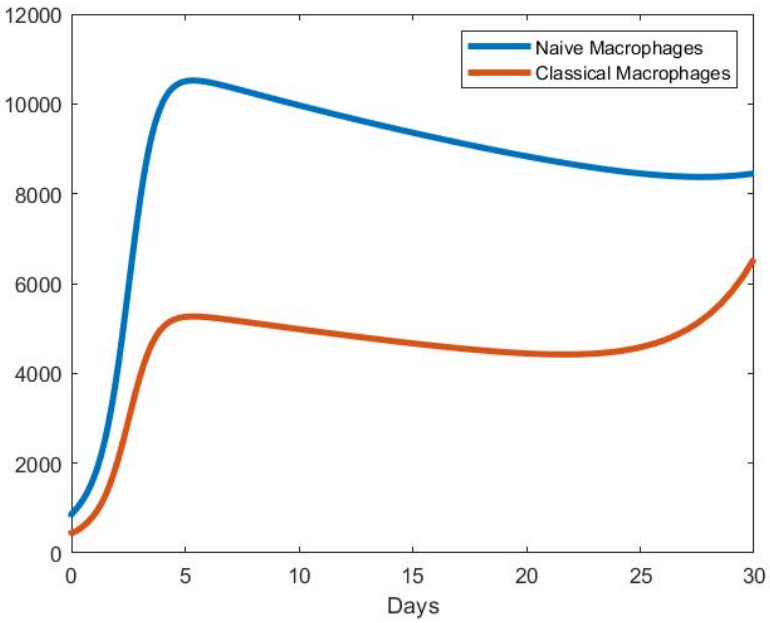

Figure 6: Numerical solution showing progression of the naive and classical macrophages with parasite switching.

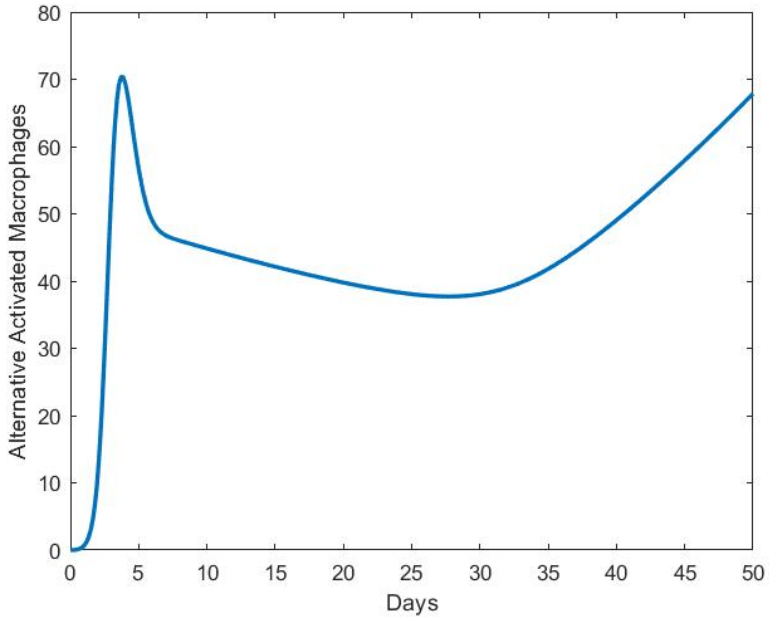

Figure 7: Numerical solution showing progression of the alternative activated macrophages with parasite switching.

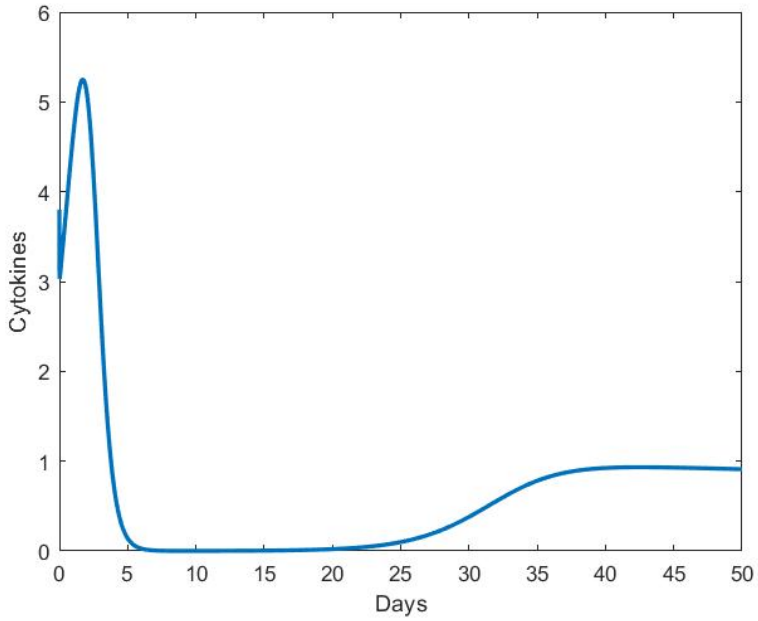

Figure 8: Numerical solution showing progression of the cytokine concentration with parasite switching.

subject to

$$\begin{cases} \dfrac{dP_1}{dt} = \alpha_1 P_1 - d_0(1-e^{-U})P_1 - s_1 P_1 - k_1 P_1 M_c - \mu_1 P_1, & P_1(0) = P_1^0; \\ \dfrac{dM_n}{dt} = \Lambda_n - \alpha_n M_n P_1 + (1-k_1)P_1 M_c + (1-k_2)P_2 M_{aa} - \alpha_c M_n - \alpha_{aa} M_n P_2 + \alpha_I M_n C \\ \qquad\qquad - \mu_n M_n - d_1(1-e^{-U})M_n, & M_n(0) = M_n^0; \\ \dfrac{dM_c}{dt} = \alpha_n M_n P_1 + \alpha_c M_n + \gamma_c M_c C - (1-k_1)P_1 M_c - \mu_c M_c - d_1(1-e^{-U})M_c, & M_c(0) = M_c^0; \\ \dfrac{dM_{aa}}{dt} = \alpha_{aa} M_n P_2 + \gamma_{aa} M_{aa} C - (1-k_2)P_2 M_{aa} - \mu_{aa} M_{aa} - d_1(1-e^{-U})M_{aa}, & M_{aa}(0) = M_{aa}^0; \\ \dfrac{dC}{dt} = \alpha_{p1} P_1 M_c + \alpha_{p2} P_2 M_{aa} - \alpha_I M_n C - \gamma_{aa} M_{aa} C - \gamma_c M_c C - \mu_s C, & C(0) = C^0; \\ \dfrac{dP_2}{dt} = s_1 P_1 + \alpha_2 P_2 - d_0(1-e^{-U})P_2 - k_2 P_2 M_{aa} - \mu_2 P_2, & P_2(0) = P_2^0; \\ \dfrac{dU}{dt} = v(t) - \mu_u U, & U(0) = U^0 \end{cases} \tag{11}$$

where $P_1^0, M_n^0, M_c^0, M_{aa}^0, C^0, P_2^0, U^0$ are positive constants at $0 \le v(t) \le v_{\max}$, with $v_{\max}$ being the maximum dosage possible.

In the model system (11), we denote the amount of drug in the human host at time t by $U(t)$. The drug kills the parasite, and we assume that the drug is toxic to the immune cells. This is represented by the fraction kill for an amount of drug introduced to the system (De Pellis and Radunskaya, 2000). The fraction kill is given by

$$z(U) = d_i(1-e^{-kU}) \qquad \text{for } i = 1, 2.$$

Certain aspects in the pharmacokinetics are still unrevealed in this current study, we let $k = 1$. We let d_1 denote the parasite drug response coefficient, with d_0 being the cell drug response coefficient with an assumption that $d_0 > d_1$. The amount of drug in the host is determined by the drug dosage $v(t)$ given at a particular time. It is assumed that the drug decays naturally at a rate μ_u. It is important to note that the control is not effective when $U = 0$ and effective when $U \neq 0$.

Theorem 5.1. *Given the optimal control variable $v(t)$, and corresponding state variables P_1, M_n, M_c, M_{aa}, C, and P_2 of the control system (11), and initial conditions in Table 2 admit a unique optimal solution $P_1^*, M_n^*, M_c^*, M_{aa}^*, C^*, P_2^*$ associated with an optimal control $v(t)$ with a fixed optimal final time t_f; moreover, there exists adjoint co-state functions $\lambda_i(t)$, $1 \le i \le 7$, satisfying $\frac{d\lambda_1}{dt} = -\frac{\partial H}{\partial P_1}$, $\frac{d\lambda_2}{dt} = -\frac{\partial H}{\partial M_n}$, $\frac{d\lambda_3}{dt} = -\frac{\partial H}{\partial M_c}$, $\frac{d\lambda_4}{dt} = -\frac{\partial H}{\partial M_{aa}}$, $\frac{d\lambda_5}{dt} = -\frac{\partial H}{\partial C}$, $\frac{d\lambda_6}{dt} = -\frac{\partial H}{\partial P_2}$, $\frac{d\lambda_7}{dt} = -\frac{\partial H}{\partial U}$ with corresponding transversality conditions $\lambda_1(t_f) = 1$, $\lambda_2(t_f) = 0$, $\lambda_3(t_f) = 0$, $\lambda_4(t_f) = 0$, $\lambda_5(t_f) = 0$, $\lambda_6(t_f) = 1$, and $\lambda_7(t_f) = 0$. The Hamiltonian function H for the optimal control problem is given by*

$$H = J + \lambda_1 \dot{P}_1 + \lambda_2 \dot{M}_n + \lambda_3 \dot{M}_c + \lambda_4 \dot{M}_{aa} + \lambda_5 \dot{C} + \lambda_6 \dot{P}_2 + \lambda_7 \dot{U}$$

Furthermore, the optimal control dosage is given by

$$v(t) = \begin{cases} 0, & \text{if } \lambda_7 > 0, \\ v_{max}, & \text{if } \lambda_7 < 0, \\ \text{undetermined}, & \text{if } \lambda_7 = 0. \end{cases}$$

Proof. According to Pontryagin maximum principle (Pontryagin et al., 1986), we have the Hamiltonian function defined as,

$$\begin{aligned} H = {} & A_1 P_1 + A_2 P_2 + \lambda_1[\alpha_1 P_1 - d_0(1-e^{-U})P_1 - s_1 P_1 - k_1 P_1 M_c - \mu_1 P_1] \\ & + \lambda_2[\Lambda_n - \alpha_n M_n P_1 + (1-k_1)P_1 M_c + (1-k_2)P_2 M_{aa} - \alpha_c M_n - \alpha_{aa} M_n P_2 + \alpha_I M_n C - \mu_n M_n - d_1(1-e^{-U})M_n] \\ & + \lambda_3[\alpha_n M_n P_1 + \alpha_c M_n + \gamma_c M_c C - (1-k_1)P_1 M_c - \mu_c M_c - d_1(1-e^{-U})M_c] \\ & + \lambda_4[\alpha_{aa} M_n P_2 + \gamma_{aa} M_{aa} C - (1-k_2)P_2 M_{aa} - \mu_{aa} M_{aa} - d_1(1-e^{-U})M_{aa}] \\ & + \lambda_5[\alpha_{p1} P_1 M_c + \alpha_{p2} P_2 M_{aa} - \alpha_I M_n C - \gamma_{aa} M_{aa} C - \gamma_c M_c C - \mu_s C] \\ & + \lambda_6[s_1 P_1 + \alpha_2 P_2 - d_0(1-e^{-U})P_2 - k_2 P_2 M_{aa} - \mu_2 P_2] \\ & + \lambda_7[v(t) - \mu_u U], \end{aligned}$$

where λ_1, λ_2, λ_3, λ_4, λ_5, λ_6, and λ_7 are the adjoint functions associated with the state functions. Applying the Pontryagin maximum principle, the adjoint system is given by

$$\begin{aligned}
\frac{d\lambda_1}{dt} &= -A_1 + \lambda_1[d_0(1-e^{-U}) + s_1 + k_1M_c - \mu_1 - \alpha_1] + \alpha_2M_n\lambda_2 + \lambda_3[(1-k_1)M_c - \alpha_nM_n] - \lambda_6s_1 - \lambda_5\alpha_{p1}M_c \\
\frac{d\lambda_2}{dt} &= \lambda_2[\alpha_nP_1 + \alpha_c - \alpha_IC + \alpha_{aa}P_2 + \mu_n + d_1(1-e^{-U})] + \lambda_5\alpha_IC - \lambda_4\alpha_{aa}P_2 - \lambda_3[\alpha_nP_1 + \alpha_c] \\
\frac{d\lambda_3}{dt} &= \lambda_1k_1P_1 - \lambda_2(1-k_1)P_1 + \lambda_3[(1-k_1)P_1 + \mu_c + d_1(1-e^{-U}) - \gamma_cC] + \lambda_5[\gamma_cC - \alpha_{p1}P_1] \\
\frac{d\lambda_4}{dt} &= \lambda_6k_2P_2 - \lambda_2(1-k_2)P_2 + \lambda_4[(1-k_2)P_2 + \mu_{aa} + d_1(1-e^{-U}) - \gamma_{aa}C] + \lambda_5[\gamma_{aa}C - \alpha_{p2}P_2] \\
\frac{d\lambda_5}{dt} &= \lambda_5[\alpha_IM_n + \gamma_{aa}M_{aa} + \gamma_cM_c + \mu_s] - \lambda_2\alpha_IM_n - \lambda_3\gamma_cM_c - \lambda_4\gamma_{aa}M_{aa} \\
\frac{d\lambda_6}{dt} &= -A_2 + \lambda_2[\alpha_{aa}M_n - (1-k_2)M_{aa}] + \lambda_4[(1-k_2)M_{aa} - \alpha_{aa}M_n] - \lambda_5\alpha_{p2}M_{aa} \\
&\qquad + \lambda_6[k_2M_{aa} + d_0(1-e^{-U}) + \mu_2 - \alpha_2] \\
\frac{d\lambda_7}{dt} &= e^{-U}(\lambda_1d_0P_1 + \lambda_2d_1M_n + \lambda_3d_1M_c + \lambda_4d_1M_{aa} + \lambda_6d_0P_2) + \lambda_7\mu_u.
\end{aligned}$$

Using the transversality condition, the initial values for the adjoint functions are obtained as

$$\lambda_1(t_f) = \left.\frac{\partial J}{\partial P_1}\right|_{t=t_f} = 1, \qquad \lambda_2(t_f) = \left.\frac{\partial J}{\partial M_n}\right|_{t=t_f} = 0, \qquad \lambda_3(t_f) = \left.\frac{\partial J}{\partial M_c}\right|_{t=t_f} = 0, \qquad \lambda_4(t_f) = \left.\frac{\partial J}{\partial M_{aa}}\right|_{t=t_f} = 0,$$
$$\lambda_5(t_f) = \left.\frac{\partial J}{\partial C}\right|_{t=t_f} = 0, \qquad \lambda_6(t_f) = \left.\frac{\partial J}{\partial P_2}\right|_{t=t_f} = 1, \qquad \lambda_7(t_f) = \left.\frac{\partial J}{\partial U}\right|_{t=t_f} = 0.$$

The drug in the whole system is dependent on the dosage given at a particular time. The aim is to minimise the Hamiltonian H, with respect to the dosage v. But H is linear in v

$$H = \lambda_7v + \lambda_8,$$

where $\lambda_8 = A_1P_1 + A_2P_2 + \lambda_1\dot{P}_1 + \lambda_2\dot{M}_n + \lambda_3\dot{M}_c + \lambda_4\dot{M}_{aa} + \lambda_5\dot{C} + \lambda_6\dot{P}_2 - \mu_u\lambda_7\dot{U}$. Thus the optimal value $v(t)$

$$v(t) = \begin{cases} 0, & \text{if } \lambda_7 > 0, \\ v_{max}, & \text{if } \lambda_7 < 0, \\ \text{undetermined}, & \text{if } \lambda_7 = 0. \end{cases}$$

The adjoint function λ_7 is the switching function for the drug dosage $v(t)$, bounded by $0 \le v(t) \le v_{\max}$; the drug should be injected at maximum rate, $v_{\max}$, whenever λ_7 is negative and should be stopped whenever λ_7 is positive. □

5.1.1 Numerical simulations of early stage stage drug

We use the steepest descent method to find the optimal control, in combination with the forward, backward sweep method for the state and co-state variables. We note that the drug dosage needs to be the same every day. The initial conditions for model (11) are given by $P_1 = 1000, M_n = 500, M_c = 300, M_{aa} = 10, C = 5, P_2 = 500$, with the assumption that intervention is implemented when the disease has progressed in the human host. The solution curve (blue) without intervention was simulated with the initial conditions in Table 2. From Figure 9, we notice the significant reduction of the parasite type 1 population in the presence of the drug as opposed to no drug in the system. From Figure 12, we notice that in spite of the drug being present in the system, parasite type 2 increases with time. This suggests that using a drug targeting the parasite population does not reduce the disease burden. We observe a decline in the macrophage populations in Figures 10, 11, and 14 when using the first stage drug. That is because the drug has a negative impact on macrophages because of the toxicity of the drug. This then means that the body loses its ability to fight parasites. Attributes shown in Figure 12 confirms that not any drug minimises the disease burden in the system. Figure 15 illustrates that early stage drugs need to be administered continuously for 10 days.

5.2 Second stage drug

In the second optimal control strategy, the specific function of the drug is to reduce the parasite load by targeting their production abilities. These are drugs that are administered in the second stage of the disease, due to their ability to cross the blood brain

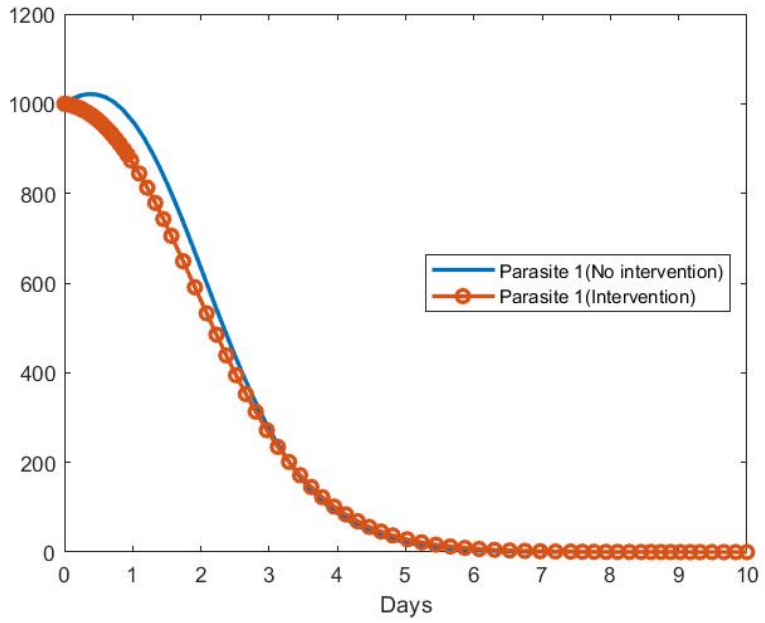

Figure 9: Numerical solutions of model system showing progression of parasite type 1 with effects of the early stage drug.

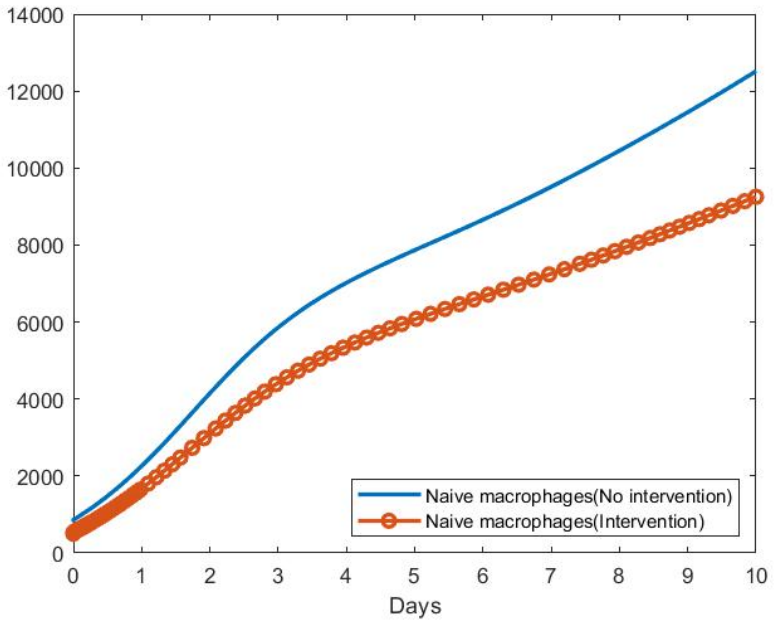

Figure 10: Numerical solutions of model system showing progression of naive macrophages with effects of the early stage drug.

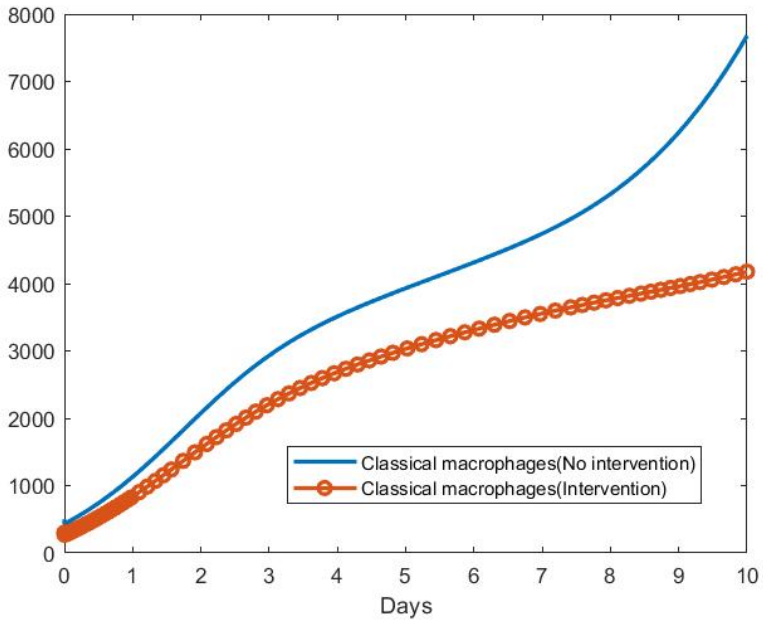

Figure 11: Numerical solutions of model system showing progression of classical macrophages with effects of the early stage drug.

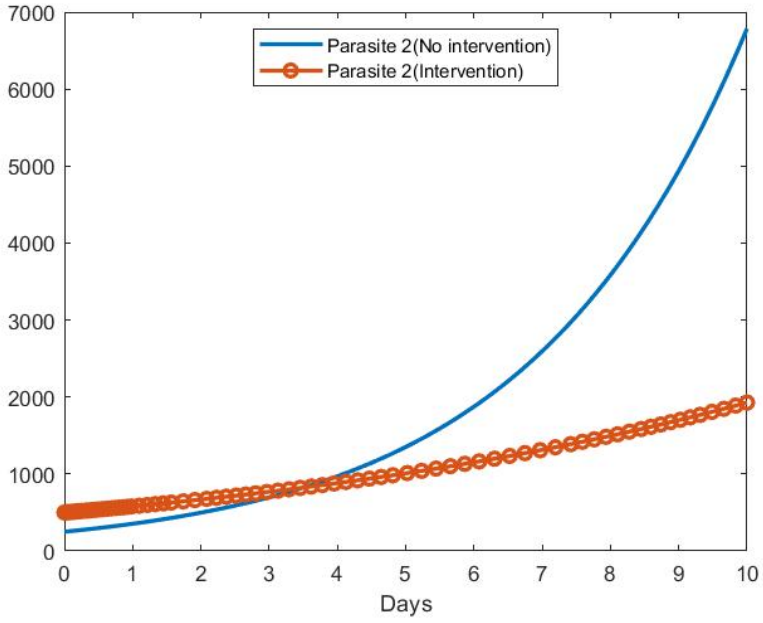

Figure 12: Numerical solutions of model system showing progression of parasite type 2 with effects of the early stage drug

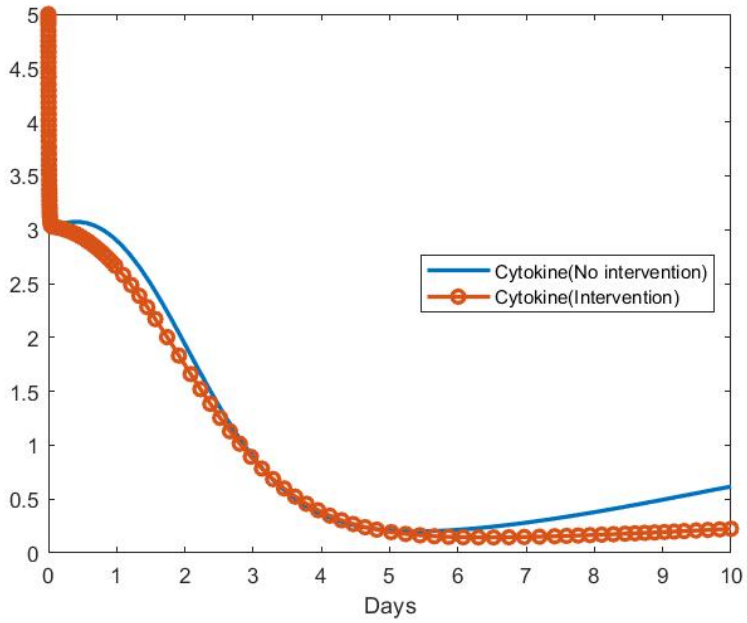

Figure 13: Numerical solutions of model system showing progression of cytokines with effects of the early stage drug.

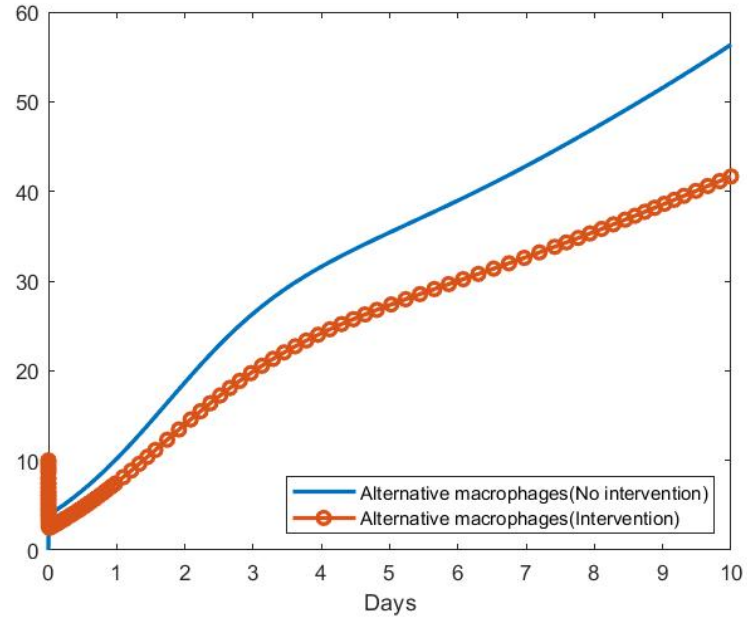

Figure 14: Numerical solutions of model system showing progression of alternative macrophages with effects of the early stage drug.

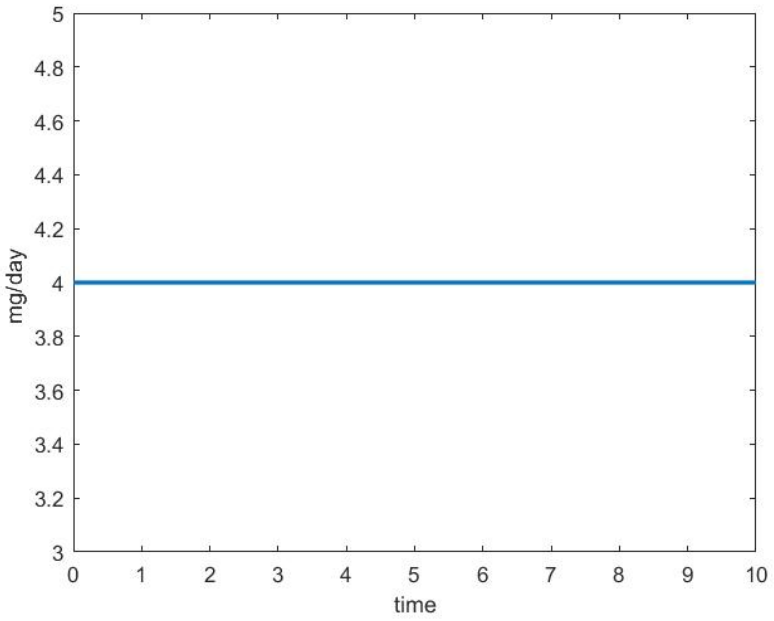

Figure 15: Drug dosage

barrier. This for instance is the case of Melarsoprol, Eflornithine, and Fexinidazole (Etchegorry et al., 2001). In this strategy, the performance measure is given by

$$J = \int_{t_0}^{t_f} \left(A_1 P_1 + A_2 P_2 + b_2 u_2^2 - b_1 u_1^2\right) dt.$$

Thus, we wish to minimise the density of parasite P_1, P_2 and the toxicity of the drug u_2, while maximising drug efficacy. The corresponding optimal control problem is

$$\text{minimise}\left\{J = \int_{t_0}^{t_f} \left(A_1 P_1 + A_2 P_2 + b_2 u_2^2 - b_1 u_1^2\right) dt\right\}.$$

subject to

$$\begin{cases} \dfrac{dP_1}{dt} = (1-u_1)\alpha_1 P_1 - s_1 P_1 - k_1 P_1 M_c - \mu_1 P_1, & P_1(0) = P_1^0; \\ \dfrac{dM_n}{dt} = \Lambda_n - \alpha_n M_n P_1 + (1-k_1) P_1 M_c + (1-k_2) P_2 M_{aa} \\ \qquad\qquad - \alpha_c M_n - \alpha_{aa} M_n P_2 + \alpha_I M_n C - (\mu_n + u_2) M_n, & M_n(0) = M_n^0; \\ \dfrac{dM_c}{dt} = \alpha_n M_n P_1 + \alpha_c M_n + \gamma_c M_c C - (1-k_1) P_1 M_c - (\mu_c + u_2) M_c, & M_c(0) = M_n^0; \\ \dfrac{dM_{aa}}{dt} = \alpha_{aa} M_n P_2 + \gamma_{aa} M_{aa} C - (1-k_2) P_2 M_{aa} - (\mu_{aa} + u_2) M_{aa}, & M_{aa}(0) = M_{aa}^0; \\ \dfrac{dC}{dt} = \alpha_{p1} P_1 M_c + \alpha_{p2} P_2 M_{aa} - \alpha_I M_n C - \gamma_{aa} M_{aa} C - \gamma_c M_c C - \mu_s C, & C(0) = C^0; \\ \dfrac{dP_2}{dt} = s_1 P_1 + (1-u_1)\alpha_2 P_2 - k_2 P_2 M_{aa} - \mu_2 P_2, & P_2(0) = P_2^0 \end{cases} \tag{12}$$

where $P_1^0, M_n^0, M_c^0, M_{aa}^0, C^0, P_2^0$ are given constants and $0 \le u_1(t) \le 1; u_2(t) \ge 0$ with $u_1 = 1$ being 100% effective and $u_1 = 0$ being no drug usage.

Theorem 5.2. *Given the optimal control variable u_1, u_2, and corresponding state variables P_1, M_n, M_c, M_{aa}, C, and P_2 of the control system (12), and initial conditions in Table 2 admits a unique optimal solution P_1^*, M_n^*, M_c^*, M_{aa}^*, C^*, P_2^* associated with an optimal control u_1, u_2 with a fixed optimal final time t_f; moreover, there exists adjoint co-state functions $\lambda_i(t)$, $1 \le i \le 6$, satisfying $\frac{d\lambda_1}{dt} = -\frac{\partial H}{\partial P_1}$, $\frac{d\lambda_2}{dt} = -\frac{\partial H}{\partial M_n}$, $\frac{d\lambda_3}{dt} = -\frac{\partial H}{\partial M_c}$, $\frac{d\lambda_4}{dt} = -\frac{\partial H}{\partial M_{aa}}$, $\frac{d\lambda_5}{dt} = -\frac{\partial H}{\partial C}$, $\frac{d\lambda_6}{dt} = -\frac{\partial H}{\partial P_2}$, $\frac{d\lambda_7}{dt} = -\frac{\partial H}{\partial U}$. The Hamiltonian function H for the optimal control problem is given by*

$$H = J + \lambda_1 \dot{P}_1 + \lambda_2 \dot{M}_n + \lambda_3 \dot{M}_c + \lambda_4 \dot{M}_{aa} + \lambda_5 \dot{C} + \lambda_6 \dot{P}_2.$$

Furthermore, the optimal control variable solutions are given as

$$u_1^* = \min\left\{\max\left\{0, -\tfrac{1}{2b_1}\left(\lambda_1\alpha_1 P_1 + \lambda_6\alpha_2 P_2\right)\right\}, 1\right\}.$$

Proof. According to the Pontryagin maximum principle (Pontryagin et al., 1986), the Hamiltonian function is defined by

$$\begin{aligned} H = {} & A_1 P_1 + A_2 P_2 + b_2 u_2^2 - b_1 u_1^2 + \lambda_1[(1-u_1)\alpha_1 P_1 - s_1 P_1 - k_1 P_1 M_c - \mu_1 P_1] \\ & + \lambda_2[\Lambda_n - \alpha_n M_n P_1 + (1-k_1)P_1 M_c + (1-k_2)P_2 M_{aa} - \alpha_c M_n - \alpha_{aa} M_n P_2 + \alpha_I M_n C - (\mu_n + u_2)M_n] \\ & + \lambda_3[\alpha_n M_n P_1 + \alpha_c M_n + \gamma_c M_c C - (1-k_1)P_1 M_c - (\mu_c + u_2)M_c] \\ & + \lambda_4[\alpha_{aa} P_2 M_n + \gamma_{aa} M_{aa} C - (1-k_2)P_2 M_{aa} - (\mu_{aa} + u_2)M_{aa}] \\ & + \lambda_5[\alpha_{p1} M_c P_1 + \alpha_{p2} P_2 M_{aa} - \alpha_I M_n C - \gamma_{aa} M_{aa} C - \gamma_c M_c C - \mu_s C] \\ & + \lambda_6[s_1 P_1 + (1-u_1)\alpha_2 P_2 - k_2 P_2 M_{aa} - \mu_2 P_2], \end{aligned}$$

where $\lambda_1, \lambda_2, \lambda_3, \lambda_4, \lambda_5, \lambda_6$ are adjoint functions of the following adjoint system:

$$\begin{aligned} \frac{d\lambda_1}{dt} &= -A_1 + \lambda_1[s_1 + k_1 M_c + \mu_1 - (1-u_1)\alpha_1] + \lambda_2[\alpha_n M_n - (1-k_1)M_c] + \lambda_3[(1-k_1)M_c - \alpha_n M_n] - \lambda_5\alpha_{p1} M_c - \lambda_6 s_1, \\ \frac{d\lambda_2}{dt} &= \lambda_2[\alpha_n P_1 + \alpha_c + \alpha_{aa} P_2 + (\mu_n + u_2) - \alpha_I C] - \lambda_3[\alpha_n P_1 + \alpha_c] - \lambda_4\alpha_{aa} P_2 + \lambda_5\alpha_I C, \\ \frac{d\lambda_3}{dt} &= \lambda_1 k_1 P_1 - \lambda_2(1-k_1)P_1 + \lambda_3[(1-k_1)P_1 + (\mu_c + u_2) - \gamma_c C] + \lambda_5[\gamma_c C - \alpha_{p1} P_1], \\ \frac{d\lambda_4}{dt} &= k_2 P_2 \lambda_6 - \lambda_2(1-k_2)P_2 + \lambda_4[(1-k_2)P_2 + (\mu_{aa} + u_2) - \gamma_{aa} C] + \lambda_5[\gamma_{aa} C - \alpha_{p2} P_2], \\ \frac{d\lambda_5}{dt} &= \lambda_5(\alpha_I M_n + \gamma_{aa} M_{aa} + \gamma_c M_c + \mu_s) - \lambda_2\alpha_I M_n - \lambda_3\gamma_c M_c - \lambda_4\gamma_{aa} M_{aa}, \\ \frac{d\lambda_6}{dt} &= -A_2 + \lambda_2[\alpha_{aa} M_n - (1-k_2)M_{aa}] + \lambda_4[(1-k_2)M_{aa} - \alpha_{aa} M_n] - \lambda_5\alpha_{p2} M_{aa} + \lambda_6[k_2 M_{aa} + \mu_2 - \alpha_2(1-u_1)]. \end{aligned}$$

Using the first derivative test, the optimal controls are obtained by solving

$$\frac{\partial H}{\partial u_1} = -2b_1 u_1 - \lambda_1\alpha_1 P_1 - \lambda_6\alpha_2 P_2 = 0, \tag{13}$$

$$\frac{\partial H}{\partial u_2} = 2b_2 u_2 - M_n\lambda_2 - M_c\lambda_3 - M_{aa}\lambda_4 = 0. \tag{14}$$

Solving for u_1 and u_2 in the system (13)–(14), the corresponding optimal control variable solutions are given by

$$\begin{aligned} u_1^* &= -\frac{1}{2b_1}\left(\lambda_1\alpha_1 P_1 + \lambda_6\alpha_2 P_2\right), \\ u_2^* &= \frac{1}{2b_2}\left(\lambda_2 M_n + M_c\lambda_3 + M_{aa}\lambda_4\right). \end{aligned}$$

□

5.2.1 Numerical simulations of second stage drug

Similarly, we use the steepest descent method to find the optimal control, in combination with the forward, backward sweep method for the state and co-state variables.

Figures 16–21 illustrate the dynamics of model (12). Model (12) incorporates the drug that targets the growth rate of the parasite. In Figure 16, we notice that parasite type one ideally reduces in the presence of the drug. In Figure 19, we observe that

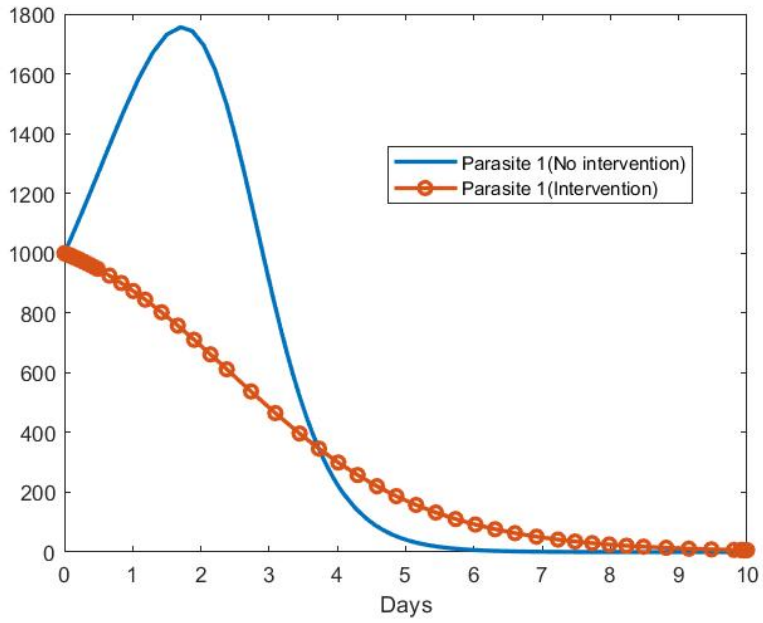

Figure 16: Numerical solutions of model system showing progression of parasite type 1 with effects of second stage drug.

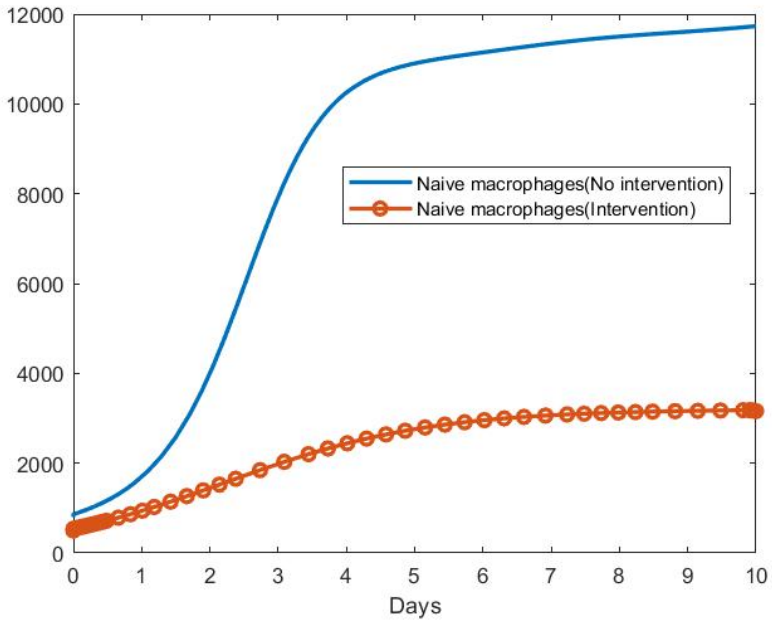

Figure 17: Numerical solutions of model system showing progression of naive macrophages with effects of second stage drug.

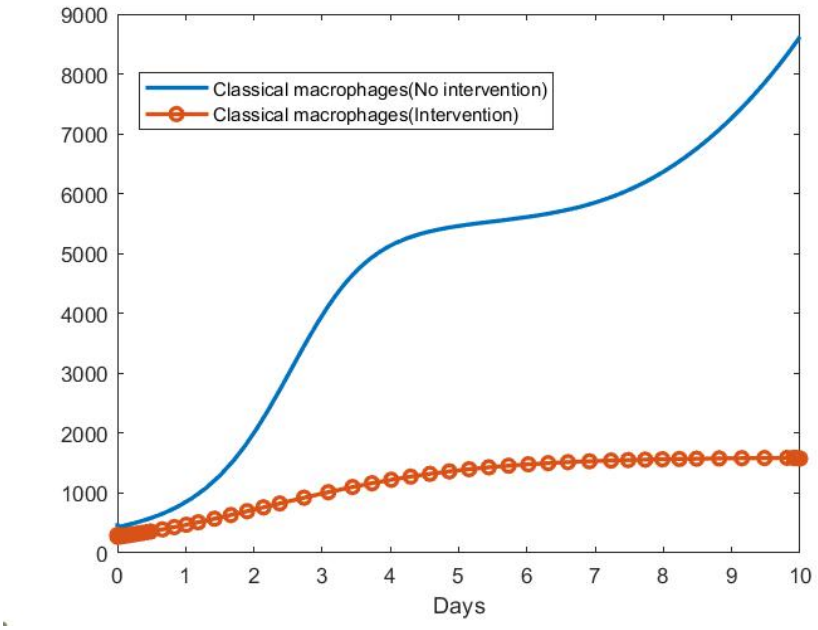

Figure 18: Numerical solutions of model system showing progression of classical macrophages with effects of second stage drug.

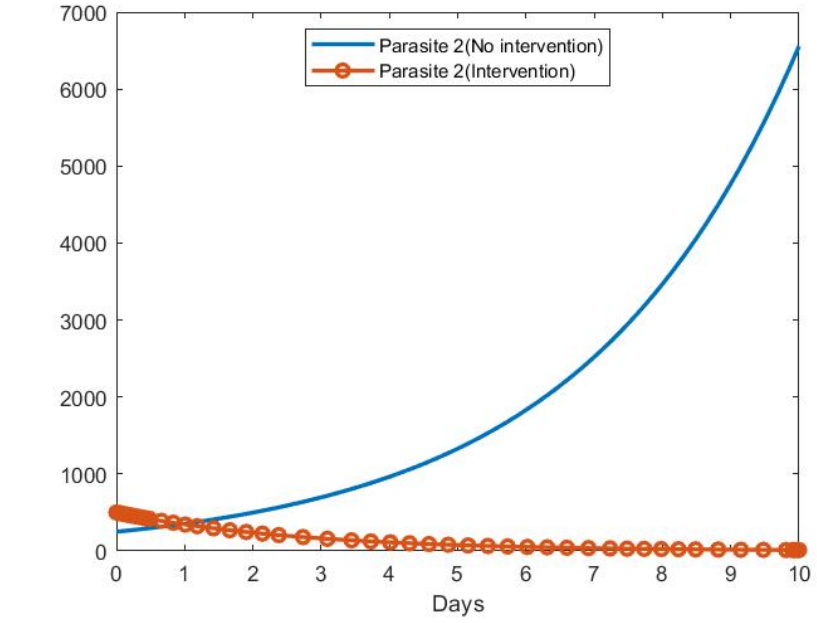

Figure 19: Numerical solutions of model system showing progression of parasite type 2 with effects of second stage drug.

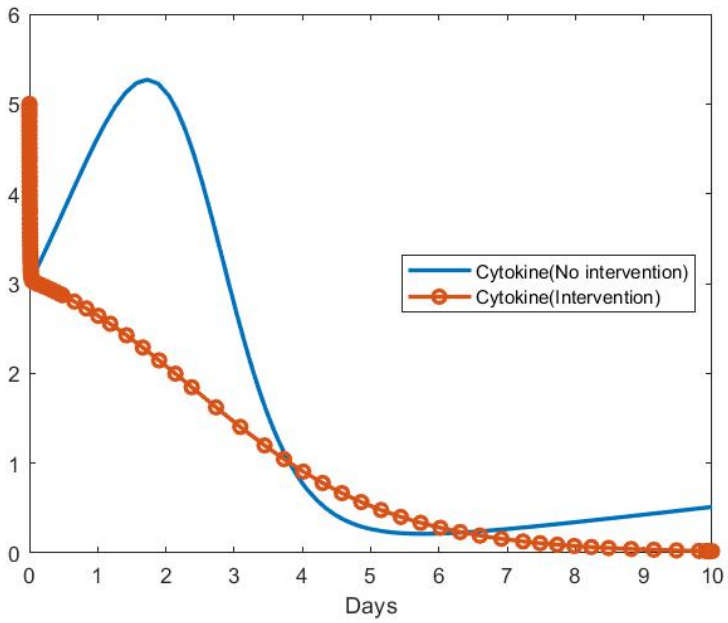

Figure 20: Numerical solutions of model system showing progression of cytokines with effects of second stage drug.

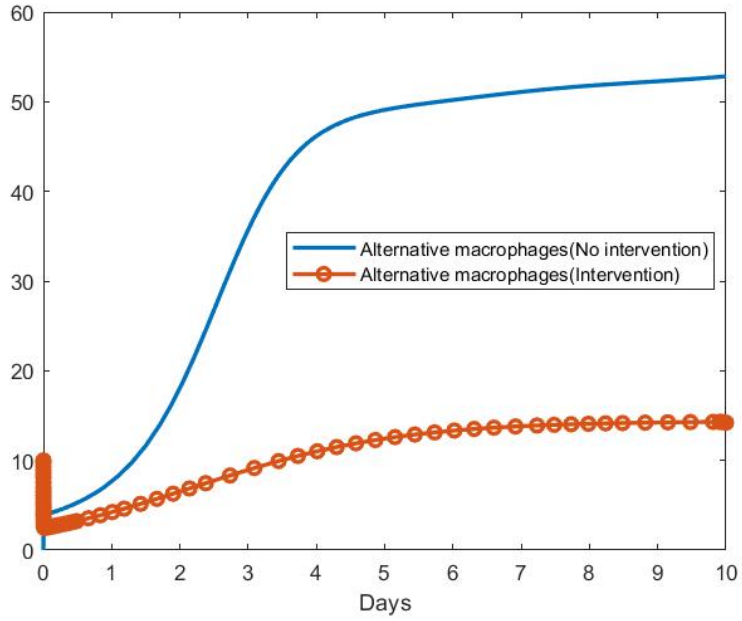

Figure 21: Numerical solutions of model system showing progression of alternative activated macrophages with effects of second stage drug.

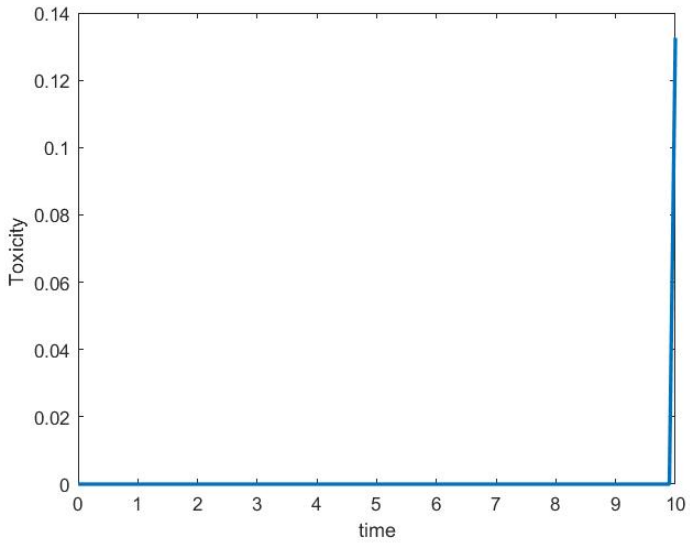

Figure 22: Numerical solutions of model system showing progression of alternative activated macrophages with effects of second stage drug.

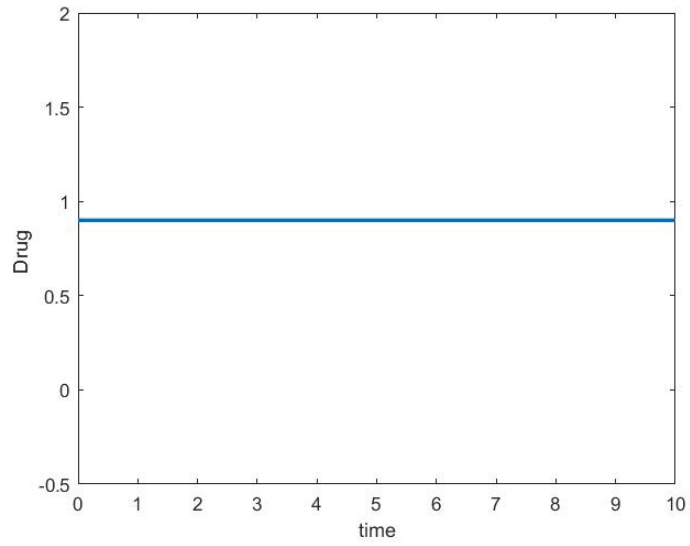

Figure 23: Numerical solutions of model system showing progression of alternative activated macrophages with effects of second stage drug.

the second parasite shows a decline over time in the presence of the second stage drug. In Figures 17, 18, and 21, we notice the drastic reduction in the macrophages, and that is due to the fact that the second stage drug is more toxic than the first stage drug.

From Figure 22, we notice the increase in the toxicity levels on the last day of treatment which explains drastic decline in the macrophages population. In this study we have discovered that for a drug to be efficient, the drug has to have an efficacy of 90% (see Figure 23). When a drug targets the population of the parasite at a given point it becomes difficult to control the parasite hence the rise on parasite type 2 still exist. In reality the parasite switches to multiple types of parasites, and in this paper we investigate using two types of parasites that.

6 Conclusion

The purpose of this study was to model and analyse the microscopic dynamics of the HAT disease within the human host. We obtained a system of six ordinary differential equations describing the switching of the parasite type 1 to type 2 and its interactions with various immune cells. There exist solutions to our system; the solutions are unique and positive. We performed a qualitative analysis of the system, and the analysis revealed the existence of one disease-free equilibrium state and two endemic equilibrium states. In addition, we carred out a stability analysis of the three equilibria using the Gershgorian circle theorem and van den Driessche and Watmough's method, and we established conditions of existence and stability of equilibrium states.

Furthermore, to investigate if the switching of the parasite from one type to the other helps the disease to persist within the host, numerical solutions of the system under consideration are presented. Figures 2, 3, and 4 show the solutions of the system of equations (1)–(6) without parasite switching. It can clearly be seen that in the absence of switching, the immune cells are able to clear the parasite from the body.

We then incorporate parasite switching in the system of equations (1)–(6). It can be observed in Figure 5 that the parasite evades the immune system even though an adaptive immune response is initiated through alternative activated macrophages, in order to deal with the new parasite type. A single switch reveals that the body is overwhelmed by the parasite load. This is indicated by the sharp increase in parasite type 2 after a few days of infection Figure 5, as well as the increase in alternative activated macrophages Figure 7. Naive and classical macrophages are part of the innate immune system, while alternatively activated macrophages are produced when the innate system fails to fight parasites.

In the effort of clearing the parasite from the host, two optimal control models are introduced. The first controlled model shows cases of all possible HAT treatments that focus on the invasion of the parasite. This example is the case of Pentamidine, Suramin. These drugs specifically kill the parasite in the blood system. In the effort to find the optimal drug dosage and at the same time reduce the toxicity of the drug, our performance measure focuses on reducing the parasite load and finding the optimal final time. The controlled model is simulated numerically and presented in Figures 9–14. It can be observed that, even though the parasites load is reduced, this type of drugs are not efficient in curing the disease due to parasite switching. It was found that the drug steers the system from the co-existing parasites states to only the parasite type 2, the endemic state, considering that in this work the parasite only switches to one other parasite type, when in reality the parasite switches to thousand different types. Furthermore, we observe a decline in macrophages, suggesting that drug toxicity is the influencing factor in reducing macrophage load with time.

The second optimal control model include treatments of HAT that specifically targets the reproduction of the parasites within the host. This example, is the case of Melarsoprol, Eflornithine, and Fexinidazole. The numerical results show that these type of drugs are quite efficient in the treatment of HAT, and more adopted to deal with the switching of the parasite of other types (see Figures 16–21). The numerical solutions confirm that there is a possibility of achieving total elimination of the HAT disease when using a growth inhibitor drug.

References

Artzrouni, M. and J. P. Gouteux (1996). A compartmental model of sleeping sickness in central Africa. *Journal of Biological Systems 4*(04), 459–477. 208

Baral, T. N. (2010). Immunobiology of African trypanosomes: need of alternative interventions. *BioMed Research International*, Article ID 389153. doi: 10.1155/2010/389153. 209

Bejarano, D. A. O., E. Ibargüen-Mondragón, and E. A. Gómez-Hernández (2018). A stability test for non linear systems of ordinary differential equations based on the Gershgorin circles. *Contemporary Engineering Sciences 11*(91), 4541–4548. 215

De Pellis, L. G. and A. Radunskaya (2000). A mathematical tumor model with immune resistance and drug therapy: an optimal control approach. *Journal of Theoretical Medicine 3*, 79–100. 221

Etchegorry, M. G., J. P. Helenport, B. Pecoul, J. Jannin, and D. Legros (2001). Availability and affordability of treatment for human African trypanosomiasis. *Tropical Medicine & International Health 6*(11), 957–959. 216, 226

Frank, S. A. (1999). A model for the sequential dominance of antigenic variants in African trypanosome infections. *Proceedings of the Royal Society of London. Series B: Biological Sciences 266*(1426), 1397–1401. 208, 209, 217

Gervas, H. E., N. K.-D. O. Opoku, S. Ibrahim (2018). Mathematical modelling of human African trypanosomiasis using control measures. *Computational and Mathematical Methods in Medicine*, Article ID 5293568. doi: 10.1155/2018/5293568. 208

Mhlanga, J. D., M. Bentivoglio, and K. Kristensson (1997). Neurobiology of cerebral malaria and African sleeping sickness. *Brain Tesearch Bulletin 44*(5), 579–589. 216

Mohamed, C. C., A. Eladdadi, and K. Mokni (2018). Activation of the immune response by cytokines and its effect on tumour cells. *Letters in Biomathematics 5*(2), S178–S200. 217

Navarrete, D. J. (2019). Parasites, clocks, and immunity: a within-host mathematical model of human African trypanosomiasis [Doctoral dissertation, Princeton University]. *Princeton University Senior Theses*, http://arks.princeton.edu/ark:/88435/dsp01ng451m33x. 208

Ndondo, A. M., J. M. W. Munganga, J. N. Mwambakana, C. M. Saad-Roy, P. Van den Driessche, and R. O. Walo (2016). Analysis of a model of gambiense sleeping sickness in humans and cattle. *Journal of Biological Dynamics 10*(1), 347–365. 208

Pienaar, E. and M. Lerm (2014). A mathematical model of the initial interaction between Mycobacterium tuberculosis and macrophages. *Journal of Theoretical Biology 342*, 23–32. 217

Pontryagin, L. S., V. G. Boltyanskii, R. V. Gamkrelize, and E. F. Mishchenko (1986). *The Mathematical Theory of Optimal Processes*. John Wiley & Sons, New York. 221, 227

Rock, K. S., C. M. Stone, I. M. Hastings , M. J. Keeling, S. J. Torr, and N. Chitnis (2015). Mathematical models of human African trypanosomiasis epidemiology. *Advances in Parasitology 87*, 53–133. 208

Rogers, D. J. (1988). A general model for the African trypanosomiases. *Parasitology 97*(1), 193–212. 207, 208

Rőszer, T. (2015). Understanding the mysterious M2 macrophage through activation markers and effector mechanisms. *Mediators of Inflammation*, Article ID 816460. doi: 10.1155/2015/816460. 209

Thieme, H. R. (1948). *Mathematics in Population Biology*. Princeton University Press. 211

Turner, M. D., B. Nedjai, T. Hurst, D. J. Pennington (2014). Cytokines and chemokines: at the crossroads of cell signalling and inflammatory disease. *Biochimica et Biophysica Acta (BBA)-Molecular Cell Research 1843*(11), 2563–2582. 208

Uniting to Combat Neglected Tropical Disease (2019). https://unitingtocombatntds.org/ntds/human-african-trypanosomiasis. 207

Wamwiri, F. N., G. Nkwengulila, and P. H. Clausen (2007). Hosts of Glossina fuscipes fuscipes and G. pallidipes in areas of western Kenya with endemic sleeping sickness, as determined using an egg-yolk (IgY) ELISA. *Annals of Tropical Medicine and Parasitology 101*(3), 225–232. 207

Wockner, L. F., I. Hoffmann, L. Webb, B. Mordmüller, S. C. Murphy, J. G. Kublin, P. O'Rourke, J. S. McCarthy, and L. Marquart (2020). Growth rate of Plasmodium falciparum: analysis of parasite growth data from malaria volunteer infection studies. *The Journal of Infectious Diseases 221*(6), 963–972. 217

World Health Organisation (2019). https://unitingtocombatntds.org/en/neglected-tropical-diseases/disease-directory/Sleeping-sickness/. 207

Zhang, J.M., and J. An (2007). Cytokines, inflammation and pain. *International Anesthesiology Clinics 45*(2), 27. 208

Chapter 3

Control analysis of sleeping sickness under the implementation of specific treatment and vector trapping

---

[1] In this chapter we explore the dynamics of a mathematical model involving three species in the context of Human African Trypanosomiasis (HAT) disease. We aimed to identify an effective control strategy for minimizing the disease burden. This study involved utilizing stage-specific treatment and vector trapping as control measures. The chapter encompasses detailed mathematical model analysis, including stability analysis.

Furthermore, we employed bifurcation analysis to determine the crucial parameters influencing the stability of the equilibrium points. A comparative analysis was conducted between scenarios with and without control measures. By doing so, we could assess the impact of control measures on the population dynamics of the model.

The effectiveness of the controls was notably pronounced given the control strategy presented, primarily attributed to treating control measures as time-dependent variables. This strategic approach gave a comprehensive understanding of the dynamics, providing valuable insights into controlling HAT disease.

[1]The work in this chapter has been presented as a poster at an international conference called Epidemics in Bologna, Italy.

ARTICLE TEMPLATE

Control analysis of sleeping sickness under the implementation of specific treatment and vector trapping

M. Makhuvha[a,b,c] and H. Mambili-Mamboundou[a]

[a] University of Kwazulu-Natal, South Africa; [b]DSI-NRF Centre of Excellence in Mathematical and Statistical Sciences (CoE-MaSS), South Africa, [c] Nelson Mandela University, South Africa

ARTICLE HISTORY
Compiled July 7, 2024

ABSTRACT
Sleeping sickness is a neglected tropical vector disease, also called Human African Trypanosomiasis (HAT). The disease continues to be a problem because it can infect multiple hosts. When multiple hosts are present, sleeping sickness is more likely to spread and persist in a community. According to the World Health Organization (WHO), depleting parasites within infected hosts is crucial. Humans, non-human animal, and tsetse flies are reservoirs for HAT disease. In this paper, we construct and analyze a three-species epidemiological mathematical model to explore disease dynamics that incorporates the role of stage-specific treatment and vector disease trapping. Human disease transmission is divided into five compartments. There are two compartments in the disease model for each population of the Tsetse fly and non-human animal reservoir. The model's mathematical properties were explored. An effective reproductive number was used to establish equilibrium points and stability conditions. The bifurcation analysis revealed that having $R_e < 1$ does not guarantee the eradication of HAT disease. In the sensitivity analysis, the biting rate was the most sensitive variable. The optimal control model was developed by applying Pontragin's maximum principle to understand the control strategy. We recommend that the control measures be used concurrently to achieve optimal time for disease interruption, with vector control implemented for a more extended period.

KEYWORDS
Human African Trypanosomiasis; vector-borne; equilibrium points; sensitivity analysis; control analysis

1. Introduction

Sub-Saharan Africa harbors one of the neglected vector-borne diseases known as sleeping sickness, or human African trypanosomiasis (HAT) [1]. Besides being transmitted through tsetse fly bites, suspicions of sexual and maternal transmission of HAT have been noted [2]. This disease poses a threat to humans, domestic animals, and wildlife animals [3]. In humans, sleeping sickness is either caused by *Trypanosoma Brucie Gambiense* or *Trypanosoma Brucie Rhodesiense* parasites, with *T.b. Gambiense* accounting for 80% of reported cases [2]. African Animal Trypanosomiasis, affecting domesticated and wild animals, is caused by *Trypanosoma Brucie Vivax*, *Trypanosoma Brucie Congolense*, and *T.b. Rhodesinse*.

CONTACT M. Makhuvha. Email: makhubamulalo@gmail.com

In addition to eliminating sleeping sickness by 2030, WHO aims to reduce the number of cases to fewer than 10,000 each year [5]. The CDC estimates that 65 million people in sub-Saharan Africa are at risk of infection [4]. Despite a near-elimination in 1960, HAT resurged following an unplanned intervention interruption. The COVID-19 outbreak raised concerns about a potential resurgence of HAT disease in endemic areas [6]. Some countries, including Benin, Burkina Faso, Ghana, Mali, Nigeria, Togo, and Côte dÍvoire, have reached the elimination stage [5]. Recently, WHO declared the eradication of the disease in Côte dÍvoire, while *T.b. gambiense* cases are predominant in the Democratic Republic of Congo (DRC), Angola, Chad, the Central African Republic, Gabon, Guinea, Congo, and South Sudan, with the DRC reporting the majority of cases [5].

The HAT disease manifests in two stages: the haemolymphatic phase and the meningoencephalitic phase. Symptoms of the first stage are nonspecific and include headaches, fatigue, weight loss, and fever, while second-stage symptoms include sleep disturbances, mental confusion, and psychiatric disorders. There is a challenge in most countries in reporting accurate information about HAT disease since, if left untreated, it can cause death.

Despite its complexity, African Trypanosomiasis has been extensively researched. Disease transmission is difficult to capture due to the possibility of different hosts, which allows parasites to live in other host populations. Rodgers' model, a prominent and general mathematical model for HAT transmission, integrates two vertebrate hosts and vector species [7]. The model was used to investigate the role of an animal reservoir in HAT disease progression dynamics, and it suggests that domestic animals play a crucial role in maintaining the disease, emphasizing the limitations of relying solely on human surveillance and treatment campaigns [7]. In addition, [8] argued that introducing animals as hosts may reduce human bites, but it was not the first time animals were introduced as hosts.

Several studies have investigated the animal reservoir and its effects over the years, such as [9], [10], [11], [12], [13], and [14], also further investigate the impact of interventions, such as treatment, education, and vector trapping, on HAT transmission. Notably, [9] proposes a three-species model emphasizing the combined impact of treatment, education, and vector trapping. Combining the three interventions has a significant impact and should be applied concurrently in endemic areas.

[14] presented a mathematical model incorporating three hosts, tsetse flies, humans, and cattle, that considers the development of tsetse flies from larval to adult stages. As a result of the model, critical parameters for control strategy were suggested, and it was found that HAT disease could be prevented by controlling the tsetse flies [14]. Similar to [14], [10] proposed a mathematical model incorporating the three hosts. As opposed to [14], this model evaluated cattle treatment for sleeping sickness in Uganda. A study demonstrated that insecticides are effective at controlling the disease. In addition, [15] also presented a species mathematical model incorporating awareness campaigns and insecticides as control measures. The role of awareness and insecticides in controlling disease was found to be both important and insecticide control had a more significant impact on preventing disease spread than awareness alone. Understanding the effects of intervention strategies on disease transmission is crucial to effectively control the disease. In 2018, [11] introduced a three-species mathematical model incorporating education, treatment, and insecticides, confirming their effectiveness in disease elimination through numerical simulations.

Over the years, diverse control measures have been employed, including passive and

active screening, treatment, and vector control. Screening identifies disease stages, and treatment varies based on stage. Common treatments include *Suramin* and *Pentamidine* for the initial stage, and *Melarsoprol* and *nifurtimox-eflornithine (NECT)* for the second stage. Vector control involves using pyramid-shaped traps made from black and blue cloth, suspended from trees and bushes near water sources, to monitor and control tsetse flies.

Research into HAT disease has led to the development of models capturing transmission between vectors, humans, and animals. This study incorporates control measures to explore transmission dynamics in the presence of interventions. Subsequently, optimal control theory will be employed to assess the effects of stage-specific treatment and vector trapping on HAT disease. These findings aim to contribute to a comprehensive understanding of effective HAT disease control through interventions.

2. Model formulation

In this section, we describe the transmission of HAT disease from humans to tsetse flies and from animals to tsetse flies and vice versa. Transmission in the human population is classified as susceptible S_H, exposed E_H, stage 1 infected I_1, stage 2 infected I_2, and treated R_H. The total human population, N_H, is defined by

$$N_H = S_H + E_H + I_1 + I_2 + R_H.$$

The transmission in the animal population is subdivided into susceptible S_N and infected I_N. The total animal reservoir population, N_N, is defined by

$$N_N = S_N + I_N.$$

Transmission in the vector population is subdivided into susceptible S_V and infected I_V. The total vector population, N_V, is defined by

$$N_V = S_V + I_V.$$

The recruitment rates are constant due to birth, with the recruitment rates for humans, animals, and vectors being π_H, π_N, and π_V, respectively. By being bitten by an infectious tsetse, the susceptible host becomes infected. A susceptible vector becomes infected when it bites an infected host. Natural death rates for human, animal, and vector populations are μ_H, μ_N, and μ_V, respectively.

The force of infection for humans is defined by

$$\lambda_H = \frac{b\beta_{VH} I_V}{N_V},$$

where b is the tsetse fly biting rate and β_{VH} is the probability that a bite on an infectious vector infects a susceptible human. The force of infection for non-humans is defined by

$$\lambda_N = \frac{b\beta_{VN} I_V}{N_V},$$

where β_{VN} is the probability that an infectious tsetse fly infects a non-human reservoir. The force of infection for vectors is defined by

$$\lambda_v = b\beta_{HV}\frac{(I_1 + I_2)}{N_H} + b\beta_{NV}\frac{I_N}{N_N},$$

where β_{HV} is the probability that a bite on an infected human infects a susceptible tsetse fly, and β_{NV} is the probability that a bite on an infected non-human reservoir infects the susceptible tsetse fly. The parameter σ_H represents the rate at which exposed individuals become infectious.

Infected individuals are divided into two groups based on their stage of infection because treatment varies by stage. Case detection is a crucial fundamental element for all HAT control programs [5] because treatment depends on the individual's stage. The suspected individuals undergo screening, leading to a stage 1 or stage 2 infection diagnosis. The probability of correct disease stage classification is given by γ_1, γ_2, respectively [11].

The parameter α_H represents the rate at which the disease progresses from stage 1 to stage 2. Assuming that infected individuals seek treatment, the likelihood of treatment success at stage 1 and stage 2 is u_1 and u_2, respectively. Therefore, the human population has a recovering rate δ_H; later, individuals lose their temporal immunity and become susceptible again. The disease-induced rates for humans and animal reservoirs are η_H and η_n, respectively. We assume vector trapping is applied at a rate of u_3 to reduce the vector population.

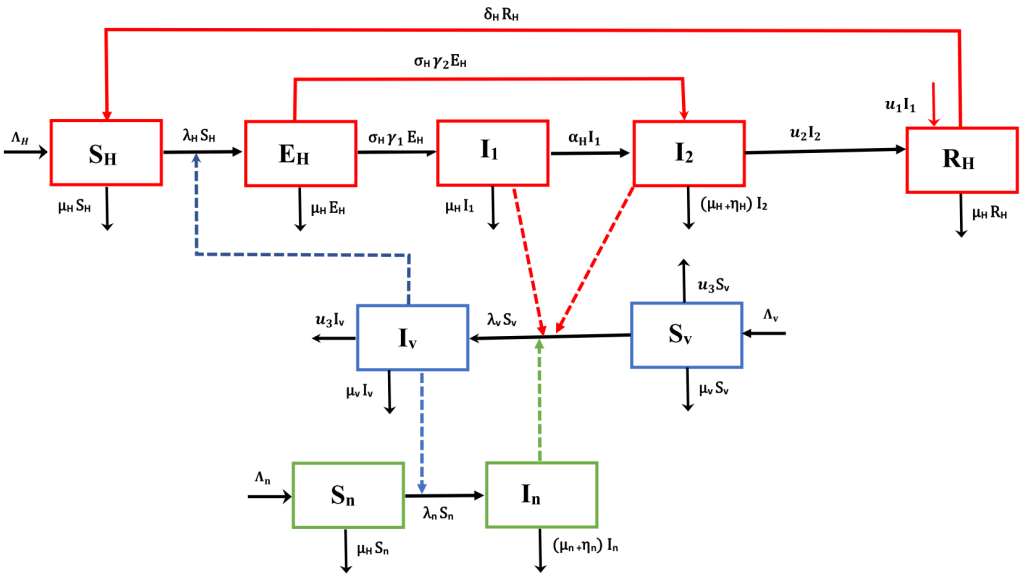

Figure 1. Compartmental model for Human African trypanosomiasis with three intervention strategies.

From the relations described in Figure 1 the following model is derived

$$\begin{cases} \frac{dS_H}{dt} &= \pi_H N_H - \lambda_H S_H + \delta_H R_H - \mu_H S_H, \\ \frac{dE_H}{dt} &= \lambda_H S_H - \sigma_H \gamma_1 E_H - \sigma_H \gamma_2 E_H - \mu_H E_H, \\ \frac{dI_1}{dt} &= \sigma_H \gamma_1 E_H - u_1 I_1 - \alpha_H I_1 - \mu_H I_1, \\ \frac{dI_2}{dt} &= \alpha_H I_1 + \sigma_H \gamma_2 E_H - \epsilon_2 I_2 - (\mu_H + \eta_H) I_2, \\ \frac{dR_H}{dt} &= u_2 I_2 + u_1 I_1 - \delta_H R_H - \mu_H R_H, \\ \frac{dS_N}{dt} &= \pi_N N_N - \lambda_N S_N - \mu_N S_N, \\ \frac{dI_N}{dt} &= \lambda_N S_N - \eta_N I_N - \mu_N I_N, \\ \frac{dS_V}{dt} &= \pi_V N_V - \lambda_V S_V - u_3 S_V - \mu_V S_V, \\ \frac{dI_V}{dt} &= \lambda_V S_V - u_3 I_V - \mu_V I_v. \end{cases} \quad (1)$$

Table 1 and Table 2 summarize the definitions of all the variables and the associated parameters.

We determine an equivalent model by using the dimensionless techniques yields the following model,

$$\begin{cases} \frac{ds_h}{dt} &= \pi_h - b\beta_{vh} i_v s_h + \delta_h r_h - \mu_h s_h, \\ \frac{de_h}{dt} &= b\beta_{vh} i_v s_h - \sigma_h \gamma_1 e_h - \sigma_h \gamma_2 e_h - \mu_h e_h, \\ \frac{di_1}{dt} &= \sigma_h \gamma_1 e_h - u_1 i_1 - \alpha_h i_1 - \mu_h i_1, \\ \frac{di_2}{dt} &= \alpha_h i_1 + \sigma_h \gamma_2 e_h - u_2 i_2 - (\mu_h + \eta_h) i_2, \\ \frac{dr_h}{dt} &= u_2 i_2 + u_1 i_1 - \delta_h r_h - \mu_h r_h, \\ \frac{ds_n}{dt} &= \pi_n - b\beta_{vn} i_v s_n - \mu_n s_n, \\ \frac{di_n}{dt} &= b\beta_{vn} i_v s_n - \eta_n i_n - \mu_n i_n, \\ \frac{ds_v}{dt} &= \pi_v - b\beta_{hv} s_v (i_1 + i_2) - b\beta_{nv} s_v i_n - u_3 s_v - \mu_v s_v, \\ \frac{di_v}{dt} &= b\beta_{hv} s_v (i_1 + i_2) + b\beta_{nv} s_v i_n - u_3 i_v - \mu_v i_v. \end{cases} \quad (2)$$

Table 1. Parameter values of the model.

Parameter	description	Range	Unit	Source
π_h	Recruitment rate for human population	0.000215 [2.15-2.365]$\times 10^{-4}$	day^{-1}	[11] Assumed
π_n	Recruitment rate for animal population	0.0001 [1-1.1]$\times 10^{-4}$	day^{-1}	Assumed
π_v	Recruitment rate for vector population	0.0505	day^{-1}	[24]
b	Vector biting rate	0.333 [0.2-0.5]	day^{-1}	[25]
η_h	Human disease-induced rate	0.002 [0.0029-0.013]	day^{-1}	[27]
β_{vh}	Proportion of bites by infectious vector on susceptible human population	0.62 [0.558-0.682]	—	[7]
δ_h	Human immunity waning rate	0.006 [0.001-0.01]	day^{-1}	[25]
μ_h	Human natural death rate	0.000046 [4.2-5.475]$\times 10^{-5}$	day^{-1}	[12]
σ_h	Human incubation rate	0.0833 [0.00093-0.0833]	day^{-1}	[7]
γ_1	Probability of correct classification in stage 1	0.66 [0.66-0.70]	—	[1]
γ_2	Probability of correct classification in stage 2	0.95 [0.93-0.95]	—	[1]
α_h	Disease progression rate	0.0019 [0.001-0.003]	day^{-1}	[25]
u_1	Efficacy stage 1 treatment (pentamidine)	0.94	—	[12]
u_2	Efficacy Stage 2 treatment (nifurtimox-eflornithine)	0.96	—	[23], [12]
η_n	Animal reservoir disease-induced rate	0.0006 [5.4-6.6]$\times 10^{-4}$	day^{-1}	Assumed
β_{vn}	Proportion of bites by infectious vector on animal reservoir population	0.62 [0.558-0.682]	—	[7]
μ_n	Animal reservoir natural death rate	0.0014 [1.4-1.54]$\times 10^{-3}$	day^{-1}	[28]
β_{hv}	Proportion of bites by susceptible vector on infectious human	0.065	—	[7]
β_{nv}	Proportion of bites by susceptible vector on infectious human	0.065	—	[7]
μ_v	Vector natural death rate	0.033 [0.03-0.16]	day^{-1}	[13]
u_3	Vector trapping rate	0.25 [0.04-0.25]	day^{-1}	Assumed

3. Model analysis

This section shows that the model system (2) has unique and positive solutions when initial conditions are non-negative. We must also show that the model is bounded, well-posed, and biologically meaningful for all $t \geq 0$.

3.1. Positivity, uniqueness, and boundedness of solutions

Lemma 3.1 (Positivity of solutions)**.** *Let the non-negative initial conditions be* $\big(s_h(0) \geq 0, e_h(0) \geq 0, i_1(0) \geq 0, i_2(0) \geq 0, r_h(0) \geq 0, s_n(0) \geq 0, i_n(0) \geq 0, s_v(0) \geq 0, i_v(0) \geq 0\big) \in \mathbb{R}^9_+$*, then all solutions of the model system (2) are positive for all* $t > 0$ *and non-negative for all* t *such that all positive solutions satisfy* $\big(s_h(t), e_h(t), i_2(t), i_2(t), r_h(t), s_n(t), i_n(t), s_v(t), i_v(t)\big)$ *for all large* t*.*

Table 2. Description of the state variables of the model.

Variables	Description
s_h	Susceptible human population
λ_h	Human force of infection
e_h	Exposed population
i_1	Stage 1 infected population
i_2	Stage 2 infected population
r_h	Treated population
λ_n	Animal reservoir force of infection
s_n	Susceptible animal reservoir population
i_n	Infected animal reservoir population
λ_v	Vector force of infection
s_v	Susceptible vector population
i_v	Infected vector population

From model system (2), we have the first equation as

$$\frac{ds_h}{dt} = \pi_h - b\beta_{vh} i_v s_h + \delta_h r_h - \mu_h s_h.$$

We then obtain the inequality to be

$$\frac{ds_h}{dt} \geq \pi_h - b\beta_{vh} i_v s_h - \mu_h s_h.$$

The inequality can be expressed as

$$\frac{ds_h}{dt} + (b\beta_{vh} i_v + \mu_h) s_h \geq \pi_h.$$

The integrating factor I is given by

$$I = \exp\left\{\mu_h t + \int_0^t b\beta_{vh} i_v(s) ds\right\}.$$

We then multiply the inequality by the integrating factor

$$\frac{d}{dt}\left[s_h \exp\left\{\mu_h t + \int_0^t b\beta_{vh} i_v(s) ds\right\}\right] \geq \pi_h \exp\left\{\mu_h t + \int_0^t b\beta_{vh} i_v(s) ds\right\}.$$

Integrate the above expression

$$\int_o^t \frac{d}{dt}\left[s_h \exp\left\{\mu_h t + \int_0^t b\beta_{vh} i_v(s) ds\right\}\right] \geq \int_o^t \pi_h \exp\left\{\mu_h t + \int_0^t b\beta_{vh} i_v(s) ds\right\}.$$

Solving the above inequality, we get

$$s_h(t)\exp\left\{\mu_h t+\int_0^t b\beta_{vh}i_v(s)ds\right\}-s_h(0)\geq\int_o^t\pi_h\exp\left\{\mu_h\upsilon+\int_0^\upsilon b\beta_{vh}i_v(q)dq\right\}d\upsilon.$$

Therefore,

$$\begin{aligned}s_h(t) &\geq s_h(0)\exp\left\{-\left(\mu_h t+\int_0^t b\beta_{vh}i_v(q)dq\right)\right\}+\exp\left\{-\left(\mu_h t+\int_0^t b\beta_{vh}i_v(q)dq\right)\right\}\times\\ &\int_o^t\pi_h\exp\left\{\mu_h\upsilon+\int_0^\upsilon b\beta_{vh}i_v(q)dq\right\}d\upsilon>0.\end{aligned}$$

Similarly, we obtain

$$\begin{aligned}i_2(t) &\geq e^{-(u_2+\mu_h+\eta_h)t}\left[i_2(0)+\alpha_h\int_0^t i_1e^{(u_2+\mu_h+\eta_h)t}dt\right],\\ r_h(t) &\geq e^{-(\delta_h+\mu_h)t}\left[r_h(0)+\epsilon_2\int_0^t i_2e^{(\delta_h+\mu_h)t}dt\right].\end{aligned}$$

From the model system (2), we have the second equation given by

$$\frac{de_h}{dt} = b\beta_{vh}i_vs_h-\sigma_h\gamma_1e_h-\sigma_h\gamma_2e_h-\mu_he_h.$$

We then have the inequality given by

$$\begin{aligned}\frac{de_h}{dt} &\geq -\sigma_h\gamma_1e_h-\sigma_h\gamma_2e_h-\mu_he_h,\\ \frac{de_h}{dt} &\geq -(\sigma_h\gamma_1+\sigma_h\gamma_2+\mu_h)e_h.\end{aligned}$$

We separate the variables to obtain

$$\frac{de_h}{e_h}\geq-(\sigma_h\gamma_1+\sigma_h\gamma_2+\mu_h)dt.$$

Solving the above inequality, we therefore obtain

$$e_h(t)\geq e_h(0)e^{-(\sigma_h\gamma_1+\sigma_h\gamma_2+\mu_h)t}.$$

Similarly, we obtain the following expressions

$$\begin{aligned}
i_1(t) &\geq i_1(0)e^{-(u_1+\alpha_h+\mu_h)t},\\
s_n(t) &\geq s_n(0)\exp\left\{-\left(\mu_n t+\int_0^t b\beta_{vn}i_v(s)ds\right)\right\},\\
i_n(t) &\geq i_n(0)e^{-(\eta_n+\mu_n)t},\\
s_v(t) &\geq s_v(0)\exp\left\{-\left((u_3+\mu_v)t+\int_0^t b\beta_{hv}s_v(s)ds\right)\right\},\\
i_v(t) &\geq i_v(0)e^{-(u_3+\mu_v)t}.
\end{aligned}$$

Therefore, we conclude that the solutions $s_h(t), e_h(t), i_1(t), i_2(t), r_h(t), s_n(t), i_n(t), s_v(t), i_v(t)$ are all positive when $t > 0$.

Lemma 3.2 (Uniqueness of solutions)**.** *Let $G : \mathbb{R}_+^{n+1} \to \mathbb{R}_+^n$ be a Lipschitz function satisfying $G_i(t, z)$ for $(t, z) \in \mathbb{R}_+ \times \mathbb{R}_+^n$. Then for every $z_0 \in \mathbb{R}_+^n$, the solution to $\frac{dz}{dt} = G(t, z), Z(0) = Z_0$ is defined on $[0, c), c > 0$ and is unique and exists with values in $\mathbb{R}_+^n$ [18].*

To show the uniqueness of the solutions of the model system we use Lemma 3.2 called Theorem A.4 in [18]. We set the equations as follows

$$\begin{aligned}
G_1(s_h, e_h, i_1, i_2, r_h, s_n, i_n, s_v, i_v) &= g_1,\\
G_2(s_h, e_h, i_1, i_2, r_h, s_n, i_n, s_v, i_v) &= g_2,\\
G_3(s_h, e_h, i_1, i_2, r_h, s_n, i_n, s_v, i_v) &= g_3,\\
G_4(s_h, e_h, i_1, i_2, r_h, s_n, i_n, s_v, i_v) &= g_4,\\
G_5(s_h, e_h, i_1, i_2, r_h, s_n, i_n, s_v, i_v) &= g_5,\\
G_6(s_h, e_h, i_1, i_2, r_h, s_n, i_n, s_v, i_v) &= g_6,\\
G_7(s_h, e_h, i_1, i_2, r_h, s_n, i_n, s_v, i_v) &= g_7,\\
G_8(s_h, e_h, i_1, i_2, r_h, s_n, i_n, s_v, i_v) &= g_8,\\
G_9(s_h, e_h, i_1, i_2, r_h, s_n, i_n, s_v, i_v) &= g_9,
\end{aligned}$$

where, g_i, $i = 1, \cdots, 9$ are the right-hand sides of the model system (2), respectively.

We have the following

$$\begin{aligned}
G_1(0, e_h, i_1, i_2, r_h, s_n, i_n, s_v, i_v) &= \pi_h + \delta_h r_h \geq 0,\\
G_2(s_h, 0, i_1, i_2, r_h, s_n, i_n, s_v, i_v) &= b\beta_{vh} i_v s_h \geq 0,\\
G_3(s_h, e_h, 0, i_2, r_h, s_n, i_n, s_v, i_v) &= \sigma_h \gamma_1 e_h \geq 0,\\
G_4(s_h, e_h, i_1, 0, r_h, s_n, i_n, s_v, i_v) &= \alpha_h i_1 + \sigma_h \gamma_2 e_h \geq 0,\\
G_5(s_h, e_h, i_1, i_2, 0, s_n, i_n, s_v, i_v) &= u_2 i_2 + u_1 i_1 \geq 0,\\
G_6(s_h, e_h, i_1, i_2, r_h, 0, i_n, s_v, i_v) &= \pi_n \geq 0,\\
G_7(s_h, e_h, i_1, i_2, r_h, s_n, 0, s_v, i_v) &= b\beta_{vn} i_v s_n \geq 0,\\
G_8(s_h, e_h, i_1, i_2, r_h, s_n, i_n, 0, i_v) &= \pi_v \geq 0,\\
G_9(s_h, e_h, i_1, i_2, r_h, s_n, i_n, s_v, 0) &= b\beta_{hv}(i_1 + i_2) s_v + b\beta_{nv} i_n s_v \geq 0,
\end{aligned}$$

We can further define $G(t, z) = G(t_+, z_+)$ where $t_+ = max\{t, 0\}$ and $z_+ = (z_1, z_2, z_3, z_4, z_5, z_6, z_7, z_8, z_9)$ are positive parts of the scalar t and vector z. We can check that $\|z_+ - y_+\| \leq \|z - y\|$ for any of the usual norms on $\mathbb{R}^n$. Hence G is a locally Lipschitz continuous vector field on $\mathbb{R}^9$ satisfies $G_i(t, z) \geq 0$ for all $t \in \mathbb{R}, x \in \mathbb{R}^9_+, z_i = 0$. According to Lemma 3.2, the equations in model system (2) have unique and positive solutions for initial conditions $s_h(0), e_h(0), i_1(0), i_2(0), r_h(0), s_n(0), i_n(0), s_v(0), i_v(0) \in \mathbb{R}^9_+$.

Lemma 3.3 (Feasible Region)**.** *Let the feasible region for the three species be* $\Omega = \Omega_h \cup \Omega_n \cup \Omega_v \in \mathbb{R}^5_+ \times \mathbb{R}^2_+ \times \mathbb{R}^2_+$, *where* $\Omega_h = \left\{s_h, e_h, i_1, i_2, r_h \in \mathbb{R}^4_+ = n_h \leq \frac{\pi_h}{\mu_h}\right\}$, $\Omega_n = \left\{s_n, i_n \in \mathbb{R}^2_+ = n_n \leq \frac{\pi_n}{\mu_n}\right\}$, $\Omega_v = \left\{s_v, i_v \in \mathbb{R}^2_+ = n_v \leq \frac{\pi_v}{\mu_v}\right\}$.

To prove the feasible region, we use the model (2) to compute the total number of human population, non-human reservoir population and vector population.

$$\frac{dn_h}{dt} = \pi_h - \eta_h i_2 - \mu_h n_h, \qquad \frac{dn_h}{dt} \leq \pi_h - \mu_h n_h, \tag{3}$$

$$\frac{dn_n}{dt} = \pi_n - \eta_n i_n - \mu_n n_n, \qquad \frac{dn_n}{dt} \leq \pi_n - \mu_n n_n, \tag{4}$$

$$\frac{dn_v}{dt} = \pi_v - u_3 n_v - \mu_v n_v, \qquad \frac{dn_v}{dt} \leq \pi_v - \mu_v n_v. \tag{5}$$

By solving equation (3)-(5) we then get the following inequalities

$$n_h(t) \leq \frac{\pi_h}{\mu_h} - \Big(\frac{\pi_h - \mu_h n_h(0)}{\mu_h}\Big) e^{-\mu_h t}, \tag{6}$$

$$n_n(t) \leq \frac{\pi_n}{\mu_n} - \Big(\frac{\pi_n - \mu_n n_n(0)}{\mu_n}\Big) e^{-\mu_n t}, \tag{7}$$

$$n_v(t) \leq \frac{\pi_v}{\mu_v} - \Big(\frac{\pi_v - \mu_v n_v(0)}{\mu_v}\Big) e^{-\mu_v t}. \tag{8}$$

Therefore,

$$\lim_{t\to\infty} \sup n_h(t) \leq \frac{\pi_h}{\mu_h}, \tag{9}$$

$$\lim_{t\to\infty} \sup n_n(t) \leq \frac{\pi_n}{\mu_n}, \tag{10}$$

$$\lim_{t\to\infty} \sup n_v(t) \leq \frac{\pi_v}{\mu_v}. \tag{11}$$

The region is therefore given by

$$\Omega_H = \{s_h, e_h, i_1, i_2, r_h \in \mathbb{R}^5_+ = n_h \leq \frac{\pi_h}{\mu_h}\}, \tag{12}$$

$$\Omega_n = \{s_n, i_n \in \mathbb{R}^2_+ = n_n \leq \frac{\pi_n}{\mu_n}\}, \tag{13}$$

$$\Omega_v = \{s_v, i_v \in \mathbb{R}^2_+ = n_v \leq \frac{\pi_v}{\mu_v}\}. \tag{14}$$

We can conclude that the region is bounded, biologically meaningful and well posed.

4. Model equilibrium analysis

In this section, we obtain the equilibrium points of the model system (2). Two equilibrium points exist for the model system (2): Disease-Free Equilibrium (DFE) and Endemic Equilibrium (EE). For each equilibrium point, we equate the right-hand side of the model system (2) equations to zero.

4.1. Disease Free Equilibrium (DFE)

The disease-free equilibrium point is when there is no disease in the population. The DFE state of the model (2) is given by

$$E_0 = \left(\frac{\pi_h}{\mu_h}, 0, 0, 0, 0, \frac{\pi_n}{\mu_n}, 0, \frac{\pi_v}{\psi + \mu_v}, 0\right). \tag{15}$$

4.2. Endemic Equilibrium (EE)

The endemic equilibrium point is a state when the disease persist in the population. The model system (2) has the endemic equilibrium point of the form

$$E_1 = (s^*_h, e^*_h, i^*_1, i^*_2, r^*_h, s^*_n, i^*_n, s^*_v, i^*_v), \tag{16}$$

with the expressions of $s_h^*, e_h^*, i_1^*, i_2^*, r_h^*, s_n^*, i_n^*, s_v^*, i_v^*$ given by

$$s_h^* = \frac{\pi_h f_1 f_2 f_3(\delta_h + \mu_h)}{f_1 f_2 f_3(\delta_h + \mu_h)(b\beta_{vh} i_v^* + \mu_h) - b\beta_{vh} i_v^* \sigma_h \delta_h f_4}, \tag{17}$$

$$e_h^* = \frac{b\beta_{vh}\pi_h f_2 f_3(\delta_h + \mu_h) i_v^*}{f_1 f_2 f_3(\delta_h + \mu_h)(b\beta_{vh} i_v^* + \mu_h) - b\beta_{vh} i_v^* \sigma_h \delta_h f_4}, \tag{18}$$

$$i_1^* = \frac{\sigma_h \gamma_1 b\beta_{vh}\pi_h f_3(\delta_h + \mu_h) i_v^*}{f_1 f_2 f_3(\delta_h + \mu_h)(b\beta_{vh} i_v^* + \mu_h) - b\beta_{vh} i_v^* \sigma_h \delta_h f_4}, \tag{19}$$

$$i_2^* = \frac{b\beta_{vh}\sigma_h \pi_h(\delta_h + \mu_h)(\alpha_h \gamma_1 + f_2\gamma_2) i_v^*}{f_1 f_2 f_3(\delta_h + \mu_h)(b\beta_{vh} i_v^* + \mu_h) - b\beta_{vh} i_v^* \sigma_h \delta_h f_4}, \tag{20}$$

$$r_h^* = \frac{b\beta_{vh}\sigma_h \pi_h f_4 i_v^*}{f_1 f_2 f_3(\delta_h + \mu_h)(b\beta_{vh} i_v^* + \mu_h) - b\beta_{vh} i_v^* \sigma_h \delta_h f_4}, \tag{21}$$

$$s_n^* = \frac{\pi_n}{b\beta_{vn} i_v^* + \mu_n}, \tag{22}$$

$$i_n^* = \frac{b\beta_{vn} i_v^* s_n^*}{(\eta_n + \mu_n)}, \tag{23}$$

$$s_v^* = \frac{\pi_v}{b\beta_{hv}(i_1^* + i_2^*) + b\beta_{nv} i_n^* + (u_3 + \mu_v)}, \tag{24}$$

$$i_v^* = \frac{b\beta_{hv}(i_1^* + i_2^*) s_v^* + b\beta_{nv} i_n^* s_v^*}{(u_3 + \mu_v)}, \tag{25}$$

where,

$$\begin{aligned} f_1 &= \sigma_h(\gamma_1 + \gamma_2) + \mu_h, \\ f_2 &= u_1 + \alpha_h + \mu_h, \\ f_3 &= u_2 + \eta_h + \mu_h, \\ f_4 &= \alpha_h \gamma_1 + \gamma_2 f_2 + f_3 \gamma_1. \end{aligned}$$

4.3. Effective Reproductive number R_e

An effective reproductive number R_e is a threshold determining the average number of secondary infections by a single infected host exposed to a susceptible population. We use the next-generation operator method [19] to determine the effective reproductive number. Using the method, we define matrix F, which comprises newly infected terms, and matrix V, which comprises transition terms evaluated at the DFE point (E_0), as follows

$$F = \begin{pmatrix} 0 & 0 & 0 & 0 & \frac{b\beta_{\rm vh}\pi_h}{\mu_h} \\ 0 & 0 & 0 & 0 & 0 \\ 0 & 0 & 0 & 0 & 0 \\ 0 & 0 & 0 & 0 & \frac{b\beta_{\rm vn}\pi_n}{\mu_n} \\ 0 & \frac{b\beta_{hv}\pi_v}{\mu_v+u_3} & \frac{b\beta_{hv}\pi_v}{\mu_v+u_3} & \frac{b\beta_{nv}\pi_v}{\mu_v+u_3} & 0 \end{pmatrix},$$

$$V = \begin{pmatrix} \sigma_h\gamma_1 + \sigma_h\gamma_2 + \mu_h & 0 & 0 & 0 & 0 \\ -\gamma_1\sigma_h & u_1 + \alpha_h + \mu_h & 0 & 0 & 0 \\ -\gamma_2\sigma_h & -\alpha_h & \eta_h + \mu_h + u_2 & 0 & 0 \\ 0 & 0 & 0 & \eta_n + \mu_n & 0 \\ 0 & 0 & 0 & 0 & \mu_v + u_3 \end{pmatrix}.$$

The inverse of V is given by

$$V^{-1} = \begin{pmatrix} \frac{1}{\mu_h+(\gamma_1+\gamma_2)\sigma_h} & 0 & 0 & 0 & 0 \\ \frac{\gamma_1\sigma_h}{(\alpha_h+u_1+\mu_h)(\mu_h+(\gamma_1+\gamma_2)\sigma_h)} & \frac{1}{\alpha_h+u_1+\mu_h} & 0 & 0 & 0 \\ b_0 & \frac{\alpha_h}{(\alpha_h+u_1+\mu_h)(u_2+\mu_h+\eta_h)} & \frac{1}{\eta_h+\mu_h+u_2} & 0 & 0 \\ 0 & 0 & 0 & \frac{1}{\eta_n+\mu_n} & 0 \\ 0 & 0 & 0 & 0 & \frac{1}{\mu_v+u_3} \end{pmatrix},$$

where,

$$b_0 = \frac{(\alpha_h(\gamma_1+\gamma_2)+\gamma_2(u_1+\mu_h))\sigma_h}{(\alpha_h+u_1+\mu_h)(u_2+\eta_h+\mu_h)(\mu_h(\gamma_1+\gamma_2)\sigma_h)}.$$

Therefore,

$$FV^{-1} = \begin{pmatrix} 0 & 0 & 0 & 0 & \frac{b\pi_h\beta_{\rm vh}}{\mu_h(\mu_v+u_3)} \\ 0 & 0 & 0 & 0 & 0 \\ 0 & 0 & 0 & 0 & 0 \\ 0 & 0 & 0 & 0 & \frac{b\pi_n\beta_{\rm vn}}{\mu_n(\mu_v+u_3)} \\ b_1 & \frac{b\pi_v\beta_{\rm hv}(\alpha_h+\eta_h+\mu_h+u_2)}{(\mu_v+u_3)(\alpha_h+\mu_h+u_1)(\eta_h+\mu_h+u_2)} & \frac{b\pi_v\beta_{\rm hv}}{(\mu_v+u_3)(\eta_h+\mu_h+u_2)} & \frac{b\pi_v\beta_{\rm nv}}{(\eta_n+\mu_n)(\mu_v+u_3)} & 0 \end{pmatrix},$$

where,

$$b_1 = \frac{b\pi_v\sigma_h\beta_{\rm hv}((\gamma_1+\gamma_2)\alpha_h+\gamma_1(\eta_h+\mu_h+u_2)+\gamma_2(\mu_h+u_1))}{(\mu_v+u_3)(\alpha_h+\mu_h+u_1)((\gamma_1+\gamma_2)\sigma_h+\mu_h)(\eta_h+\mu_h+u_2)}.$$

The effective reproductive number is the spectral radius of the matrix (FV^{-1}), R_e is given by

$$R_e = \sqrt{\frac{b^2\pi_v\pi_h\beta_{vh}\beta_{hv}\mu_n\sigma_h(\eta_n+\mu_n)f_4 + b^2\pi_v\pi_n\beta_{nv}\beta_{vn}\mu_h f_2 f_3 f_1}{\mu_h\mu_n f_2 f_3 f_1(\eta_n+\mu_n)(u_3+\mu_v)^2}}, \quad (26)$$

$$R_e = \sqrt{\frac{b^2\pi_h\pi_v\beta_{hv}\beta_{vh}\sigma_h f_4}{\mu_h f_2 f_3 f_1(u_3+\mu_v)^2} + \frac{b^2\pi_n\pi_v\beta_{nv}\beta_{vn}}{\mu_n(\eta_n+\mu_n)(u_3+\mu_v)^2}}, \quad (27)$$

$$R_e = \sqrt{R_{eh}+R_{en}}, \quad (28)$$

where

$$\begin{aligned} f_1 &= \sigma_h(\gamma_1+\gamma_2)+\mu_h, \\ f_2 &= u_1+\alpha_h+\mu_h, \\ f_3 &= u_2+\eta_h+\mu_h, \\ f_4 &= \alpha_h\gamma_1+\gamma_2 f_2+f_3\gamma_1. \end{aligned}$$

The human reproductive number R_{eh} and animal reproductive number R_{en} determine the effective reproductive number. Therefore, we can conclude that an infected human in a susceptible non-human population will cause at least R_{en} infected non-human reservoirs. One infected animal reservoir will also produce R_{eh} infected humans within a susceptible population. In essence, R_e determines the spread of the disease in the sense that the disease will die out when $R_e < 1$, and it will persist when it is above $R_e > 1$.

4.3.1. Existence of endemic point

Substituting equation (19), (20), (23), (24) into equation (25) and simplifying the resulting equation, we obtain the following polynomial for i_v^*

$$g(i_v^*) = a_1 i_v^{*3} + a_2 i_v^{*2} + a_3 i_v^* = 0, \quad (29)$$

which simplifies to the following,

$$g(i_v^*) = i_v^*(a_1 i_v^{*2} + a_2 i_v^* + a_3) = 0, \quad (30)$$

where,

$$\begin{aligned}
a_1 &= b^3 f_4 \pi_h \sigma_h \beta_{\mathrm{hv}} \beta_{\mathrm{vh}} \beta_{\mathrm{vn}} (\delta_h + \mu_h)(\eta_n + \mu_n)(\mu_v + u_3) \\
&\quad - b^2 f_4 \delta_h \sigma_h \beta_{\mathrm{vh}} \beta_{\mathrm{vn}} (\mu_v + u_3)(b\pi_n \beta_{\mathrm{nv}} + (\eta_n + \mu_n)(\mu_v + u_3)) \\
&\quad + b^2 f_1 f_2 f_3 \beta_{\mathrm{vh}} \beta_{\mathrm{vn}} (\delta_h + \mu_h)(\mu_v + u_3)(b\pi_n \beta_{\mathrm{nv}} + (\eta_n + \mu_n)(\mu_v + u_3)), \\
a_2 &= b^2 f_4 \pi_h \sigma_h \beta_{\mathrm{hv}} \beta_{\mathrm{vh}} (\delta_h + \mu_h)(\eta_n + \mu_n)(\mu_n (\mu_v + u_3) - b\pi_v \beta_{\mathrm{vn}}) \\
&\quad + b f_4 \delta_h \sigma_h \beta_{\mathrm{vh}} \left(b^2 \pi_n \pi_v \beta_{\mathrm{nv}} \beta_{\mathrm{vn}} - \mu_n (\eta_n + \mu_n)(\mu_v + u_3)^2\right) \\
&\quad + b^2 f_1 f_2 f_3 \pi_n \beta_{\mathrm{nv}} \beta_{\mathrm{vn}} (\delta_h + \mu_h)(\mu_h (\mu_v + u_3) - b\pi_v \beta_{\mathrm{vh}}) \\
&\quad + b f_1 f_2 f_3 (\delta_h + \mu_h)(\eta_n + \mu_n)(\mu_v + u_3)^2 (\mu_h \beta_{\mathrm{vn}} + \mu_n \beta_{\mathrm{vh}}), \\
a_3 &= f_1 f_2 f_3 \mu_h \mu_n (\eta_n + \mu_n)(\delta_h + \mu_h)(\mu_v + u_3)^2 (1 - R_e^2).
\end{aligned}$$

All parameters in the model system (2) are all non-negative for $t > 0$; it then follows that the possible positive roots of the polynomial lie on the signs a_1, a_2 and a_3. Therefore, we then determine the possible number of positive roots of the quadratic equation in equation (30) by using Descartes' rule of signs. Table 3 gives a list of possible signs.

Table 3. Number of possible positive real roots of $g(i_v^*)$.

Case	a_1	a_2	a_3	Reproductive number	Sign change	Possible positive roots
1	+	+	+	$R_e < 1$	0	0
2	+	+	-	$R_e > 1$	1	1
3	+	-	+	$R_e < 1$	2	0 or 2
4	+	-	-	$R_e > 1$	1	1

The model system (2) admit that

(i) Two endemic equilibria E_1 if $R_e < 1$, when case 3 is satisfied.
(ii) A unique endemic equilibrium exists if $R_e > 1$, when case 2 and 4 holds.
(iii) No endemic point when $R_e < 1$, when case 1 holds.

The positive solutions of i_v^* are given by

$$i_v^* = \frac{-a_2 \pm \sqrt{a_2^2 - 4a_1 a_3}}{2a_1}.$$

Basically we get two unique endemic points when $a_1 > 0, a_2 < 0, a_3 > 0$ and $\Delta > 0$. The table shows that the model has two positive endemic equilibria for different values of R_e when $R_e < 1$. For the system to have positive roots, it occurs at $\Delta > 0$. To investigate the critical value, we use $\Delta = 0$ so that

$$\Delta = a_2^2 - 4a_1 a_3.$$

Thus, the critical value denoted by R_{ec}, is

$$R_{ec} = 1 - \frac{a_2^2}{4a_1 f_1 f_2 f_3 \mu_h \mu_n \mu_n (\eta_n + \mu_n)(\delta_h + \mu_h)(u_3 + \mu_v)^2}. \tag{31}$$

Therefore, the system has two positive equilibrium values for $R_{ec} < R_e < 1$.

4.3.2. Bifurcation simulation

A bifurcation occurs when a slight change in the system's inputs (parameter values) leads to a topological change. The system's behavior (2) is investigated when the bifurcation parameter R_e is varied. Following is an expression of the polynomial coefficients:

$$g(i_v^*) = a_4 i_v^{*2} + a_5 i_v^* + a_3 = 0, \tag{32}$$

where,

$$\begin{aligned}
a_4 &= b^2\beta_{vn}\beta_{vh}(u_3+\mu_v)\left[b\pi_n\beta_{nv} + (\eta_n+\mu_n)(u_3+\mu_v)\right]\left[f_1f_2f_3(\delta_h+\mu_h) - f_4\delta_h\sigma_h\right] \\
&\quad + \frac{b\mu_h f_1 f_2 f_3 \beta_{vn}(u_3+\mu_v)^3(\eta_n+\mu_n)(\delta_h+\mu_h)}{\pi_v} R_{eh}, \\
a_5 &= bf_1f_2f_3\mu_h\beta_{vn}(\eta_n+\mu_n)(\delta_h+\mu_h)(u_3+\mu_v)^2(1-R_{eh}) \\
&\quad + bf_1f_2f_3\mu_n\beta_{vh}(\eta_n+\mu_n)(\delta_h+\mu_h)(u_3+\mu_v)^2(1-R_{en}) \\
&\quad + bf_4\delta_h\sigma_h\beta_{vh}\mu_n(\eta_n+\mu_n)(u_3+\mu_v)^2(R_{en}-1) \\
&\quad + \frac{(\eta_n+\mu_n)(\delta_h+\mu_h)(u_3+\mu_v)^3 f_1f_2f_3\mu_n\mu_h}{\pi_v} R_e^2, \\
a_3 &= f_1f_2f_3\mu_h\mu_n(\eta_n+\mu_n)(\delta_h+\mu_h)(u_3+\mu_v)^2(1-R_e^2).
\end{aligned}$$

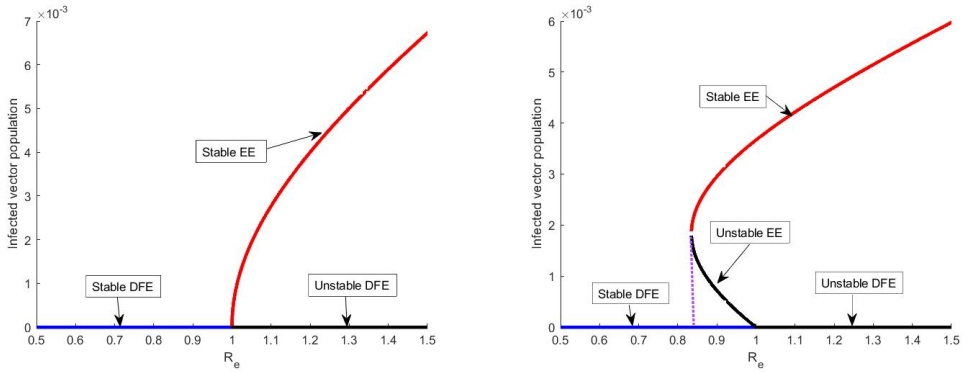

(a) Forward bifuraction. (b) Backward bifuraction.

Figure 2. Forward bifurcation: $\beta_{vh} = 0.62, \gamma_1 = 0.68, \sigma_h = 0.083$, and backward bifurcation: $\beta_{vh} = 0.92, \gamma_1 = 0.038, \sigma_h = 0.00093$. The rest of the parameter values are: $u_1 = 0.94, u_2 = 0.96$, $\beta_{vn} = 0.62, \gamma_2 = 0.95, \delta_h = 0.006, \mu_h = 0.00046, \alpha_h = 0.0019, \pi_v = 0.0505, \pi_n = 0.0001, \mu_n = 0.0014$, $\eta_n = 0.0006, \mu_v = 0.033, \beta_{nv} = 0.065, \pi_h = 0.000215, b = 0.333, \beta_{hv} = 0.065$

The model system displays both forward and backward bifurcations, as depicted in Figure 2, based on the specified parameters. Managing the disease poses a challenge, primarily due to the presence of a backward bifurcation. This is influenced by a high rate of incorrect diagnoses and the failure to decrease the proportion of bites from an infectious vector to susceptible humans. The complexity arises from the coexistence of the Disease-Free Equilibrium (DFE) and the Endemic Equilibrium (EE) for values between R_{ec} and 1. To effectively control HAT disease, it is crucial to ensure accurate diagnosis of infected humans. Additionally, the use of vector traps proves valuable in reducing direct contact between humans and infectious vectors.

4.4. Local Stability of DFE

In this section, we determine the local stability for DFE by finding the eigenvalues of the Jacobian matrix. The equilibrium point is stable if the eigenvalues have negative real parts.

Theorem 4.1. *The disease free equilibrium point is locally asymptotically stable if* $R_e < 1$ *and unstable if* $R_e > 1$.

The Jacobian matrix of the model evaluated at DFE point is given by:

$$J(E_0) = \begin{pmatrix} -\mu_h & 0 & 0 & 0 & \delta_h & 0 & 0 & 0 & -\frac{b\beta_{vh}\pi_h}{\mu_h} \\ 0 & -c_1 & 0 & 0 & 0 & 0 & 0 & 0 & \frac{b\beta_{vh}\pi_h}{\mu_h} \\ 0 & \sigma_h\gamma_1 & -c_2 & 0 & 0 & 0 & 0 & 0 & 0 \\ 0 & \sigma_h\gamma_2 & \alpha_h & -c_3 & 0 & 0 & 0 & 0 & 0 \\ 0 & 0 & \epsilon_1 & \epsilon_2 & -c_4 & 0 & 0 & 0 & 0 \\ 0 & 0 & 0 & 0 & 0 & -\mu_n & 0 & 0 & -\frac{b\beta_{vn}\pi_n}{\mu_n} \\ 0 & 0 & 0 & 0 & 0 & 0 & -c_5 & 0 & \frac{b\beta_{vn}\pi_n}{\mu_n} \\ 0 & 0 & -c_7 & -c_7 & 0 & 0 & -c_8 & -c_6 & 0 \\ 0 & 0 & c_7 & c_7 & 0 & 0 & c_8 & 0 & -c_6 \end{pmatrix},$$

$$c_1 = \sigma_h(\gamma_1+\gamma_2)+\mu_h, \quad c_2 = \alpha_h + u_1 + \mu_h, \quad c_3 = u_2 + \eta_h + \mu_h, \quad c_4 = \delta_h + \mu_h,$$
$$c_5 = \eta_n + \mu_n, \quad c_6 = u_3 + \mu_v, \quad c_7 = \frac{b\pi_v\beta_{hv}}{u_3+\mu_v}, \quad c_8 = \frac{b\beta_{nv}\pi_v}{u_3+\mu_v}.$$

We test for local stability of the disease-free equilibrium point by calculating the eigenvalues of Jacobian matrix J at the point E_0 as follows:

$$|J - I\lambda| = 0,$$

$$|J-\lambda| = \begin{pmatrix} -\mu_h-\lambda & 0 & 0 & 0 & \delta_h & 0 & 0 & 0 & -\frac{b\beta_{vh}\pi_h}{\mu_h} \\ 0 & -c_1-\lambda & 0 & 0 & 0 & 0 & 0 & 0 & \frac{b\beta_{vh}\pi_h}{\mu_h} \\ 0 & \sigma_h\gamma_1 & -c_2-\lambda & 0 & 0 & 0 & 0 & 0 & 0 \\ 0 & \sigma_h\gamma_2 & \alpha_h & -c_3-\lambda & 0 & 0 & 0 & 0 & 0 \\ 0 & 0 & \epsilon_1 & \epsilon_2 & -c_4-\lambda & 0 & 0 & 0 & 0 \\ 0 & 0 & 0 & 0 & 0 & -\mu_n-\lambda & 0 & 0 & -\frac{b\beta_{vn}\pi_n}{\mu_n} \\ 0 & 0 & 0 & 0 & 0 & 0 & -c_5-\lambda & 0 & \frac{b\beta_{vn}\pi_n}{\mu_n} \\ 0 & 0 & -c_7 & -c_7 & 0 & 0 & -c_8 & -c_6-\lambda & 0 \\ 0 & 0 & c_7 & c_7 & 0 & 0 & c_8 & 0 & -c_6-\lambda \end{pmatrix}.$$

Therefore, by solving the above matrix we get the characteristic equation

$$\begin{aligned} &(-\mu_h-\lambda)(-c_1-\lambda)(-c_2-\lambda)(-c_3-\lambda)(-c_4-\lambda)(-c_5-\lambda)(-c_6-\lambda)^2(-\mu_n-\lambda) \\ &+b\beta_{vn}(-\mu_h-\lambda)(-c_1-\lambda)(-c_2-\lambda)(-c_3-\lambda)(-c_4-\lambda)(-c_6-\lambda)^2(-\mu_n-\lambda) \\ &-b\beta_{vh}\sigma_h\gamma_1\alpha_h c_7(-\mu_h-\lambda)(-c_4-\lambda)(-\mu_n-\lambda)(-c_5-\lambda)(-c_6-\lambda) \\ &+b\beta_{vh}\sigma_h\gamma_1(-\mu_h-\lambda)(-c_3-\lambda)(-c_4-\lambda)(-\mu_n-\lambda)(-c_5-\lambda)(-c_6-\lambda) \\ &+b\beta_{vh}\sigma_h c_7\gamma_2(-\mu_h-\lambda)(-c_2-\lambda)(-c_4-\lambda)(-\mu_n-\lambda)(-c_5-\lambda)(-c_6-\lambda)=0 \\ &(-\mu_h-\lambda)(-c_4-\lambda)(-c_6-\lambda)(-\mu_n-\lambda)[\lambda^5+\phi_1\lambda^4+\phi_2\lambda^3+\phi_3\lambda^2+\phi_4\lambda+\phi_5]=0. \end{aligned}$$

Certainly the characteristic equation has four obvious eigenvalues that is $\lambda_1 = -\mu_h, \lambda_2 = -\mu_n, \lambda_3 = -c_4$, and $\lambda_4 = -c_6$. The remaining eigenvalues of the given polynomial of degree five,

$$P(\lambda) = \lambda^5 + \phi_1\lambda^4 + \phi_2\lambda^3 + \phi_3\lambda^2 + \phi_4\lambda + \phi_5,$$

can be identified using the Routh-Hurwitz criteria in A.1. where,

$$\begin{aligned}
\phi_1 &= c_1 + c_2 + c_3 + c_5 + c_6,\\
\phi_2 &= -bc_8\beta_{\text{vn}} + c_1c_2 + c_3c_2 + c_5c_2 + c_6c_2 + c_1c_3 + c_1c_5 + c_3c_5 + c_1c_6 + c_3c_6 + c_5c_6,\\
\phi_3 &= -bc_7\gamma_1\sigma_h\beta_{\text{vh}} - bc_7\gamma_2\sigma_h\beta_{\text{vh}} - bc_8c_3\beta_{\text{vn}} - bc_1c_8\beta_{\text{vn}} - bc_2c_8\beta_{\text{vn}} + c_1c_2c_3 + c_1c_5c_3\\
&\quad + c_2c_5c_3 + c_1c_6c_3 + c_2c_6c_3 + c_5c_6c_3 + c_1c_2c_5 + c_1c_2c_6 + c_1c_5c_6 + c_2c_5c_6,\\
\phi_4 &= -bc_7\gamma_1\alpha_h\sigma_h\beta_{\text{vh}} - bc_7\gamma_1c_5\sigma_H\beta_{\text{vh}} - bc_7\gamma_2c_5\sigma_h\beta_{\text{vh}} - bc_3c_7\gamma_1\sigma_h\beta_{\text{vh}} - bc_2c_7\gamma_2\sigma_H\beta_{\text{vh}} - bc_1c_2c_8\beta_{\text{vn}}\\
&\quad - bc_1c_3c_8\beta_{\text{vn}} - bc_2c_3c_8\beta_{\text{vn}} + c_1c_2c_3c_5 + c_1c_2c_6c_5 + c_1c_3c_6c_5 + c_2c_3c_6c_5 + c_1c_2c_3c_6,\\
\phi_5 &= c_1c_2c_3c_5c_6\mu_h\mu_n(1 - R_e^2).
\end{aligned}$$

Using Theorem A.1, we can conclude that since the determinant of the Hurwitz matrices given the above conditions we can conclude that there exist negative real roots. Therefore, the DFE point is locally asymptomatically stable when $R_e < 1$.

4.5. Local stability of EE

Theorem 4.2. *The endemic equilibrium point is locally asymptotically stable if $R_e < 1$ and unstable if $R_e > 1$.*

The Jacobian matrix evaluated at the endemic equilibrium is given by

$$J(E_1) = \begin{pmatrix}
-b\beta_{vh}i_v^* - \mu_h & 0 & 0 & 0 & \delta_h & 0 & 0 & 0 & -b\beta_{vh}s_h^*\\
b\beta_{vh}i_v^* & -L_1 & 0 & 0 & 0 & 0 & 0 & 0 & b\beta_{vh}s_h^*\\
0 & \gamma_1\sigma_h & -L_2 & 0 & 0 & 0 & 0 & 0 & 0\\
0 & \gamma_2\sigma_h & \alpha_h & -L_3 & 0 & 0 & 0 & 0 & 0\\
0 & 0 & u_1 & u_2 & -\delta_h - \mu_h & 0 & 0 & 0 & 0\\
0 & 0 & 0 & 0 & 0 & -b\beta_{vn}i_v^* - \mu_n & 0 & 0 & -b\beta_{vn}s_n^*\\
0 & 0 & 0 & 0 & 0 & b\beta_{vn}i_v^* & -\eta_n - \mu_n & 0 & b\beta_{vn}s_n^*\\
0 & 0 & -b\beta_{hv}s_v^* & -b\beta_{hv}s_v^* & 0 & 0 & -b\beta_{nv}s_v^* & -L_4 - L_5 & 0\\
0 & 0 & b\beta_{hv}s_v^* & b\beta_{hv}s_v^* & 0 & 0 & b\beta_{nv}s_v^* & L_4 & -L_5
\end{pmatrix}.$$

where

$$\begin{aligned}
L_1 &= \sigma_h(\gamma_1 + \gamma_2) + \mu_h, & L_2 &= \alpha_h + u_1 + \mu_h, \quad L_3 = u_2 + \eta_h + \mu_h,\\
L_4 &= b\beta_{hv}(i_1^* + i_2^*) + b\beta_{nv}i_n^*, & L_5 &= u_3 + \mu_v.
\end{aligned}$$

We find the eigenvalues using the Gershgorian Circle Theorem, where $n = 9$ [21].

Lemma 4.3 (Gershgorian theorem)**.** *Let M be a size $n \times n$ with real entries M_{ij}. If the diagonal elements of that matrix satisfy $m_{ij} < -r_i$ where $r_i = \sum_{j=1, j\neq 1}^{n} |m_{ij}|$ for $i, j = 1, \cdots, n$, the eigenvalues of M are negative or have negative real parts [21].*

Using Theorem 4.3, the first hypothesis $J_{ii} < 0$, for $i = 1, \cdots, 9$, clearly all the diagonal entries of J_{E1} are negative.

The second hypothesis is equivalent to $r_i < |J_{ii}|$ for $i = 1, \cdots, 9$ is true if and only if

$$\frac{b\beta_{vh}i_v^*}{b\beta_{vh}i_v^* + \mu_h} < 1, \qquad \frac{\alpha_h + u_1}{L_2} < 1, \quad \frac{u_2}{L_3} < 1, \tag{33}$$

$$\frac{\sigma_H(\gamma_1 + \gamma_2)}{L_1} < 1, \qquad \frac{\delta_h}{\delta_h + \mu_h} < 1, \quad 0 < \eta_n + \mu_n, \tag{34}$$

$$\frac{b\beta_{vn}i_v^*}{b\beta_{vn}i_v^* + \mu_n} < 1, \qquad \frac{L_4}{L_4 + L_5} < 1, \quad 0 < u_3 + \mu_v. \tag{35}$$

Therefore, if (33), (34), and (35) are satisfied then the endemic point E_1 is locally asymptomatically stable.

4.6. Global stability of DFE

Theorem 4.4. *The disease-free equilibrium of the model (2) is globally asymptotic stable if $R_e < 1$.*

Lemma 4.5. *Consider a model written in the form*

$$\begin{aligned} \tfrac{dX_1}{dt} &= F(X_1, X_2), \\ \tfrac{dX_2}{dt} &= G(X_1, X_2), \qquad\qquad G(X_1, 0) = 0, \end{aligned} \tag{36}$$

where $X_1 \in \mathbb{R}^m$ denotes (its components) the number of uninfected individuals and $X_2 \in \mathbb{R}^n$ denotes (its components) the number of infected individuals including latent, infectious, etc; $X_0 = (X_1^*, 0)$ denotes the disease-free equilibrium of the system [22].

Also assume the conditions (H_1) and (H_2) below:

(H_1) *For $\frac{dX_1}{dt} = F(X_1, 0)$, X_1^* is globally asymptotically stable;*

(H_2) *$G(X_1, X_2) = AX_2 - \hat{G}(X_1, X_2) \geq 0$ for $(X_1, X_2) \in \Omega$, where the Jacobian $A = \frac{\partial G}{\partial X_2}(X_1^*, 0)$ is the M matrix (the off diagonal elements of A are nonnegative) and Ω is the region where the model makes biological sense.*

Then the DFE $X_0 = (X_1^*, 0)$ is globally asymptotically stable provided that $R_0 < 1$.

Proof. We need to show that conditions (H_1) and (H_2) in Lemma 4.5 when $R_0 < 1$. from the model (2) we have $X_1 = (s_h, r_h, s_n, s_v)$ and $X_2 = (e_h, i_1, i_2, i_n, i_v)$ and $X_1 = \left(\frac{\pi_h}{\mu_h}, 0, \frac{\pi_n}{\mu_n}, \frac{\pi_v}{\psi + \mu_v}\right)$. Using Lemma 4.5, we have

(H_1)

$$\frac{dX_1}{dt} = F(X_1, 0) = \begin{bmatrix} \pi_h - \mu_h s_h \\ -\delta_h r_h - \mu_h r_h \\ \pi_n - \mu_n s_n \\ \pi_v - u_3 s_v - \mu_v s_v \end{bmatrix}$$

is linear and its solution can be easily found as

$$\begin{aligned} s_h(t) &= \frac{\pi_h}{\mu_h} + \left(s_h(0) - \frac{\pi_h}{\mu_h} \right) e^{-\mu_h t}, \\ r_H(t) &= r_h(0) e^{-(\delta_h + \mu_h)t}, \\ s_n(t) &= \frac{\pi_n}{\mu_n} + \left(s_n(0) - \frac{\pi_n}{\mu_n} \right) e^{-\mu_n t}, \\ s_v(t) &= \frac{\pi_v}{u_3 + \mu_v} + \left(s_v(0) - \frac{\pi_v}{u_3 + \mu_v} \right) e^{-(u_3 + \mu_v)t}. \end{aligned}$$

Clearly $S_h(t) \to \frac{\pi_H}{\mu_h}$, $r_h(t) \to 0$, $s_n(t) \to \frac{\pi_n}{\mu_n}$ and $s_v(t) \to \frac{\Lambda_v}{u_3 + \mu_v}$ as $t \to \infty$, regardless of the values of $s_h(0), r_h(0), s_n(0), s_v(0)$. Thus $X_1 = \left(\frac{\pi_H}{\mu_H}, 0, \frac{\pi_n}{\mu_n}, \frac{\pi_v}{u_3 + \mu_v} \right)$ is globally asymptomatically stable.

(H_2)
We then have

$$G(X_1, X_2) = \begin{bmatrix} b\beta_{vh} i_v s_h - \sigma_h \gamma_1 e_h - \sigma_h \gamma_2 e_h - \mu_h e_h \\ \sigma_h \gamma_1 e_h - u_1 i_1 - \alpha_h i_1 - \mu_h i_1 \\ \alpha_h i_1 + \sigma_h \gamma_2 e_h - u_2 i_2 - \mu_h i_2 - \eta_h i_2 \\ b\beta_{vn} i_n s_n - \eta_n i_n - \mu_n i_n \\ b\beta_{hv} i_1 s_v + b\beta_{Hv} i_2 s_v + b\beta_{nv} i_n s_v - u_3 i_v - \mu_v i_v \end{bmatrix}.$$

We then obtain the M matrix to be given by

$$A = \begin{bmatrix} -(\sigma_h \gamma_1 + \sigma_h \gamma_2 + \mu_h) & 0 & 0 & 0 & \frac{b\beta_{vH}\pi_h}{\mu_h} \\ \sigma_h \gamma_1 & -(u_1 + \alpha_h + \mu_h) & 0 & 0 & 0 \\ \sigma_h \gamma_2 & \alpha_h & -(u_2 + \mu_h + \eta_h) & 0 & 0 \\ 0 & 0 & 0 & -(\eta_n + \mu_n) & \frac{b\beta_{vn}\pi_n}{\mu_n} \\ 0 & \frac{b\beta_{hv}\pi_v}{u_3 + \mu_v} & \frac{b\beta_{hv}\pi_v}{u_3 + \mu_v} & \frac{b\beta_{nv}\pi_v}{u_3 + \mu_v} & -(u_3 + \mu_v) \end{bmatrix}.$$

Therefore,

$$\hat{G}(X_1, X_2) = \begin{bmatrix} b\beta_{vh} i_v \left(\frac{\pi_h - s_h \mu_h}{\mu_h}\right) \\ 0 \\ 0 \\ b\beta_{vn} i_v \left(\frac{\pi_n - s_n \mu_n}{\mu_n}\right) \\ \left[b\beta_{hv}(i_1{+}_2) + b\beta_{nv} I_n\right] \left(\frac{\pi_v - s_v(u_3+\mu_v)}{(u_3+\mu_v)}\right) \end{bmatrix}.$$

We observe that $\hat{G}(X_1, X_2) \geq 0$ if and only if these conditions hold:

$$\pi_h \geq s_h \mu_h, \qquad \pi_n \geq s_n \mu_n \qquad \pi_v \geq s_v(u_3 + \mu_v).$$

□

5. Sensitivity analysis

In this section, we introduce the sensitivity analysis, a method that measure how changes in input values impact the outcomes of the model. Given the uncertainty associated with numerous parameters, variations in model outputs are expected due to this inherent variability.

Table 4. Sensitivity indices of the effect reproduction number.

Parameter	Sensitivity index (R_e)	Parameter	Sensitivity index (R_e)
π_h	0.115559	u_1	2.51e-06
π_n	0.884441	u_2	0.000145
π_v	1	η_n	-0.265332
b	2	β_{vn}	0.884441
η_h	-1.42E-04	μ_n	-1.503550
β_{vh}	0.115559	β_{hv}	0.115559
γ_2	-3.46E-05	β_{nv}	0.884441
μ_h	-0.115604	α_h	-1.98E-07
σ_h	3.98E-05	u_3	-1.76678
γ_1	7.43E-05	μ_v	-0.241758

The normalized forward sensitivity index is calculated to determine each parameter's impact on the effective reproductive number. The normalized forward sensitivity index is defined as

$$\Gamma_x^{R_e} = \frac{\partial R_e}{\partial x} \times \frac{x}{R_e}. \tag{37}$$

The sensitivity indices presented in Table 4 are calculated from (37) using the parameter values outlined in Table 1. Looking at Table 4, we can see that parameters

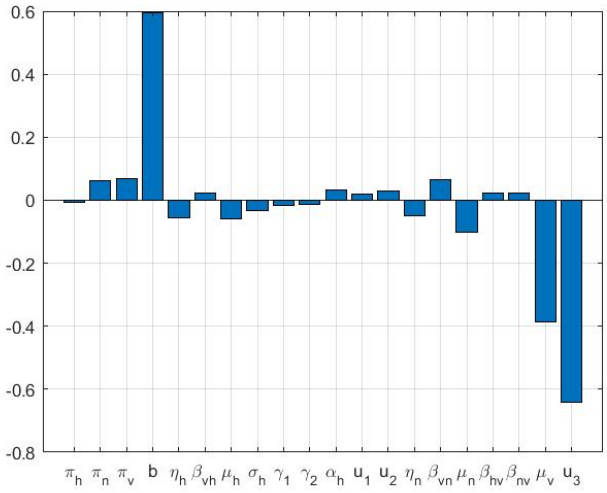

Figure 3. Partial Rank Correlation coefficients showing effects of parameter Coefficients of the effective Reproductive number (R_e)

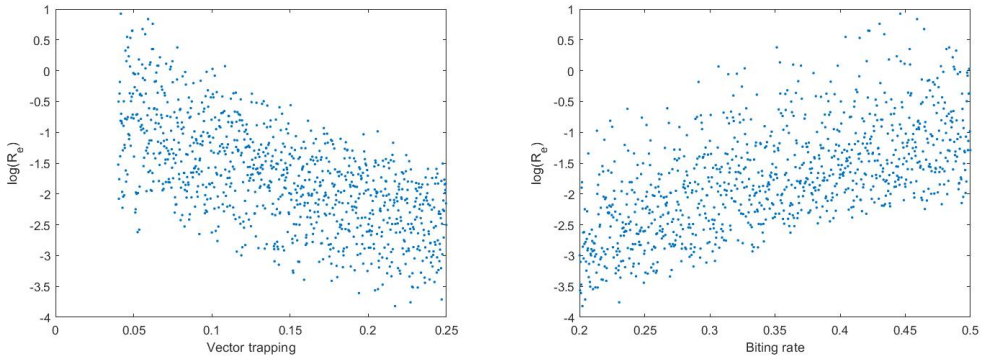

Figure 4. Monte-Carlo simulations of 1000 sample values for two parameters (vector tapping and bitting rate chosen via Latin Hypercube Sampling.)

like $\pi_h, \pi_n, \pi_v, b, \beta_{vh}, \sigma_h, \gamma_1, u_1, u_2, \beta_{vn}, \beta_{hv}$, and β_{nv} have positive indices, this suggests that increasing these parameters has the potential to raise the effective reproductive number (R_e). When these parameters rise and others stay constant, the disease persists. On the flip side, parameters such as $\eta_h, \mu_h, \gamma_1, \alpha_h, \eta_n, \mu_n, \mu_v$, and u_3 show negative indices, this implies that an increase in these parameters tends to lower R_e, thereby reducing the disease burden.

To explore variations, we also employ widely used techniques, Latin Hypercube Sampling (LHS) and Partial Rank Correlation Coefficients (PRCC). LHS efficiently analyzes how parameters vary across uncertain ranges simultaneously. PRCC illustrates how each parameter influences the outcome. Figure 3 explains the PRCC with the effective reproductive number as the output variable and 20 parameters as inputs. The sensitivity analysis indicates that the biting rate significantly influences the outcome.

Figure 4 demonstrates that when the biting rate goes up, R_e surpasses 1, signi-

fying an increased risk of disease spread. Conversely, when the vector trapping rate increases, R_e decreases. Effectively controlling disease transmission hinges on managing the vector population. To diminish disease spread, trapping an adequate number of vectors is essential. If vector trapping is done at a lower rate, the disease will likely persist, leading to many hosts contracting it. High biting rates contribute to more hosts getting infected, sustaining the disease. Therefore, trapping enough vectors to reduce the transmission rate is crucial, ensuring $R_e < 1$ and enabling disease control.

6. Optimal control Strategies

In this section, we solve the model (2) using the Pontryagin's Maximum Principle. The aim is to find a control strategy that minimizes the population of i_1, i_2, s_v, and i_v while reducing the cost associated with control measures. Control measures are defined as linear functions $u_i(t) \in [0, 1]$, for $i = 1, 2, 3$. It is to be noted that $u_i(t) = 0$ means that no control has been implemented over the model, and $u_1(t) = 1$ indicates that all individuals with stage 1 diagnoses are receiving stage 1 treatment; $u_2(t) = 1$ suggests that all individuals with stage 2 diagnoses are receiving stage 2 treatments, and $u_3(t) = 1$ indicates vector trapping being implemented.

Theorem 6.1. *There exist an optimal control* $u^* = (u_1^*, u_2^*, u_3^*)$ *such that*

$$J(u_1^*, u_2^*, u_3^*) = \min_{(u_1,u_2,u_3)} J(u_1, u_2, u_3) \tag{38}$$

subject to the model system (2) with non-negative initial conditions.

The objective function J is defined as

$$J(u_1, u_2, u_3) = \int_0^{t_f} \Big(A_1 i_1 + A_2 i_2 + A_3 s_v + A_4 i_v + b_1 u_1^2 + b_2 u_2^2 + b_3 u_3^2 \Big) dt, \tag{39}$$

where $A_1, A_2, A_3, A_4, b_1, b_2$, and b_3 are positive coefficients. The expression $b_i u_i^2$ represents the cost associated with u_i. Quantities A_1 and A_2 represent the cost of minimizing the stage 1 and stage 2 infected populations, and quantities A_3 and A_4 represent the cost of minimizing the susceptible and infected vectors, respectively. The assumption is that the costs are linear and the cost functions are nonlinear.

The Hamilton $\mathcal{H}$ is defined following Pontryagin's Maximum Principle [30] as

$$\begin{aligned}
\mathcal{H} &= \mathcal{L}(i_1, i_2, s_v, i_v, u_1, u_2, u_3) + \lambda_1 \frac{ds_h}{dt} + \lambda_2 \frac{de_h}{dt} + \lambda_3 \frac{di_1}{dt} + \lambda_4 \frac{di_2}{dt} + \lambda_5 \frac{dr_h}{dt} \\
&\quad + \lambda_6 \frac{ds_n}{dt} + \lambda_7 \frac{di_n}{dt} + \lambda_8 \frac{ds_v}{dt} + \lambda_9 \frac{di_v}{dt}, \\
&= A_1 i_1 + A_2 i_2 + A_3 s_v + A_4 i_v + b_1 u_1^2 + b_2 u_2^2 + b_3 u_3^2 + \lambda_1[\pi_h - b\beta_{vh} i_v s_h + \delta_h r_h - \mu_h s_h] \\
&\quad + \lambda_2[b\beta_{vh} i_v s_h - \sigma_h \gamma_1 e_h - \sigma_h \gamma_2 e_h - \mu_h e_h] + \lambda_3[\sigma_h \gamma_1 e_h - u_1 i_1 - \alpha_h i_1 - \mu_h i_1] \\
&\quad + \lambda_4[\alpha_h i_1 + \sigma_h \gamma_2 e_h - u_2 i_2 - (\mu_h + \eta_h) i_2] + \lambda_5[u_2 i_2 + u_1 i_1 - \delta_h r_h - \mu_h r_h] \\
&\quad + \lambda_6[\pi_n - b\beta_{vn} i_v s_n - \mu_n s_n] + \lambda_7[b\beta_{vn} i_v s_n - \eta_n i_n - \mu_n i_n] \\
&\quad + \lambda_8[\pi_v - b\beta_{hv} s_v (i_1 + i_2) - b\beta_{nv} s_v i_n - u_3 s_v - \mu_v s_v] \\
&\quad + \lambda_9[b\beta_{hv} s_v (i_1 + i_2) + b\beta_{nv} s_v i_n - u_3 i_v - \mu_v i_v],
\end{aligned}$$

where $\lambda_1, \lambda_2, \lambda_3, \lambda_4, \lambda_5, \lambda_6, \lambda_7, \lambda_8, \lambda_9$ are the adjoint variables.

Theorem 6.2. *Given that $s_h^*, e_h^*, i_1^*, i_2^*, r_h^*, s_n^*, i_n^*, s_v^*$, and i_v^* are the solutions of the optimal control model associated with the optimal control variables (u_1^*, u_2^*, u_3^*) which minimizes $J(u_1, u_2, u_3)$ over then there exist an adjoint system which satisfies*

$$\frac{d\lambda_i}{dt} = -\frac{\partial \mathcal{H}}{\partial x_i}, x_i \in \{s_h, e_h, i_1, i_2, r_h, s_n, i_n, s_v, i_v\},$$

The differential equations of adjoint variables are obtained by $\frac{d\lambda_i}{dt} = -\frac{\partial \mathcal{H}}{\partial x_i}$ with transversality boundary conditions defined as

$$\lambda_1(t_f) = \lambda_2(t_f) = \lambda_3(t_f) = \lambda_4(t_f) = \lambda_5(t_f) = \lambda_6(t_f) = \lambda_7(t_f) = \lambda_8(t_f) = \lambda_9(t_f) = 0.$$

We give the control solution u_1^*, u_2^*, u_3^* as follows

$$u_1^* = \max\left\{0, \min\left(1, u_1^*\right)\right\}, \tag{40}$$

$$u_2^* = \max\left\{0, \min\left(1, u_2^*\right)\right\}, \tag{41}$$

$$u_3^* = \max\left\{0, \min\left(1, u_3^*\right)\right\}. \tag{42}$$

Where the permissible control functions u_1^*, u_2^*, u_3^*, are obtained by setting $\frac{\partial \mathcal{H}}{\partial u_i} = 0, i = 1, 2, 3$, given by

$$u_i^* = \begin{cases} 0, & \text{if} \quad u_i \leq 0, \\ u_i, & \text{if} \quad 0 < u_i < 1, \\ 1, & \text{if} \quad u_i \geq 1. \end{cases}$$

Proof. Using Pontragin's maximum principle, we get the adjoint system

$$\begin{cases} \frac{d\lambda_1}{dt} &= \mu_h\lambda_1 + b\beta_{vh}i_v(\lambda_1 - \lambda_2), \\ \frac{d\lambda_2}{dt} &= \mu_h\lambda_2 + \sigma_h\gamma_1(\lambda_2 - \lambda_3) + \sigma_h\gamma_2(\lambda_2 - \lambda_4), \\ \frac{d\lambda_3}{dt} &= \mu_h\lambda_3 - A_1 + u_1(\lambda_3 - \lambda_5) + \alpha_h(\lambda_3 - \lambda_4) + b\beta_{hv}s_v(\lambda_8 - \lambda_9), \\ \frac{d\lambda_4}{dt} &= (\mu_h + \eta_h)\lambda_4 - A_2 + u_2(\lambda_4 - \lambda_5) + b\beta_{hv}s_v(\lambda_8 - \lambda_9), \\ \frac{d\lambda_5}{dt} &= \mu_h\lambda_5 + \delta_h(\lambda_5 - \lambda_1), \\ \frac{d\lambda_6}{dt} &= \mu_n\lambda_6 + b\beta_{vn}i_v(\lambda_6 - \lambda_7), \\ \frac{d\lambda_7}{dt} &= (\eta_n + \mu_n)\lambda_7 + b\beta_{nv}s_v(\lambda_8 - \lambda_9), \\ \frac{d\lambda_8}{dt} &= (u_3 + \mu_v)\lambda_8 - A_3 + b\beta_{hv}(i_1 + i_2)(\lambda_8 - \lambda_9) + b\beta_{nv}i_n(\lambda_8 - \lambda_9), \\ \frac{d\lambda_9}{dt} &= (u_3 + \mu_v)\lambda_9 - A_4 + b\beta_{vh}s_h(\lambda_1 - \lambda_2) + b\beta_{vn}s_n(\lambda_6 - \lambda_7), \end{cases} \tag{43}$$

with transversality boundary conditions defined as

$$\lambda_1(t_f) = \lambda_2(t_f) = \lambda_3(t_f) = \lambda_4(t_f) = \lambda_5(t_f) = \lambda_6(t_f) = \lambda_7(t_f) = \lambda_8(t_f) = \lambda_9(t_f) = 0.$$

Consequently

$$\begin{cases} \frac{\partial H}{\partial u_1^*} &= 2b_1u_1^* + i_1(\lambda_5 - \lambda_3) = 0, \\ \frac{\partial H}{\partial u_2^*} &= 2b_2u_2^* + i_2(\lambda_5 - \lambda_3) = 0, \\ \frac{\partial H}{\partial u_3^*} &= 2b_3u_3^* - s_v\lambda_8 - i_v\lambda_9 = 0. \end{cases} \tag{44}$$

From equation (44), we solve u_1^*, u_2^*, and u_3^* to obtain their respective control solutions, which are

$$\begin{cases} u_1^* &= \frac{(\lambda_3-\lambda_5)i_1}{2b_1}, \\ u_2^* &= \frac{(\lambda_4-\lambda_5)i_2}{2b_2}, \\ u_3^* &= \frac{s_v\lambda_8+i_v\lambda_9}{2b_3}. \end{cases} \tag{45}$$

The optimal control can be characterized as

$$u_1^* = \max\left\{0, \min\left(1, \frac{(\lambda_3 - \lambda_5)i_1}{2b_1}\right)\right\}, \tag{46}$$

$$u_2^* = \max\left\{0, \min\left(1, \frac{(\lambda_4 - \lambda_5)i_2}{2b_2}\right)\right\}, \tag{47}$$

$$u_3^* = \max\left\{0, \min\left(1, \frac{S_v\lambda_8 + i_v\lambda_9}{2b_3}\right)\right\}. \tag{48}$$

□

6.1. Numerical solutions

In this section, we delve into the numerical simulations of the optimal control problem alongside the model without control, employing the forward-backward sweep method to determine the optimal controls u_1^*, u_2^*, u_3^* [29]. The simulations encompass the model system (2), the adjoint system (43), and the optimal control (45), facilitated through MATLAB. The forward state is solved using the fourth-order Runge-Kutta method, while the adjoint is addressed backward in time through a modified Runge-Kutta approach. Most parameter values are derived from published literature, and assumptions are made where data is lacking. For this section, the control variables u_1, u_2, and u_3 are time-dependent variables, while the parameters values are drawn from Table 1. The initial conditions for simulation are set as $s_h = 0.2, e_h = 0.1, i_1 = 0.5, i_2 = 0.55, r_h = 0, s_n = 0.01, i_n = 0.1, s_v = 0.6$, and $i_v = 1.6$, and weight constant values are assigned as $A_1 = 1, A_1 = 2, A_3 = 2, A_4 = 2, b_1 = 2, b_2 = 10$ and $b_3 = 15$ [11].

The simulation accounts for the cumulative impact of all three controls on the model system (43), wherein all infected humans receive treatments and vector traps are employed to curtail contact rates. The strategy involves implementing all control measures, and the graphical representation in Fig. 5-13 illustrates the dynamics of various populations. Notably, the susceptible human and animal populations witness an increase with control compared to the scenario without control. The implementation of control measures results in the completion of treatments for stage 1 and stage 2 infected humans within 50 days. The number of exposed humans under control conditions is also slightly higher than the number without control. Figures 15 and 16 depict a decrease in both susceptible and infected vectors in the presence of control measures.

Furthermore, Figures 14, 15, and 16 provide insights into the profiles of the control measures. The strategic application of control measures, commencing treatment at maximum and gradually reducing it, followed by continuous administration after 50 days at a constant rate, coupled with vector traps initiated at maximum, steadily reduced, and maintained at a constant rate for extended periods, demonstrates the potential for HAT disease eradication.

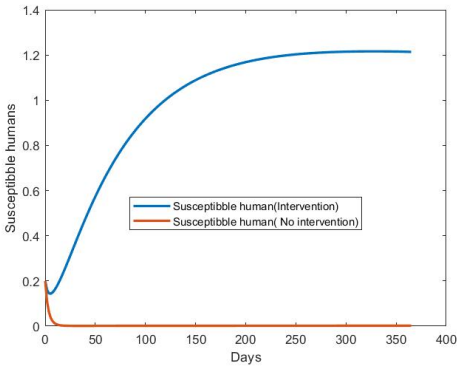

Figure 5. Susceptible human population

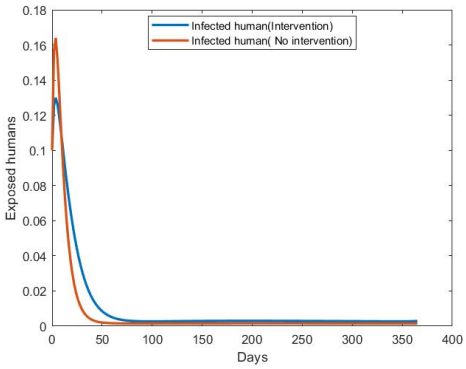

Figure 6. Exposed human population

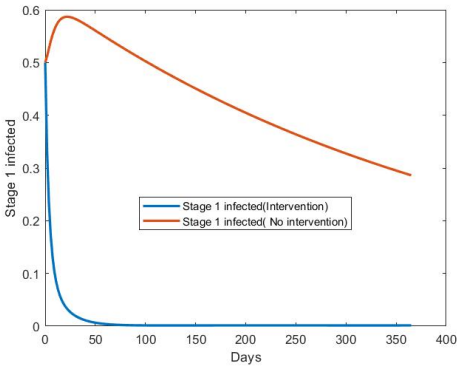

Figure 7. Stage 1 infected human population.

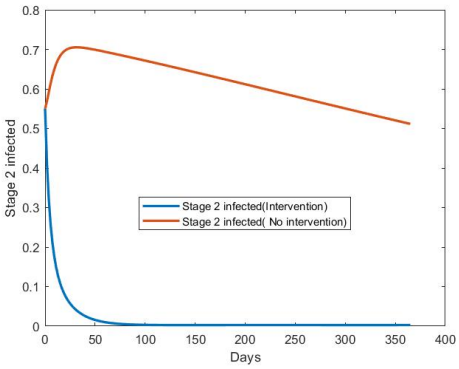

Figure 8. Stage 2 infected human population.

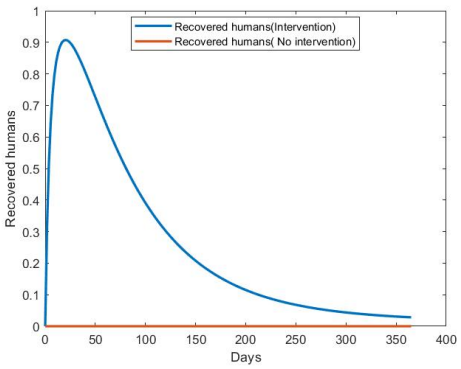

Figure 9. Recovered human population.

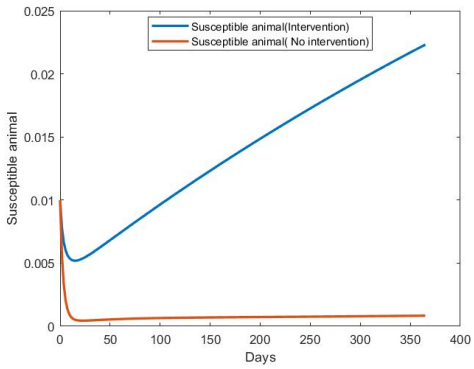

Figure 10. Susceptible animal population.

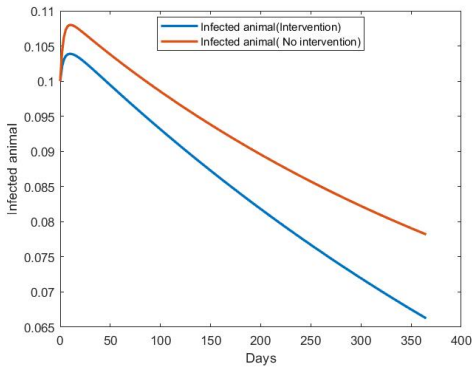

Figure 11. Infected animal population.

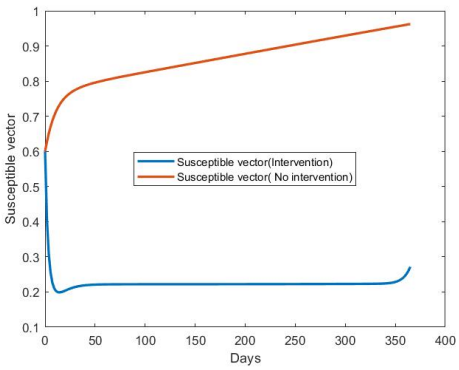

Figure 12. Susceptible vector population.

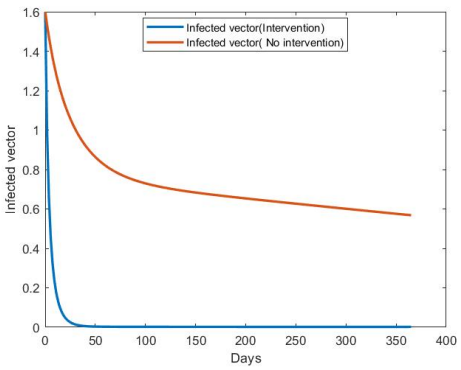

Figure 13. Infected vector population.

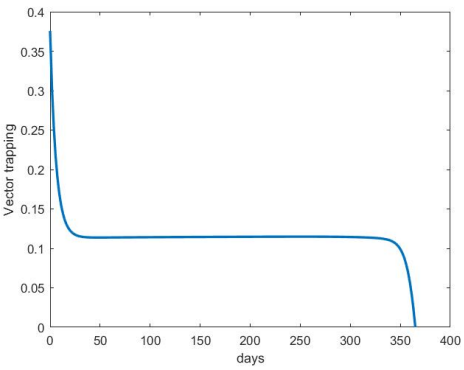

Figure 14. Vector trapping profile.

7. Conclusions

In this study, our focus is on developing and analyzing the impact of stage-specific treatment and vector trapping on Human African Trypanosomiasis (HAT) disease. Utilizing a deterministic mathematical model that integrates various control mea-

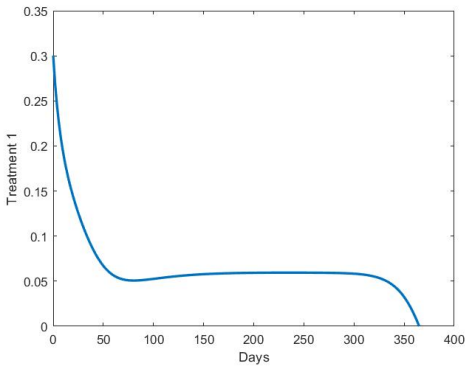

Figure 15. Treatment 1 profile.

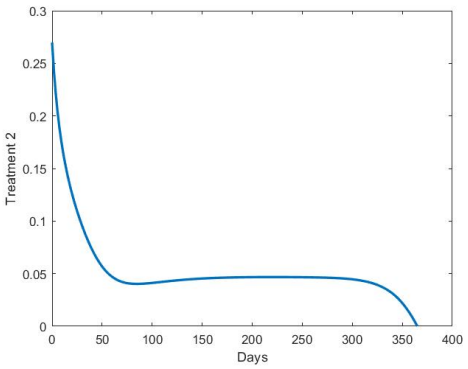

Figure 16. Treatment 2 profile.

sures, we delve into investigating disease transmission dynamics. The applied control measures within the model comprise of stage 1 treatment (u_1), stage 2 treatment (u_2), and vector trapping (u_3). The model comprises nine ordinary differential equations; the first five describe the human host, the next two describe the animal host, and the remaining two represent a vector. Through rigorous analysis, we establish the existence of positive, unique, and bounded solutions.

Two equilibrium points, namely disease-free and endemic, are presented along with the respective conditions of their existence. Furthermore, we calculate the effective reproductive number for the system and employ it to scrutinize the stability conditions associated with the model equilibrium points.

The study extends to exploring bifurcation phenomena, revealing the presence of both backward and forward bifurcations under specific conditions. Notably, the bifurcation analysis uncovers the co-existence of the Disease-Free Equilibrium (DFE) and the Endemic Equilibrium (EE) when the effective reproductive number, denoted as R_{ec}, falls below 1. This scenario poses a challenge to disease eradication. Moreover, we conduct a sensitivity analysis of the effective reproductive number concerning various model inputs. Remarkably, the biting rate emerges as the most sensitive parameter, exerting a substantial influence on disease transmission. Figure 3 visually demonstrates that vector trapping can effectively reduce disease burden.

To refine our approach, we redefine the controls as time-dependent variables and determine optimal controls for HAT disease. Using the Pontryagin's maximum principle, we solve the optimal control problem and scrutinize the conditions associated with optimal control. Utilizing the forward-backward sweep method, we find that numerical simulations support the notion that incorporating disease stage treatment and vector trapping can effectively reduce the disease burden compared to a model without control. Notably, concurrent implementation of control measures, with treatment initiated at a maximum rate and gradually decreasing over time and later having it administered at a constant rate, proves to be a strategic approach to minimizing the disease burden.

Acknowledgment

The support of the DSI-NRF Centre of Excellence in Mathematical and Statistical Sciences (CoE-MaSS) and the University of Kwazulu-Natal, School of Mathematics, Statistics and Computer Science, Pietermaritzburg Campus towards this research is hereby acknowledged. Opinions expressed and conclusions arrived at, are those of the author and are not necessarily to be attributed to the CoE.

References

[1] Checchi F., Funk S., Chandramohan D., Chappuis F. and Haydon D.T. 2018. The impact of passive case detection on the transmission dynamics of gambiense Human African Trypanosomiasis. *PLoS neglected tropical diseases*. 12(4): p.e0006276.

[2] HSTalks(2021). Human African Trypanosomiasis. 31 January. Available at:https://hstalks.com/t/4284/human-african-trypanosomiasis/?biosci (Accessed:07 June 2022)

[3] Kasozi K.I., Zirintunda G., Ssempijja F., Buyinza B., Alzahrani K.J., Matama K., Nakimbugwe H.N., Alkazmi L., Onanyang D., Bogere P. and Ochieng J.J. 2021. Epidemiology of trypanosomiasis in wildlife—implications for humans at the wildlife interface in Africa. *Frontiers in Veterinary Science*. 8: p.565.

[4] Centers for disease control and prevention. 2022. Available at:https://www.cdc.gov/parasites/sleepingsickness/epi.html. Accessed on the 02-May-2022.

[5] World Health Organisation. 2019. https://www.who.int/news-room/fact-sheets/detail/trypanosomiasis-human-African-(sleeping-sickness). Accessed on the 01-June-2019.

[6] Toor J., Adams E.R., Aliee M., Amoah B., Anderson R.M., Ayabina D., Bailey R., Basáñez M.G., Blok D.J., Blumberg S. and Borlase A. 2021. Predicted impact of COVID-19 on neglected tropical disease programs and the opportunity for innovation. *Clinical Infectious Diseases*. 72(8): pp.1463-1466.

[7] Rogers D.J. 1988. A general model for the African trypanosomiases. *Parasitology*. 97(1): 193-212.

[8] Shaier S. and Burke M. 2019. A Mathematical Model for the Effect of Domestic Animals on Human African Trypanosomiasis (Sleeping Sickness). *The Kennesaw Journal of Undergraduate Research*. 6(1): p.1.

[9] Liana Y.A., Shaban N., Mlay G. and Phibert A. 2020. African Trypanosomiasis Dynamics: Modelling the Effects of Treatment, Education, and Vector Trapping. *International Journal of Mathematics and Mathematical Sciences*.

[10] Meisner J., Barnabas R.V. and Rabinowitz P.M. 2019. A mathematical model for evaluating the role of trypanocide treatment of cattle in the epidemiology and control of Trypanosoma brucei rhodesiense and T. b. gambiense sleeping sickness in Uganda. *Parasite epidemiology and control*. 5: p.e00106.

[11] Gervas H.E., Opoku N.K.D.O. and Ibrahim S. 2018. Mathematical modelling of human African trypanosomiasis using control measures. *Computational and mathematical methods in medicine*.

[12] Pandey, A., Atkins, K.E., Bucheton, B., Camara, M., Aksoy, S., Galvani, A.P. and Ndeffo-Mbah, M.L., 2015. Evaluating long-term effectiveness of sleeping sickness control measures in Guinea. *Parasites & vectors*, 8(1), pp.1-10.

[13] Kajunguri D., Hargrove J.W., Ouifki R., Mugisha J.Y.T., Coleman P.G. and Welburn, S.C. 2014. Modelling the use of insecticide-treated cattle to control tsetse and Trypanosoma brucei rhodesiense in a multi-host population. *Bulletin of Mathematical biology* 76(3):pp.673-696.

[14] Ndondo, A.M., Munganga, J.M.W., Mwambakana, J.N., Saad-Roy, C.M., Van den Driessche, P. and Walo, R.O., 2016. Analysis of a model of gambiense sleeping sickness in humans

and cattle. *Journal of biological dynamics*. 10(1): pp.347-365.

[15] Kgosimore M., Kuznetsov D. and Mushayabasa S. 2020. Dynamical and optimal control analysis of a seasonal Trypanosoma brucei rhodesiense model. *Mathematical Biosciences and Engineering*

[16] Gyapong J. and Boatin B. eds. 2016. Neglected tropical diseases-sub-Saharan Africa. Springer International Publishing.

[17] Abd-Alla A.M., Bergoin M., Parker A.G., Maniania N.K., Vlak J.M., Bourtzis K., Boucias D.G. and Aksoy S. 2013. Improving sterile insect technique (SIT) for tsetse flies through research on their symbionts and pathogens. *Journal of invertebrate pathology*. 112: pp.S2-S10.

[18] Thieme H.R. 1948. Mathematics in population biology. *Princeton University Press*. John Wiley and sons.

[19] Van den Driessche P., and Watmough J. 2002. Reproduction numbers and sub-threshold endemic equilibria for compartmental models of disease transmission. *Mathematical biosciences*. 180(1-2): pp.29-48.

[20] Mahardika R. and Sumanto Y.D. 2019. Routh-hurwitz criterion and bifurcation method for stability analysis of tuberculosis transmission model. *Journal of Physics: Conference Series*. 1217: No. 1, p. 012056. IOP Publishing.

[21] Bejarano D.A.O., Ibargüen-Mondragón E., and Gómez-Hernández E.A. 2018. A stability test for non linear systems of ordinary differential equations based on the Gershgorin circles. *Contemporary Engineering Sciences*. 11(91): 4541-4548.

[22] Castillo-Chavez C., Blower S., Van den Driessche P., Kirschner D., and Yakubu, A.A. 2002. Mathematical approaches for emerging and reemerging infectious diseases: models, methods, and theory. *Springer Science & Business Media*. (Vol. 126)

[23] Priotto, G., Kasparian, S., Mutombo, W., Ngouama, D., Ghorashian, S., Arnold, U., Ghabri, S., Baudin, E., Buard, V., Kazadi-Kyanza, S. and Ilunga, M., 2009. Nifurtimox-eflornithine combination therapy for second-stage African Trypanosoma brucei gambiense trypanosomiasis: a multicentre, randomised, phase III, non-inferiority trial. The Lancet, 374(9683), pp.56-64.

[24] Rock, K.S., Torr, S.J., Lumbala, C. and Keeling, M.J., 2017. Predicting the impact of intervention strategies for sleeping sickness in two high-endemicity health zones of the Democratic Republic of Congo. PLoS neglected tropical diseases, 11(1), p.e0005162.

[25] Aliee, M., Keeling, M.J. and Rock, K.S., 2021. Modelling to explore the potential impact of asymptomatic human infections on transmission and dynamics of African sleeping sickness. PLoS computational biology, 17(9), p.e1009367.

[26] Marino, S., Hogue, I.B., Ray, C.J. and Kirschner, D.E., 2008. A methodology for performing global uncertainty and sensitivity analysis in systems biology. *Journal of theoretical biology*. 254(1), pp.178-196.

[27] Stone, C.M. and Chitnis, N., 2015. Implications of heterogeneous biting exposure and animal hosts on Trypanosomiasis brucei gambiense transmission and control. PLoS computational biology, 11(10), p.e1004514.

[28] Mahamat, M.H., Peka, M., Rayaisse, J.B., Rock, K.S., Toko, M.A., Darnas, J., Brahim, G.M., Alkatib, A.B., Yoni, W., Tirados, I. and Courtin, F., 2017. Adding tsetse control to medical activities contributes to decreasing transmission of sleeping sickness in the Mandoul focus (Chad). PLoS neglected tropical diseases, 11(7), p.e0005792.

[29] Lenhart S. and Workman J.T. 2007. Optimal control applied to biological models. CRC press.

[30] Pontryagin L.S., Boltyanskii V.G., Gamkrelidze R.V., Mishchenko E. The Mathematical Theory of Optimal Processes (Translated by D.E. Brown) A Pergamon Press Book; The Macmillan Company: New York, NY, USA,1964; pp. 56–57.

Chapter 4

Multiscle modeling of Sleeping sickness

---

[1] In this chapter we developed and analyzed an embedded multicale model that captures within-host dynamics and vector dynamics of sleeping sickness. The model emphasizes the dependency of each scale on each other in the disease transmission of sleeping sickness. We determine analytical and numerical solutions for the embedded multiscale model. Additionally, We formulate and analyze the optimal control problem, incorporating human treatment and vector trapping.

[1]The work in this chapter has been submitted to a Journal of Mathematical Biology.

A general Human African Trypanosomiasis multiscale model

Mulalo Makhuvha[1,2*] and Hermane Mambili-mamboundou[1†]

[1]Mathematics department, University of Kwazulu-Natal, Durban, 4000, South Africa.
[2]DSI-NRF Centre of Excellence in Mathematical and Statistical Sciences (CoE-MaSS), South Africa.

*Corresponding author(s). E-mail(s): makhubamulalo@gmail.com;
Contributing authors: mambilimamboundou@ukzn.ac.za;
†These authors contributed equally to this work.

Abstract

In disease modeling, multiscale modeling involves the integration of epidemiological and immunological dynamics. Historically, immunological and epidemiological dynamics have been studied independently. Nevertheless, recognizing that these two processes occur concurrently has yielded new insights when coupled. This study focuses on modeling sleeping sickness, also known as Human African Trypanosomiasis (HAT), a neglected tropical disease. The disease is transmitted to hosts after a bite by blood-sucking tsetse flies. Humans, wild or domesticated animals, and tsetse flies are reservoirs that allow HAT to persist in a population. According to the World Health Organization (WHO), depleting parasite reservoirs could potentially halt transmission of this neglected tropical vector disease. Using a multiscale model, we investigate how human within-host dynamics influence epidemiological disease dynamics. In this context, we propose a model that couples within-host and vector dynamics for HAT transmission. The multiscale model system we present integrates within-host and between-host dynamics for the two hosts of HAT disease. We employ seven ordinary differential equations to describe the pathogen's transition from the within-host to the between-host scale. Our analysis encompasses the mathematical properties, presentation of steady states for the model, and stability analysis of the model's steady states, incorporating the reproductive number ($\boldsymbol{R_0}$). Furthermore, we implement control measures to mitigate infection in the population. In addition, we investigate the persistence and reduction of the parasite in the presence of control measures using the Pontryagin maximum principle.

Keywords: Optimal control, immuno-epidemiological model, vector-borne disease, Human African Trypanosomiasis

1 Introduction

One of the neglected tropical diseases is sleeping sickness, a form of trypanosomiasis called Human African Trypanosomiasis (HAT). HAT disease is classified as a type *II* vector-borne disease transmitted by tsetse flies [1]. The disease is caused by the parasites *Trypanosoma brucie gambiense* and *Trypanosoma brucie rhodesiense*. The parasites are transferred from one host to the other after a bite by blood-sucking tsetse flies. HAT disease can infect humans and non-humans, such as cattle and wild animals. According to the World Health Organization [2], for the period 2016-2020, 55 million people were considered at risk, with only 3 million considered moderate to high risk. The disease is prevalent in remote areas with limited healthcare facilities and is challenging to detect and analyze because it manifests complex dynamics due to multiple hosts. HAT disease manifests in two distinct stages, and symptoms differ according to the stage at which an individual is diagnosed. Severe symptoms appear at the second stage of HAT, and it is imperative to find cost-effective public health interventions since the disease is a neglected tropical disease. In spite of the lack of a vaccine, there are therapeutic treatments available depending on the stage of the disease. The HAT disease has been modeled with models at a single scale: epidemiological scale and immunological model separately; disease transmission complexity demands innovative approaches to modeling transmission dynamics and intervention strategies. Rogers proposed the classical framework of an epidemiological model for the disease citeROGER88, presenting a general mathematical model involving one vector and two vertebrate hosts. In this setting, the construction of between-host transmission dynamics using multiple host mathematical models includes [3], [4], [5], [6], [7] [8], [9], [10], and [11] to name a few. There is a notable gap in within-host scale research, and to the best of our knowledge, the following are the only work that presents a within-host model for HAT that focuses on the interaction between the antigenic variation and the body's defense system together with the parasite replication [12], [13], [14], and [15]. In modeling, multiscale modeling provides a comprehensive and integrated framework for understanding disease dynamics at multiple scales. A multiscale model links the within-host and between-host scales, giving a detailed characterization of the system involved in infectious diseases. There are five identified categories of multiscale models: individual-based multiscale models (IMSMs), nested multiscale models (NMSMs), embedded multiscale models (EMSMs), hybrid multiscale models (HMSMs) and coupled multiscale models (CMSMs) [16]. Linking the within-host and between-host scales has challenges, ranging from understanding the complexity of immune responses, capturing and modeling super-infection, linking processes across scales, and developing methods to incorporate two or more scales into a single scale framework. The idea to develop a multiscale model for HAT stems from the lack of multiscale models for the disease. [17] presents a model that links the within-host and between-host scales,

developed using the nested modeling framework. The study illustrated the role of antigen structure in determining parasite success in a single host and how it could affect the between-host dynamics. The model incorporates parasite genetics to predict antigen switch rates, new variants from the switches, and host heterogeneity but ignores crucial aspects such as immune response and parasite replication.

In this study, we develop a multiscale mathematical model for HAT that incorporates the immune response, parasite super-infection, and parasite growth rate to the interaction between vectors and the other two hosts, which was later extended by incorporating control measures. We would like to know whether multiscale modeling can be used to eliminate or eradicate neglected diseases. Moreover, we investigated the effects of the intervention using the Pontryagin maximum principle.

2 Model formulation

Developing a multiscale model involves thoroughly comprehending individual scales, as each scale serves as a foundational element for the comprehensive multiscale model. Our approach establishes a connection between the dynamics occurring within a single infected human host and between-hosts by using embedded multiscale model catergory by a minimal set of variables. The multiscale model designed for sleeping sickness encompasses two principal components: the within-host sub-model and the between-host sub-model. These components collectively form a comprehensive framework that captures the complex dynamics of the disease at both individual and population levels.

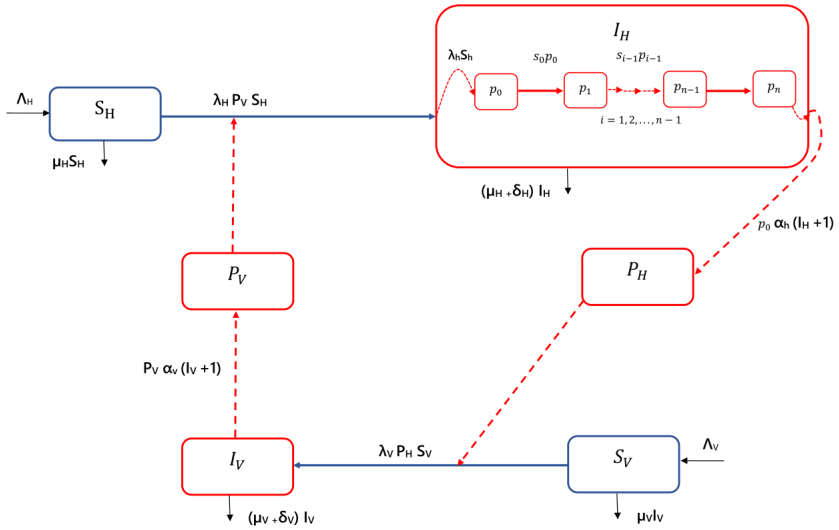

Fig. 1 A conceptual diagram of a multiscale model for Human African Trypanosomiasis (HAT).

$$
\begin{cases}
\frac{dS_H(t)}{dt} &= \Lambda_H - \frac{bP_V(t)S_H(t)}{V_0+P_V(t)} - \mu_H S_H(t), \\
\frac{dI_H(t)}{dt} &= \frac{bP_V(t)S_H(t)}{V_0+P_V(t)} - \mu_H I_H(t) - \delta_H I_H(t), \\
\frac{dp_0(t)}{dt} &= \frac{bP_V(t)[S_H(t)-1]}{[V_0+P_V(t)]\Theta_H[I_H(t)+1]} + \alpha_0 p_0(t) - k_0 p_0(t) - \mu_0 p_0(t) - \alpha_h p_0(t), \\
\frac{dP_H(t)}{dt} &= (I_H(t)+1)\alpha_h p_0(t) - \sigma_H P_H(t), \\
\frac{dS_V(t)}{dt} &= \Lambda_V - \frac{bP_H(t)S_V(t)}{H_0+P_H(t)} - \mu_V S_V(t), \\
\frac{dI_V(t)}{dt} &= \frac{bP_H(t)S_V(t)}{H_0+P_H(t)} - \mu_V I_V(t) - \delta_V I_V(t), \\
\frac{dP_V(t)}{dt} &= (I_V(t)+1)\alpha_V - \sigma_V P_V(t).
\end{cases} \tag{1}
$$

The within-host model explains the dynamics of parasite evolution within a single infected human host. In parallel, the between-host sub-model outlines the complex interplay of disease dynamics between the vector host and the human host. Transmission between hosts occurs when an infected human transmits the disease to a susceptible tsetse fly and vice versa, from an infected vector host to a susceptible human host. The mathematical expressions for the multiscale model are derived from the relationships illustrated in Figure 1 and are summarized in the model system (1). Table 1 and Table 2 summarize the definitions of all the variables and the associated parameters.

The first equation in the model system (1) describes the rate of change of a susceptible human population over time t. This population changes through recruitment via the birth rate at Λ_H, exposure to the force of infection, and natural mortality at a rate μ_H. The force of infection rate, a variable rate, is defined as $(bP_V(t))/(V_0 + P_V(t))$, where b represents the vector bite rate, and V_0 represents the half-saturation constant associated with infection of humans. Consequently, when an infected vector bites a human during a blood meal, it introduces the parasite into the human, resulting in an infected human individual. The second equation in the model system (1) characterizes the rate at which the infected human population changes over time t. The presence of infected humans is determined by new infections attributed to the force of infection and natural and death-induced death rates, denoted as μ_H and δ_H, respectively.

The third equation provides insight into the dynamics of a single infected host. This study focuses on monitoring the evolution of the parasite within an individual human host. The parasite population is influenced by new infections, growth, immune response, death rate, and parasite excretion to various body parts, including the skin, brain, and other regions. The average rate at which an individual takes up trypomastigote parasites from an infected vector host during a blood meal is expressed

as

$$\lambda_h(t)s_h(t) = \frac{bP_V(t)[S_H(t) - 1]}{[V_0 + P_V(t)]\Theta_H[I_H(t) + 1]},$$

with Θ_H being the downscaling parameter. Parasite growth is defined by binary fusion at a rate α_0. Infection on a single host is defined by

$$(S_H(t), I_H(t)) \to (S_H(t) - 1, I_H(t) + 1).$$

Following the uptake of the parasite, the parasite is killed by the body's defense mechanism, the immune system, at a rate of k_0. It has been observed that parasites may switch to different types to evade the immune system. For the sake of simplicity, our multiscale model employs a single parasite type. The parasite population decreases due to the natural death rate and excretion into the skin, μ_0 and α_h, respectively. The fourth equation in the model system (1) explains the rate of change of the human pathogen load population within the community over time t. Human pathogen load is calculated based on the infectious reservoir in the community and the elimination rate of the community pathogen load at a rate σ_H. The fifth equation captures the rate of change of the susceptible vector population over time t. Similarly to the susceptible human host population, the susceptible vector population undergoes increases due to the birth rate at Λ_V, decreases due to the force of infection, and natural death at a constant rate μ_V. The force of infection for vectors is defined as $(bP_H(t))/(H_0+P_H(t))$, and H_0 is the half-saturation constant associated with the tsetse fly infection. The sixth equation describes the rate of change of infected vectors at any time t. The vector infection rate experiences an increase due to the force of infection, and the population undergoes a decrease due to the natural death rate μ_V and the disease-induced death rate δ_V. The final equation represents the rate at which the vector pathogen load population within the community changes over time t. In the same way as the human pathogen load, the vector pathogen load is determined by the infectious reservoir in the community and the elimination rate of the community pathogen load represented by σ_V.

Table 1 Description of the state variables of the model.

Variables	Description	Initial value
$S_H(t)$	Susceptible human population	1000
$I_H(t)$	Infected human population	100
$p_0(t)$	Trypomastigote parasite population	500
$P_H(t)$	Human community load	200
$S_V(t)$	Susceptible vector population	2000
$I_V(t)$	Infected vector population	150
$P_V(t)$	Vector community load	100

Table 2 Parameter values of the model.

Parameter	Description	Value	units	Source
Λ_H	Recruitment rate for human population	42 (per 1000 people)	day^{-1}	[18]
b	Vector biting rate	0.333	day^{-1}	[11]
Θ_H	Down scaling parameter	0.0001	day^{-1}	[1]
V_0	Half saturation constant associated with infection of humans	5000	day^{-1}	[1]
μ_H	Human natural death rate	0.000046	day^{-1}	[4]
δ_H	Human disease induced rate	0.002	day^{-1}	[5]
α_0	Growth rate of parasite	0.01	day^{-1}	Assumed
k_0	Killing rate of parasite by immune system (classical macrophages)	0.00045	day^{-1}	[19]
μ_0	Natural death rate of the parasite	0.0045	day^{-1}	Assumed
α_h	Excretion of the parasite to different body parts	0.000546	day^{-1}	[1]
σ_H	Elimination rate of the human parasite community load	0.00546	day^{-1}	Assumed
Λ_V	Recruitment rate for vector population	150	day^{-1}	Assumed
H_0	Half saturation constant associated with tsetse fly infection	30 000	day^{-1}	Assumed
μ_V	Vector natural death rate	0.033	day^{-1}	[21]
δ_V	Vector disease induced rate	0.01	day^{-1}	Assumed
σ_V	Elimination rate of the tsetse-fly parasite community load	0.1	day^{-1}	Assumed
α_V	Excretion of the parasite from the vector	0.001	day^{-1}	Assumed

3 Mathematical analysis

This section presents mathematical analysis results for the HAT embedded multiscale model (1). For all time $t \geq 0$, the solution to the model system (1) exists, is non-negative, and is unique within a region $\omega \in \mathbb{R}^7_+$ of biological interest. Furthermore, this section presents the equilibrium points of the system along with the reproductive number. A subsequent stability analysis of these equilibrium points uses the reproductive number.

3.1 Positivity of solutions

Given positive initial conditions, we must prove that all variables remain non-negative for all time $t \geq 0$.

Proposition 1 (Positivity of solutions)**.** *Let the non-negative initial conditions be* $\big(s_H(0) \geq 0, I_H(0) \geq 0, p_0(0) \geq 0, S_V(0) \geq 0, I_V(0) \geq 0\big) \in \mathbb{R}^5_+$*, then all solutions of the model system (1) are positive for all* $t > 0$ *and non-negative for all* t *such that all positive solutions satisfy* $\big(S_H(t), I_H(t), p_0(t), S_V(t), I_V(t)\big)$ *for all large* t*.*

From model system (1) the first equation is given by

$$\frac{dS_H}{dt} = \Lambda_H - \lambda_H S_H - \mu_H S_H.$$

The inequality then follows as

$$\frac{dS_H}{dt} \geq -\lambda_H S_H - \mu_H S_H.$$

It then follows that the inequality can be expressed as

$$\frac{dS_H}{dt} + (\lambda_H + \mu_H)S_H \geq 0.$$

The integrating factor I is given by

$$I = \exp\Big\{\mu_H t + \int_0^t \lambda_H(s)ds\Big\}.$$

By multiplying the inequality by the integrating factor, we get

$$\frac{d}{dt}\Big(S_H \exp\Big\{\mu_H t + \int_0^t \lambda_H(s)ds\Big\}\Big) \geq 0.$$

Take the above expression and integrate it, then the solution is given by

$$S_H(t) \geq S_H(0)\exp\left\{-(\mu_H t + \int_0^t \lambda_H(s)ds)\right\}.$$

Since $\big(\mu_H t + \int_0^t \lambda_H(s)ds\big)$, therefore, $S_H(t) > 0$.
In a similar manner,

$$S_V(t) \geq S_V(0)\exp\left\{-(\mu_V t + \int_0^t \lambda_V(s)ds)\right\} > 0.$$

The third equation from the model system (1) is given by

$$\frac{dp_0}{dt} = \lambda_h s_h + \alpha_0 p_0 - k_0 p_0 - \mu_0 p_0 - \alpha_h p_0,$$

the following inequality results

$$\frac{dp_0}{dt} \geq \alpha_0 p_0 - k_0 p_0 - \mu_0 p_0 - \alpha_h p_0.$$

By separating the variables, we can obtain

$$\frac{dp_0}{p_0} \geq (\alpha_0 - k_0 - \mu_0 - \alpha_h)dt.$$

As a result of solving the inequality above, we obtain

$$p_0(t) \geq p_0(0)e^{(\alpha_0 - k_0 - \mu_0 - \alpha_h)t},$$

$(\alpha_0 - k_0 - \mu_0 - \alpha_h) < 0$, when $\alpha_0 < (k_0 + \mu_0 + \alpha_h)$, therefore, $p_0(t) > 0$.

In the same way, the following expressions can be obtained for the remaining variables:

$$I_H(t) \geq I_H(0)e^{-(\mu_H + \delta_H)t} > 0,$$

$$
\begin{aligned}
I_V(t) &\geq I_V(0)e^{-(\mu_V+\delta_V)t} > 0,\\
P_H(t) &\geq P_H(0)e^{-\sigma_H t} > 0,\\
P_V(t) &\geq P_V(0)e^{-\sigma_V t} > 0.
\end{aligned}
$$

The analysis concludes that for all time instances $t > 0$, the solutions $S_H(t), I_H(t), p_0(t), P_H(t), S_V(t), I_V(t), P_V(t)$ are strictly positive. This finding affirms that, under positive initial conditions for all variables, the solutions to the model system (1) remain non-negative for all $t > 0$.

3.2 Feasible region

In this subsection, our objective is to determine the feasible region employing Proposition 2.

Proposition 2 (Feasible Region)**.** *Let the feasible region for the multiscale model be* $\omega = \{S_H, I_H, p_0, P_H, S_V, I_H, P_V \in \mathbb{R}^7_+ : 0 \leq S_H + I_H \leq \frac{\Lambda_H}{\mu_H}, 0 \leq p_0 \leq m_1,$
$0 \leq P_H \leq m_2, 0 \leq S_V + I_V \leq \frac{\Lambda_V}{\mu_V}, 0 \leq P_V \leq m_3\}$.

Let $N_H = S_H + I_H$, and $N_V = S_V + I_V$, we obtain

$$
\begin{cases}
\frac{dN_H}{dt} &= \Lambda_H - \mu_H N_H - \delta_H I_H,\\
\frac{dN_V}{dt} &= \Lambda_V - \mu_H N_V - \delta_V I_V.
\end{cases}
$$

It then follows that

$$
\begin{cases}
\frac{dN_H}{dt} \leq \Lambda_H - \mu_H N_H,\\
\frac{dN_V}{dt} \leq \Lambda_V - \mu_H N_V.
\end{cases}
$$

Which gives us

$$
\begin{cases}
N_H(t) \leq N_H(0)e^{-\mu_H t} + \frac{\Lambda_H}{\mu_H}[1 - e^{-\mu_H t}],\\
N_V(t) \leq N_V(0)e^{-\mu_V t} + \frac{\Lambda_V}{\mu_V}[1 - e^{-\mu_v t}].
\end{cases}
$$

Therefore, we get

$$
\begin{cases}
\lim\limits_{t\to\infty} \sup(N_H(t)) \leq \frac{\Lambda_H}{\mu_H},\\
\lim\limits_{t\to\infty} \sup(N_V(t)) \leq \frac{\Lambda_V}{\mu_V}.
\end{cases}
$$

We substitute $N_V(t) \leq \frac{\Lambda_V}{\mu_V}$ to obtain

$$
P_V(t) \leq P_V(0)e^{-\sigma_V t} + \frac{\alpha_V(\Lambda_V + \mu_V)}{\mu_V \sigma_V}[1 - e^{-\sigma_V t}],
$$

therefore we get

$$\lim_{t\to\infty} \sup(P_V(t)) \leq \frac{\alpha_V\left(\Lambda_V+\mu_V\right)}{\mu_V\sigma_V}.$$

Similarly, we get the following

$$\begin{cases} p_0(t) & \leq \frac{b\alpha_V(\Lambda_H-\mu_H)(\Lambda_V+\mu_V)}{\Theta_H(\Lambda_H+\mu_H)(-\alpha_0+\alpha_h+k_0+\mu_0)(\alpha_V(\Lambda_V+\mu_V)+V_0\mu_V\sigma_V)} \\ P_H(t) & \leq \frac{b\alpha_h\alpha_V(\Lambda_H-\mu_H)(\Lambda_V+\mu_V)}{\Theta_H\mu_H\sigma_H(-\alpha_0+\alpha_h+k_0+\mu_0)(\alpha_V(\Lambda_V+\mu_V)+V_0\mu_V\sigma_V)} \end{cases}$$

The analysis reveals that positive solutions persist when $\alpha_0 < k_0 + \mu_0 + \alpha_h$ within the designated region ω. This finding concludes that the embedded multiscale model, initiated with positive initial conditions, maintains bounded solutions within the specified region ω. The condition $\alpha_0 < k_0 + \mu_0 + \alpha_h$ serves as a critical threshold, ensuring that the model's dynamics, as defined by the model equations, remain well-behaved and do not exhibit unbounded growth.

3.3 Existence and uniqueness of the multiscale solutions

This subsection establishes solutions' existence and uniqueness for our embedded multiscale model system (1). The inquiry involves determining the conditions under which solutions exist and identifying the circumstances that lead to the uniqueness of these solutions. Our approach draws upon the groundwork laid by [22], providing a framework to ascertain the well-posedness of the model.

Theorem 3 (Uniqueness of solutions)**.** *Let D denote the domain:*

$$|t-t_0| \leq a, ||x-x_0|| \leq b, x = (x_1, x_2, \ldots, x_n), x_0 = (x_{10}, x_{20}, \ldots, x_{n0}) \tag{2}$$

and supposed that $f(t,x)$ satisfies the Lipschitz condition:

$$||f(t,x_1) - f(t,x_2)|| \leq k||x_1 - x_2||, \tag{3}$$

and whenever the pairs (t,x_1) and (t,x_2) belong to the domain D, where k is used to represent a positive constant. Then, there exist a constant $\delta > 0$ such that there exists a unique (exactly one) continuous vector solution $x(t)$ of the system

$$x^{'} = f(t,x), x(t_0) = x_0,$$

in the interval $|t-t_0| \leq \delta$. It is important to note that conditions (3) is satisfied by requirement that:

$$\left\{ \quad \frac{\partial f_i}{\partial x_j}, \quad i,j = 1,2,\ldots,n \right.$$

be continuous and bounded in domain D.

Proposition 4. *If $f(t,x)$ has continuous partial derivative $\frac{\partial f_i}{\partial x_j}$ on a bounded closed vortex domain $\mathcal{R}$ (i.e convex set of real numbers), where $\mathcal{R}$ is used to denotes real numbers, then it satisfies a Lipschitz condition in $\mathcal{R}$. Our interest is in the domain:*

$$1 \leq \epsilon \leq \mathcal{R}. \tag{4}$$

So, we look for the bounded solution of the form

$$0 < \mathcal{R} < \infty.[22]$$

The following is a proof of the existence theorem. Let D denote the domain defined in (2) such that (3) and (4) hold. Then, there exists a solution of the model system (1), which is bounded in the domain D.

Proof. Let

$$\begin{cases} f_1 &= \Lambda_H - \frac{bP_V}{V_0+P_V}S_H - \mu_H S_H, \\ f_2 &= \frac{bP_V}{V_0+P_V}S_H - \mu_H I_H - \delta_H I_H, \\ f_3 &= \frac{bP_V[S_H-1]}{[V_0+P_V]\Theta_H[I_H+1]} + \alpha_0 p_0 - k_0 p_0 - \mu_0 p_0 - \alpha_h p_0, \\ f_4 &= (I_H+1)\alpha_h p_0 - \sigma_H P_H, \\ f_5 &= \Lambda_V - \frac{bP_H}{H_0+P_H}S_V - \mu_V S_V, \\ f_6 &= \frac{bP_H}{H_0+P_H}S_V - \mu_V I_V - \delta_V I_V, \\ f_7 &= (I_V+1)\alpha_V P_V - \sigma_v P_v. \end{cases} \tag{5}$$

We have to show that $\frac{\partial f_i}{\partial x_j}$, for $i,j = 1,2,3,4,5,6,7$ are continuous and bounded. The following partial derivatives were explored for the model system (5).

From the first equation from system (5)

$$\begin{cases} \frac{\partial f_1}{\partial S_H} &= -\frac{bP_V}{V_0+P_V} - \mu_H, \quad ||\frac{\partial f_1}{\partial S_H}|| = ||-\frac{bP_V}{V_0+P_V} - \mu_H|| < \infty, \\ \frac{\partial f_1}{\partial I_H} &= 0, \quad \left|\frac{\partial f_1}{\partial I_H}\right| = |0| < \infty, \\ \frac{\partial f_1}{\partial p_0} &= 0, \quad \left|\frac{\partial f_1}{\partial p_0}\right| = |0| < \infty, \\ \frac{\partial f_1}{\partial P_H} &= 0, \quad \left|\frac{\partial f_1}{\partial P_H}\right| = |0| < \infty, \\ \frac{\partial f_1}{\partial S_V} &= 0, \quad \left|\frac{\partial f_1}{\partial S_V}\right| = |0| < \infty, \\ \frac{\partial f_1}{\partial I_V} &= 0, \quad \left|\frac{\partial f_1}{\partial I_V}\right| = |0| < \infty, \\ \frac{\partial f_1}{\partial P_V} &= -\frac{bS_H V_0}{(P_0+P_V)^2}, \quad ||\frac{\partial f_1}{\partial P_V}|| = ||-\frac{bS_H V_0}{(P_0+P_V)^2}|| < \infty. \end{cases}$$

The second equation from system (5) yields

$$\begin{cases} \frac{\partial f_2}{\partial S_H} = \frac{bP_V}{V_0+P_V}, & ||\frac{\partial f_2}{\partial S_H}|| = ||\frac{bP_V}{V_0+P_V}|| < \infty, \\ \frac{\partial f_2}{\partial I_H} = -\delta_H - \mu_H, & \left|\frac{\partial f_2}{\partial I_H}\right| = |-\delta_H - \mu_H| < \infty, \\ \frac{\partial f_2}{\partial p_0} = 0, & \left|\frac{\partial f_2}{\partial p_0}\right| = |0| < \infty, \\ \frac{\partial f_2}{\partial P_H} = 0, & \left|\frac{\partial f_2}{\partial P_H}\right| = |0| < \infty, \\ \frac{\partial f_2}{\partial S_V} = 0, & \left|\frac{\partial f_2}{\partial S_V}\right| = |0| < \infty, \\ \frac{\partial f_2}{\partial I_V} = 0, & \left|\frac{\partial f_2}{\partial I_V}\right| = |0| < \infty, \\ \frac{\partial f_2}{\partial P_V} = \frac{bS_H V_0}{(P_0+P_V)^2}, & ||\frac{\partial f_2}{\partial P_V}|| = ||\frac{bS_H V_0}{(P_0+P_V)^2}|| < \infty. \end{cases}$$

The third equation from system (5) gives

$$\begin{cases} \frac{\partial f_3}{\partial S_H} = \frac{bP_V}{[V_0+P_V]\Theta_H[I_H+1]}, & ||\frac{\partial f_3}{\partial S_H}|| = ||\frac{bP_V}{[V_0+P_V]\Theta_H[I_H+1]}|| < \infty, \\ \frac{\partial f_3}{\partial I_H} = -\frac{bP_V(S_H-1)}{[V_0+P_V]\Theta_H[I_H+1]^2}, & ||\frac{\partial f_3}{\partial I_H}|| = ||-\frac{bP_V(S_H-1)}{[V_0+P_V]\Theta_H[I_H+1]^2}|| < \infty, \\ \frac{\partial f_3}{\partial p_0} = \alpha_0 - k_0 - \mu_0 - \alpha_h, & \left|\frac{\partial f_3}{\partial p_0}\right| = |\alpha_0 - k_0 - \mu_0 - \alpha_h| < \infty, \\ \frac{\partial f_3}{\partial P_H} = 0, & \left|\frac{\partial f_3}{\partial P_H}\right| = |0| < \infty, \\ \frac{\partial f_3}{\partial S_V} = 0, & \left|\frac{\partial f_3}{\partial S_V}\right| = |0| < \infty, \\ \frac{\partial f_3}{\partial I_V} = 0, & \left|\frac{\partial f_3}{\partial I_V}\right| = |0| < \infty, \\ \frac{\partial f_3}{\partial P_V} = \frac{bV_0(S_H-1)}{(V_0+P_V)^2\Theta_H(I_H+1)}, & ||\frac{\partial f_3}{\partial P_H}|| = ||\frac{bV_0(S_H-1)}{(V_0+P_V)^2\Theta_H(I_H+1)}|| < \infty. \end{cases}$$

Using the fourth equation from system (5)

$$\begin{cases} \frac{\partial f_4}{\partial S_H} = 0, & \left|\frac{\partial f_4}{\partial S_H}\right| = |0| < \infty, \\ \frac{\partial f_4}{\partial I_H} = \alpha_h p_0, & ||\frac{\partial f_4}{\partial I_H}|| = ||\alpha_h p_0|| < \infty, \\ \frac{\partial f_4}{\partial p_0} = \alpha_h(I_H+1), & ||\frac{\partial f_4}{\partial p_0}|| = ||\alpha_h(I_H+1)|| < \infty, \\ \frac{\partial f_4}{\partial P_H} = -\sigma_H, & \left|\frac{\partial f_4}{\partial P_H}\right| = |-\sigma_H| < \infty, \\ \frac{\partial f_4}{\partial S_V} = 0, & \left|\frac{\partial f_4}{\partial S_V}\right| = |0| < \infty, \\ \frac{\partial f_4}{\partial I_V} = 0, & \left|\frac{\partial f_4}{\partial I_V}\right| = |0| < \infty, \\ \frac{\partial f_4}{\partial P_V} = 0, & \left|\frac{\partial f_4}{\partial P_V}\right| = |0| < \infty. \end{cases}$$

We have the fifth equation from system (5) giving

$$\begin{cases} \frac{\partial f_5}{\partial S_H} = 0, & \left|\frac{\partial f_5}{\partial S_H}\right| = |0| < \infty, \\ \frac{\partial f_5}{\partial I_H} = 0, & \left|\frac{\partial f_5}{\partial I_H}\right| = |0| < \infty, \\ \frac{\partial f_5}{\partial p_0} = 0, & \left|\frac{\partial f_5}{\partial p_0}\right| = |0| < \infty, \\ \frac{\partial f_5}{\partial P_H} = -\frac{bH_0S_V}{(H_0+P_H)^2}, & \left|\frac{\partial f_5}{\partial P_H}\right| = || - \frac{bH_0S_V}{(H_0+P_H)^2}|| < \infty, \\ \frac{\partial f_5}{\partial S_V} = -\frac{bP_H}{H_0+P_H} - \mu_0, & \left|\frac{\partial f_5}{\partial S_V}\right| = || - \frac{bP_H}{H_0+P_H} - \mu_0|| < \infty, \\ \frac{\partial f_5}{\partial I_V} = 0, & \left|\frac{\partial f_5}{\partial I_V}\right| = |0| < \infty, \\ \frac{\partial f_5}{\partial P_V} = 0, & \left|\frac{\partial f_5}{\partial P_V}\right| = |0| < \infty. \end{cases}$$

The sixth equation from system (5) giving

$$\begin{cases} \frac{\partial f_6}{\partial S_H} = 0, & \left|\frac{\partial f_6}{\partial S_H}\right| = |0| < \infty, \\ \frac{\partial f_6}{\partial I_H} = 0, & \left|\frac{\partial f_6}{\partial I_H}\right| = |0| < \infty, \\ \frac{\partial f_6}{\partial p_0} = 0, & \left|\frac{\partial f_6}{\partial p_0}\right| = |0| < \infty, \\ \frac{\partial f_6}{\partial P_H} = \frac{bH_0S_V}{(H_0+P_H)^2}, & ||\frac{\partial f_6}{\partial P_H}|| = ||\frac{bH_0S_V}{(H_0+P_H)^2}|| < \infty, \\ \frac{\partial f_6}{\partial S_V} = \frac{bP_H}{H_0+P_H}, & ||\frac{\partial f_6}{\partial S_V}|| = ||\frac{bP_H}{H_0+P_H}|| < \infty, \\ \frac{\partial f_6}{\partial I_V} = -\mu_V - \delta_V, & \left|\frac{\partial f_6}{\partial I_V}\right| = |-\mu_V - \delta_V| < \infty, \\ \frac{\partial f_6}{\partial P_V} = 0, & \left|\frac{\partial f_6}{\partial P_V}\right| = |0| < \infty, \end{cases}$$

Finally, we have the seventh equation from system (5) giving

$$\begin{cases} \frac{\partial f_7}{\partial S_H} = 0, & \left|\frac{\partial f_7}{\partial S_H}\right| = |0| < \infty, \\ \frac{\partial f_7}{\partial I_H} = 0, & \left|\frac{\partial f_7}{\partial I_H}\right| = |0| < \infty, \\ \frac{\partial f_7}{\partial p_0} = 0, & \left|\frac{\partial f_7}{\partial p_0}\right| = |0| < \infty, \\ \frac{\partial f_7}{\partial P_H} = 0, & \left|\frac{\partial f_7}{\partial P_H}\right| = |0| < \infty, \\ \frac{\partial f_7}{\partial S_V} = 0, & \left|\frac{\partial f_7}{\partial S_V}\right| = |0| < \infty, \\ \frac{\partial f_7}{\partial I_V} = \alpha_V, & \left|\frac{\partial f_7}{\partial I_V}\right| = |\alpha_V| < \infty, \\ \frac{\partial f_7}{\partial P_V} = -\sigma_V, & \left|\frac{\partial f_7}{\partial P_V}\right| = |-\sigma_V| < \infty. \end{cases}$$

Since all partial derivatives are continuous and bounded, it invokes Theorem (3), suggesting that unique solutions exist for the model system (1) within the specified region D. This Theorem, which presumably pertains to the continuity and boundedness of partial derivatives, serves as a critical criterion for ensuring the well-posedness of the model. □

3.4 Equilibrium points

In this section, we determine the equilibrium points for the multiscale model system (1). This involves setting the system of equations to zero, seeking solutions that correspond to both the Disease-Free Equilibrium (DFE) and the Endemic Equilibrium (EE).

3.4.1 DFE of the multiscale moddel

The disease-free equilibrium point (DFE) of the embedded multiscale model (1) is derived by setting the system of equations to zero and assuming the absence of disease, which implies $I_H = p_0 = P_H = I_V = P_V = 0$. Therefore, the disease-free state is given by

$$E_0 = \left(\frac{\Lambda_H}{\mu_H}, 0, 0, 0, \frac{\Lambda_V}{\mu_V}, 0, 0\right)$$

3.4.2 EE of the multiscale model

The endemic point is when the pathogen level is above the minimum infection dose. The endemic equilibrium point (EE) of the embedded multiscale model (1) is determined by setting the system of equations to zero, signifying a steady state where the disease persists. Unlike the disease-free equilibrium, at the endemic equilibrium, variables such as I_H, p_0, P_H, I_V, P_V take non-zero values, indicating a stable presence of the disease within the population. Upon solving the model system (1), endemic equilibrium is therefore defined by

$$E_1 = (S_H^*, I_H^*, p_0^*, P_H^*, S_V^*, I_V^*, P_V^*),$$

with

$$\begin{aligned}
S_H^* &= \frac{\Lambda_H \left(P_V^* + V_0\right)}{bP_V^* + \mu_H P_V^* + V_0\mu_H}, \\
I_H^* &= \frac{bS_H^* P_V^*}{\left(P_V^* + V_0\right)\left(\delta_H + \mu_H\right)}, \\
p_0^* &= \frac{b\left(S_H^* - 1\right)P_V^*}{\Theta_H \left(I_H^* + 1\right)\left(P_V^* + V_0\right)\left(\alpha_h + k_0 + \mu_0 - \alpha_0\right)}, \\
P_H^* &= \frac{\alpha_h \left(I_H^* + 1\right) p_0^*}{\sigma_H}, \\
S_V^* &= \frac{\left(P_H^* + H_0\right)\Lambda_V}{bP_H^* + P_H^*\mu_V + H_0\mu_V}, \\
I_V^* &= \frac{bP_H^* S_V^*}{\left(P_H^* + H_0\right)\left(\delta_V + \mu_V\right)}, \\
P_V^* &= \frac{\alpha_V \left(I_V^* + 1\right)}{\sigma_V}.
\end{aligned}$$

3.4.3 Existence of EE model

P_V^* is the positive root of the cubic polynomial equation as follows,

$$g(P_V^*) = a_1 P_V^{*3} + a_2 P_V^{*2} + a_3 P_V^* + a_4 = 0, \tag{6}$$

where $a_1 \neq 0$, with

$$\begin{aligned}
a_1 &= H_0\Theta_H\sigma_H\mu_V\sigma_V\left(b+\mu_H\right)\left(\delta_V+\mu_V\right)\left(-\alpha_0+\alpha_h+k_0+\mu_0\right)\\
&\quad -b\alpha_h\sigma_V\left(b+\mu_V\right)\left(\delta_V+\mu_V\right)\left(b-\Lambda_H+\mu_H\right),\\
a_2 &= -H_0\Theta_H\sigma_H\alpha_V\mu_V\left(b+\mu_H\right)\left(\delta_V+\mu_V\right)\left(-\alpha_0+\alpha_h+k_0+\mu_0\right)\\
&\quad +H_0V_0\Theta_H\sigma_H\mu_V\sigma_V\left(b+\mu_H\right)\left(\delta_V+\mu_V\right)\left(-\alpha_0+\alpha_h+k_0+\mu_0\right)\\
&\quad -bV_0\alpha_h\sigma_V\left(b+\mu_V\right)\left(\mu_H-\Lambda_H\right)\left(\delta_V+\mu_V\right)\\
&\quad +b\alpha_h\alpha_V\left(b-\Lambda_H+\mu_H\right)\left(\delta_V\left(b+\mu_V\right)+b\Lambda_V+\mu_V\left(b+\mu_V\right)\right)\\
&\quad +H_0V_0\Theta_H\mu_H\sigma_H\mu_V\sigma_V\left(\delta_V+\mu_V\right)\left(-\alpha_0+\alpha_h+k_0+\mu_0\right),\\
a_3 &= -H_0V_0\Theta_H\sigma_H\alpha_V\mu_V\left(b+\mu_H\right)\left(\delta_V+\mu_V\right)\left(-\alpha_0+\alpha_h+k_0+\mu_0\right)\\
&\quad +bV_0\alpha_h\alpha_V\left(\mu_H-\Lambda_H\right)\left(\delta_V\left(b+\mu_V\right)+b\Lambda_V+\mu_V\left(b+\mu_V\right)\right)\\
&\quad +H_0V_0^2\Theta_H\mu_H\sigma_H\mu_V\sigma_V\left(\delta_V+\mu_V\right)\left(-\alpha_0+\alpha_h+k_0+\mu_0\right)\\
&\quad -H_0V_0\Theta_H\mu_H\sigma_H\alpha_V\mu_V\left(\delta_V+\mu_V\right)\left(-\alpha_0+\alpha_h+k_0+\mu_0\right),\\
a_4 &= -H_0V_0^2\Theta_H\mu_H\sigma_H\alpha_V\mu_V\left(\delta_V+\mu_V\right)\left(-\alpha_0+\alpha_h+k_0+\mu_0\right).
\end{aligned}$$

The equation $g(P_V^*)$ is a third-order equation, it is very difficult to find explicit expressions of positive roots of the equation explicitly in terms of the other parameters involved in the system. All parameters are non-negative for $t > 0$; it then follows that positive roots of the polynomial lie on the sign a_1, a_2, a_3, and a_4. Possible number of positive roots of the cubic equation in (6) by using Descartes' rule of signs.

Table 3 Number of possible positive real roots of $g(P_V^*)$.

Case	a_1	a_2	a_3	a_3	Possible positive roots
1	+	+	+	+	0 (No positive roots exist)
2	+	+	+	-	1
3	+	+	-	+	2
4	+	+	-	-	2
5	+	-	+	+	2
6	+	-	-	+	2
7	+	-	-	-	1
8	-	-	-	-	0 (No positive roots exist)
9	-	+	+	+	1
10	-	+	-	+	3 or 1 (at most three positive roots exist)
11	-	-	+	+	1
12	-	-	-	+	1
13	+	-	+	-	3 or 1 (at most three positive roots exist)

The model system can either have $0, 1, 2$, or 3 roots depending on sign of the coefficient. When all of the coefficients have the same sign therefore no root exist, otherwise at least one root exist when the coefficients have different signs. We can

conclude that the endemic equilibrium point of the model system (1) does exist provide the signs of the coefficients are met.

3.5 Reproductive number

In this section, determining the reproductive number, denoted as R_0, is crucial for analyzing the stability of equilibrium points. R_0 serves as a threshold that helps ascertain the potential for secondary infections resulting from a single infection. We employ the next-generation operator to compute R_0 for the embedded multiscale model, following the methodology outlined in [23].

The embedded multiscale model system (1) needs to be expressed in a specific form conducive to calculating R_0. This formulation is typically achieved by structuring the equations to highlight the contribution of new infections and their subsequent impact on the disease transmission dynamics. The embedded multiscale model system (1) must be written in the form

$$\begin{cases} \frac{dX}{dt} &= f(X,Y,Z), \\ \frac{dY}{dt} &= g(X,Y,Z), \\ \frac{dZ}{dt} &= h(X,Y,Z), \end{cases}$$

where

(i) $X = (S_H, S_V)$ represents all compartments of individuals who are not infected,

(ii) $Y = (I_H, p_0, I_V)$ represents all compartments of individuals who are infected who are not capable of infecting others,

(iii) $Z = (P_H, P_V)$ represents all compartments of individuals who are infected who are capable of infecting others.

The disease free equilibrium of the model is given by

$$\overline{U}_0 = \left(\frac{\Lambda_H}{\mu_H}, 0, 0, 0, \frac{\Lambda_V}{\mu_V}, 0, 0\right).$$

Following [23], we let

$$\tilde{g}(X^*, Z) = (\tilde{g}_1(X^*, Z), \tilde{g}_2(X^*, Z), \tilde{g}_3(X^*, Z)),$$

with

$$\begin{cases} \tilde{g}_1(X^*, Z) &= \frac{b\Lambda_H P_V}{\mu_H(\mu_H+\delta_H)(V_0+P_V)}, \\ \tilde{g}_2(X^*, Z) &= \frac{bP_V(\delta_H+\mu_H)(\Lambda_H-\mu_H)}{\Theta_H(\alpha_h+k_0+\mu_0-\alpha_0)[P_V(b\Lambda_H+\mu_H(\delta_H+\mu_H))+V_0\mu_H(\delta_H+\mu_H)]}, \\ \tilde{g}_3(X^*, Z) &= \frac{bP_H\Lambda_V}{\mu_V(H_0+P_H)(\delta_V+\mu_V)}. \end{cases}$$

We then define the

$$h(X, Y, Z) = (h_1(X, Y, Z), h_2(X, Y, Z)),$$

with

$$\begin{cases} h_1(X, Y, Z) &= \frac{b\alpha_h(\Lambda_H-\mu_H)P_V}{\Theta_H\mu_H(\alpha_h+k_0+\mu_0-\alpha_0)(P_V+V_0)} - P_H\sigma_H, \\ h_2(X, Y, Z) &= \frac{b\alpha_V\Lambda_V P_H}{\mu_V(\delta_V+\mu_V)(P_H+H_0)} - P_V\sigma_V. \end{cases}$$

The matrix

$$A = D_Z h(X^*, \tilde{g}(X^*, 0), 0) = \begin{bmatrix} -\sigma_H & \frac{b\alpha_h(\Lambda_H-\mu_H)}{V_0\Theta_H\mu_H(\alpha_h+k_0+\mu_0-\alpha_0)} \\ \frac{b\alpha_V\Lambda_V}{H_0\mu_V(\delta_V+\mu_V)} & -\sigma_V \end{bmatrix},$$

such that it can be written as $A = M - D$,

$$M = \begin{bmatrix} 0 & \frac{b\alpha_h(\Lambda_H-\mu_H)}{V_0\Theta_H\mu_H(\alpha_h+k_0+\mu_0-\alpha_0)} \\ \frac{b\alpha_V\Lambda_V}{H_0\mu_V(\delta_V+\mu_V)} & 0 \end{bmatrix},$$

$$D = \begin{bmatrix} \sigma_H & 0 \\ 0 & \sigma_V \end{bmatrix}.$$

The basic reproductive number of the embedded multiscale model system is given by the dominant eigenvalue of the matrix MD^{-1} that is $R_0 = \rho(MD^{-1})$, therefore

$$R_0 = \sqrt{\left[\frac{\alpha_h(\Lambda_H-\mu_H)}{H_0\Theta_H\mu_H\sigma_H(\alpha_h+k_0+\mu_0-\alpha_0)}\right]\left[\frac{b^2\alpha_V\Lambda_V}{V_0\mu_V\sigma_V(\delta_V+\mu_V)}\right]}. \tag{7}$$

Which can be written as

$$R_0 = \sqrt{R_{0H}}\sqrt{R_{0V}},$$

where

$$R_{0H} = \frac{\alpha_h(\Lambda_H-\mu_H)}{H_0\Theta_H\mu_H\sigma_H(\alpha_h+k_0+\mu_0-\alpha_0)},$$

$$R_{0V} = \frac{b^2\alpha_V\Lambda_V}{V_0\mu_V\sigma_V(\delta_V+\mu_V)}.$$

For R_0 to exist, the following conditions have to hold: $\alpha_h + k_0 + \mu_0 > \alpha_0$ and $\Lambda_H - \mu_H > 0$. Therefore,

$$\frac{\alpha_h + k_0 + \mu_0}{\alpha_0} > 1, \qquad \frac{\Lambda_H}{\mu_H} > 1.$$

To understand biological meaning we observe that the overall parasite decreasing rate should be greater than the parasite growth rate for the disease to potentially infect secondary hosts. To satisfy the boundary conditions, the growth rate should always be less than the rate at which p_0 is being removed from the system. It is also necessary to ensure that human recruitment is higher than the natural death of humans.

The analysis leads to the conclusion that the reproduction number (7) for the embedded multiscale model is a function of both the between-host scale and within-host scale parameters.

3.6 Local stability of DFE

This subsection presents the local stability of the Disease-Free Equilibrium (DFE) of the embedded multiscale model system (1). The model system's equations are linearized to obtain the Jacobian matrix. Subsequently, we evaluate the Jacobian matrix at the disease-free equilibrium, denoted as E_0. The Jacobian matrix of the embedded model system (1) evaluated at the disease-free equilibrium point (E_0) is given by

$$J(E_0) = \begin{pmatrix} -\mu_H & 0 & 0 & 0 & 0 & 0 & -\frac{b\Lambda_H}{V_0\mu_H} \\ 0 & -\delta_H-\mu_H & 0 & 0 & 0 & 0 & \frac{b\Lambda_H}{V_0\mu_H} \\ 0 & 0 & \alpha_0-\alpha_h-k_0-\mu_0 & 0 & 0 & 0 & \frac{b(\Lambda_H-\mu_H)}{V_0\Theta_H\mu_H} \\ 0 & 0 & \alpha_h & -\sigma_H & 0 & 0 & 0 \\ 0 & 0 & 0 & -\frac{b\Lambda_V}{H_0\mu_V} & -\mu_V & 0 & 0 \\ 0 & 0 & 0 & \frac{b\Lambda_V}{H_0\mu_V} & 0 & -\delta_V-\mu_V & 0 \\ 0 & 0 & 0 & 0 & 0 & \alpha_V & -\sigma_V \end{pmatrix}. \tag{8}$$

In order to determine the stability of DFE, the eigenvalues of the Jacobian matrix given by (8) are determined. The characteristic equation for the eigenvalues is given by

$$(-\mu_H-\lambda)((-\delta_H-\mu_H)-\lambda)(-\mu_V-\lambda)[\lambda^4+\phi_1\lambda^3+\phi_2\lambda^2+\phi_3\lambda+\phi_4] = 0, \tag{9}$$

where

$$\begin{aligned}
\phi_1 &= (\alpha_h+k_0-\alpha_0+\mu_0)+(\sigma_H+\delta_V+\mu_V+\sigma_V),\\
\phi_2 &= (\alpha_h+k_0-\alpha_0+\mu_0)(\sigma_H+\delta_V+\mu_V+\sigma_V)+(\delta_V+\mu_V)(\sigma_H+\sigma_V)+\sigma_H\sigma_V,\\
\phi_3 &= (\alpha_h+k_0+\mu_0-\alpha_0)\left[(\delta_V+\mu_V)(\sigma_H+\sigma_V)+\sigma_H\sigma_V\right]+\sigma_H\sigma_V(\delta_V+\mu_V),\\
\phi_4 &= \sigma_H\sigma_V(\delta_V+\mu_V)(\alpha_h+k_0+\mu_0-\alpha_0)(1-R_0).
\end{aligned}$$

From equation (9), it can be noted that there are three negative eigenvalues $(\mu_H, (\delta_H + \mu_H)$, and $\mu_V)$. To conclude the stability of DFE, Routh-Hurwitz criteria is used to determine the sign of the coefficients of the polynomial of the fourth order. The Routh-Hurwitz criterion states that an equilibrium point of a model system is stable if and only if the determinants of the characteristic (9) are positive, that is

$$\det(H_j) > 0; j = 1, 2, 3, 4$$

where

$$\begin{cases} H_1 = \begin{pmatrix} \phi_1 \end{pmatrix}, H_2 = \begin{pmatrix} \phi_1 & 1 \\ \phi_3 & \phi_2 \end{pmatrix}, \\ H_3 = \begin{pmatrix} \phi_1 & 1 & 0 \\ \phi_3 & \phi_2 & \phi_1 \\ 0 & \phi_4 & \phi_3 \end{pmatrix}, \\ H_4 = \begin{pmatrix} \phi_1 & 1 & 0 & 0 \\ \phi_3 & \phi_2 & \phi_1 & 1 \\ 0 & \phi_4 & \phi_3 & \phi_2 \\ 0 & 0 & 0 & \phi_4 \end{pmatrix}. \end{cases} \tag{10}$$

When Routh-Hurwitz criterion is applied to the expressions in equation (10), therefore we have the following

$$\begin{aligned} D_1 &= \phi_1 > 0, \\ D_2 &= \phi_1\phi_2 - \phi_3 > 0, \\ D_3 &= \phi_1\phi_2\phi_3 - \phi_3^2 - \phi_1^2\phi_4 > 0, \\ D_4 &= \phi_1\phi_2\phi_3\phi_4 - \phi_3^2\phi_4 - \phi_1^2\phi_4^2 > 0. \end{aligned}$$

To guarantee the local stability of the model system's disease-free equilibrium point (1), the following conditions must be met:

$$\begin{cases} C1 : \phi_1 > 0, \phi_2 > 0, \phi_3 > 0, \phi_4 > 0, \phi_5 > 0, \\ C2 : \phi_1\phi_2\phi_3 > \phi_3^2 + \phi_1^2\phi_4. \end{cases}$$

We can conclude that from (9) and (10), the coefficients of the polynomial are greater than zero whenever $R_0 < 1$. Additionally, the stipulated condition for a positive solution $\alpha_0 < k_0 + \mu_0 + \alpha_h$ is satisfied. The results can be concluded using Theorem 5.

Theorem 5. *The disease-free equilibrium point of the embedded multiscale model system (1) is locally stable whenever* $R_0 < 1$.

3.7 Local stability of EE

This subsection presents the local asymptotic stability of the endemic equilibrium point of the model system (1). Similarly, we use the Jacobian matrix evaluated at endemic equilibrium point denoted by E_1. The Jacobian matrix at the endemic equilibrium point is given by

$$J(E_1) = \begin{pmatrix} -L_1-\mu_H & 0 & 0 & 0 & 0 & 0 & -L_2 \\ L_1 & -\delta_H-\mu_H & 0 & 0 & 0 & 0 & L_2 \\ L_3 & L_4 & L_5 & 0 & 0 & 0 & L_6 \\ 0 & p_0\alpha_h & \alpha_h(I_H^*+1) & -\sigma_H & 0 & 0 & 0 \\ 0 & 0 & 0 & -L_7 & -L_8-\mu_V & 0 & 0 \\ 0 & 0 & 0 & L_7 & L_8 & -\delta_V-\mu_V & 0 \\ 0 & 0 & 0 & 0 & 0 & \alpha_V & -\sigma_V \end{pmatrix}, \tag{11}$$

where

$$\begin{cases} L_1 = \frac{bP_V^*}{P_V^*+V_0}, & L_2 = \frac{bV_0S_H^*}{(P_V^*+V_0)^2}, \\ L_3 = \frac{bP_V^*}{(P_V^*+V_0)(I_H^*+1)\Theta_H}, & L_4 = \frac{bP_V^*(S_H^*-1)}{(P_V^*+V_0)(I_H^*+1)^2\Theta_H} \\ L_5 = \alpha_0-\alpha_h-k_0-\mu_0, & L_6 = \frac{bV_0(S_H^*-1)}{(P_V^*+V_0)^2(I_H^*+1)\Theta_H}, \\ L_7 = \frac{bH_0S_V^*}{(H_0+P_H^*)^2}, & L_8 = \frac{bP_H^*}{H_0+P_H^*}. \end{cases}$$

The eigenvalues of the Jacobian matrix (11) are used to determine the stability of EE, and the sign of the eigenvalues is found by using the Gershgorin theorem described in [24]. Applying the Gershgorin theorem to the matrix $J(E_1)$ of size 7×7, we get the following inequality:

$$\frac{bP_V\left(\Theta_H\left(I_H^*+1\right)+1\right)}{\Theta_H\left(I_H^*+1\right)\left(P_V^*\left(b+\mu_H\right)+V_0\mu_H\right)}<1, \qquad \frac{bV_0\left(S_H^*-1\right)}{\Theta_H\left(I_H^*+1\right)\left(P_V^*+V_0\right)^2\sigma_V}<1, \tag{12}$$

$$\frac{p_0\alpha_h\Theta_H(P_V^*+V_0)(I_H^*+1)^2-bP_V^*(S_H^*-1)}{(P_V^*+V_0)(I_H^*+1)^2\Theta_H(\delta_H+\mu_H)}<1, \qquad \frac{\alpha_h(I_H^*+1)}{\alpha_0-\alpha_h-k_0-\mu_0}<1, \tag{13}$$

$$\frac{\alpha_V}{\delta_V+\mu_V}<1, \qquad 0<\sigma_H, \qquad 0<\mu_V. \tag{14}$$

The condition $\alpha_V<\delta_V+\mu_V$ is identified as crucial for stability, indicating that the stability of E_1 hinges on the relationship between the parasites excreted by the vector α_V and the combined rate of decrease of the vector $\delta_V+\mu_V$. To explain further, when the excretion of parasites by the vector is less than the overall diminishing rate

of the vector population, that is, $\alpha_V < \delta_V + \mu_V$, the equilibrium point E_1 is asserted to be locally stable. It is imperative to note that the conditions outlined in equations (12) - (14) collectively contribute to the local stability of E_1.

4 Optimal control problem

This section outlines a comprehensive strategy for controlling Human African Trypanosomiasis (HAT) disease, employing a time-dependent control approach within the framework of an embedded multiscale model system. The proposed strategy involves the introduction of two time-dependent controls: $u_1(t)$, representing the treatment applied to the infected human population, and $u_2(t)$, denoting vector traps. The optimal control problem is formulated by appropriately fixing these controls to achieve the most effective disease control outcomes. The optimal control problem is given by

$$\begin{cases} \frac{dS_H(t)}{dt} &= \Lambda_H - \frac{bP_V S_H}{V_0+P_V} - \mu_H S_H, \\ \frac{dI_H(t)}{dt} &= \frac{bP_V S_H}{V_0+P_V} - \mu_H I_H - \delta_H I_H, \\ \frac{dp_0(t)}{dt} &= \frac{bP_V[S_H-1]}{[V_0+P_V]\Theta_H[I_H+1]} + \alpha_0(1-u_1(t))p_0 - k_0 p_0 - \mu_0 p_0 - \alpha_h p_0, \\ \frac{dP_H(t)}{dt} &= (I_H+1)\alpha_h p_0 - \sigma_H P_H, \\ \frac{dS_V(t)}{dt} &= \Lambda_V - \frac{bP_H S_V}{H_0+P_H} - \mu_V S_V - u_2(t)S_V, \\ \frac{dI_V(t)}{dt} &= \frac{bP_H S_V}{H_0+P_H} - \mu_V I_V - \delta_V I_V - u_2(t)I_V, \\ \frac{dP_V(t)}{dt} &= (I_V+1)\alpha_V - \sigma_V P_V. \end{cases} \tag{15}$$

Theorem 6. *There exist an optimal control* $u^* = (u_1^*, u_2^*, u_3^*)$ *such that*

$$\mathcal{J}(u_1^*, u_2^*) = \min_{(u_1,u_2)} J(u_1, u_2), \tag{16}$$

subject to the model system (15) with initial conditions in Table 1.

The objective function is given by

$$\mathcal{J}(u_1^*, u_2^*) = \int_0^{T_f} \left(A_1 p_0 + A_2 S_V + A_3 I_V + b_1 u_1^2 + b_2 . u_2^2\right) dt$$

The Lagrangian of the model (15) is given by

$$\mathcal{L}(p_0, S_V, I_V, u_1, u_2) = A_1 p_0 + A_2 S_V + A_3 I_V + b_1 u_1^2 + b_2 u_2^2.$$

The Pontryagin's maximum principle will be employed to determine the necessary and sufficient conditions for the optimal control problem (15) to hold. The principle

will convert the model (15) and the equation (16) to a minimization problem pointwise Hamiltonian ($\mathcal{H}$) with respect to u_1 and u_2. The Hamiltonian function will be defined by

$$\begin{aligned}
\mathcal{H} &= A_1p_0 + A_2S_V + A_3I_V + b_1u_1^2 + b_2u_2^2 + \lambda_1\frac{dS_H}{dt} + \lambda_2\frac{dI_H}{dt} + \lambda_3\frac{dp_0}{dt} + \lambda_4\frac{dP_H}{dt} + \lambda_5\frac{dS_V}{dt} \\
&= +\lambda_6\frac{dI_V}{dt} + \lambda_7\frac{dP_V}{dt} \\
&= A_1p_0 + A_2S_V + A_3I_V + b_1u_1^2 + b_2u_2^2 + \lambda_1\left[\Lambda_H - \frac{bP_VS_H}{V_0+P_V} - \mu_HS_H\right] \\
&\quad +\lambda_3\left[\frac{bP_V[S_H-1]}{[V_0+P_V]\Theta_H[I_H+1]} + \alpha_0(1-u_1(t))p_0 - k_0p_0 - \mu_0p_0 - \alpha_hp_0\right] \\
&\quad +\lambda_2\left[\frac{bP_VS_H}{V_0+P_V} - \mu_HI_H - \delta_HI_H\right] + \lambda_4\Big[(I_H+1)\alpha_hp_0 - \sigma_HP_H\Big] \\
&\quad +\lambda_5\left[\Lambda_V - \frac{bP_HS_V}{H_0+P_H} - \mu_VS_V - u_2(t)S_V\right] + \lambda_6\left[\frac{bP_HS_V}{H_0+P_H} - \mu_VI_V - \delta_VI_V - u_2I_V\right] \\
&\quad +\lambda_7\Big[(I_V+1)\alpha_V - \sigma_VP_V\Big],
\end{aligned}$$

where $\lambda_1, \lambda_2, \lambda_3, \lambda_4, \lambda_5, \lambda_6, \lambda_7$ are adjoint state variables.

Theorem 7. *Given the optimal control u_1, u_2, and solutions $S_H^*, I_H^*, p_0^*, P_H^*, S_V^*, I_V^*, P_V^*$ of the model system (15) that optimizes $J(u_i)$ over u, then there exist adjoint variables $\lambda_1, \lambda_2, \lambda_3, \lambda_4, \lambda_5, \lambda_6, \lambda_7$ satisfying $\frac{\partial\lambda_i}{dt} = \frac{-\partial\mathcal{H}}{\partial i}$, $\lambda_i(t) = 0$, where $i = S_H, I_H, p_0, P_H, S_V, I_V, P_V$.*

The adjoint state variables are given by

$$\begin{cases}
\frac{d\lambda_1}{dt} &= \mu_H\lambda_1 + \frac{bP_V^*}{V_0+P_V^*}(\lambda_1-\lambda_2) - \frac{bP_V^*}{(V_0+P_V^*)\Theta_H(I_H^*+1)}\lambda_3, \\
\frac{d\lambda_2}{dt} &= (\mu_H+\delta_H)\lambda_2 - \alpha_hp_0^*\lambda_4 - \frac{bP_V^*(S_H-1)}{(V_0+P_V^*)\Theta_H(I_H^*+1)^2}\lambda_3, \\
\frac{d\lambda_3}{dt} &= -A_1 + (k_0+\mu_0+\alpha_h)\lambda_3 - \alpha_0(1-u_1(t))\lambda_3 - \alpha_h(I_H^*+1)\lambda_4, \\
\frac{d\lambda_4}{dt} &= \sigma_H\lambda_4 + \frac{bH_0S_V^*}{(H_0+P_H^*)^2}(\lambda_5-\lambda_6), \\
\frac{d\lambda_5}{dt} &= -A_2 + (\mu_V+u_2(t))\lambda_5 + \frac{bP_H^*}{H_0+P_H^*}(\lambda_5-\lambda_6), \\
\frac{d\lambda_6}{dt} &= -A_3 + (\mu_V+\delta_V+u_2(t))\lambda_6 - \alpha_V\lambda_7, \\
\frac{d\lambda_7}{dt} &= \frac{bV_0S_H^*}{(V_0+P_V^*)^2}(\lambda_1-\lambda_2) - \frac{bV_0(S_H^*-1)}{(V_0+P_V^*)^2\Theta_H(I_H^*+1)}\lambda_3 + \sigma_V\lambda_7.
\end{cases}$$

The transversality solutions $\lambda_1 = 0, \lambda_2 = 0, \lambda_3 = 0, \lambda_4 = 0, \lambda_5 = 0, \lambda_6 = 0, \lambda_7 = 0$, *and the control* u *satisfying the optimality conditions given by* $\frac{\partial \mathcal{H}}{\partial u_i} = 0$, $i = 1, 2$

$$\begin{cases} \frac{\partial H}{\partial u_1^*} &= 2b_1 u_1^* - \alpha_0 p_0 \lambda_3 = 0, \\ \frac{\partial H}{\partial u_2^*} &= 2b_2 u_2^* - S_V^* \lambda_4 - I_V \lambda_6 = 0. \end{cases} \tag{17}$$

Solving equation (17), therefore the optimal control is given by

$$\begin{cases} u_1^* &= \frac{\alpha_0 p_0^* \lambda_3}{2b_1}, \\ u_2^* &= \frac{S_V^* \lambda_4 + I_V^* \lambda_6}{2b_2}. \end{cases}$$

Consider the control bounds, then we get

$$\begin{cases} u_1^* &= \max\left\{0, \min\left(1, \frac{\alpha_0 p_0^* \lambda_3}{2b_1}\right)\right\}, \\ u_2^* &= \max\left\{0, \min\left(1, \frac{S_V^* \lambda_4 + I_V^* \lambda_6}{2b_2}\right)\right\}. \end{cases}$$

5 Results and discussion of numerical simulations

In this section, we delve into the numerical solutions of the embedded multiscale model (1), aiming to explore the dynamics of the Human African Trypanosomiasis (HAT) disease. The investigation entails demonstrating the reciprocal influence of within-host parameters on between-host dynamics and vice versa through numerical simulations. Furthermore, the dynamics of the HAT disease are examined under scenarios with and without implementation of control measures.

The initial conditions for the state variables are outlined in Table 1 and The parameter values employed in these numerical simulations are detailed in Table 2, offering the necessary inputs to drive the model and observe its behavior under various scenarios. These numerical simulations are crucial for gaining insights into the complex interplay of factors influencing the dynamics of HAT, enabling a comprehensive understanding of the disease's behavior in different contexts.

5.1 Influence of within-host on the between-host disease transmission

In this subsection, we present numerical simulations demonstrating the influence of the within-host scale on certain variables of the embedded multiscale model (1). Figures 2 to 9 illustrate the impact of variations of two within-host parameters (α_0, k_0) on the dynamics of four key between-host variables (I_H, P_H, I_V, P_V). The parameter values employed for parasite growth rate are α_0: $\alpha_0 = 0.05, \alpha_0 = 0.10$, and $\alpha_0 = 0.9$, while the other parameter represents the killing effect of the immune system with values

$k_0 = 0.045$ and $k_0 = 0.5$. Variations in parasite growth rate significantly influence disease transmission dynamics, as shown in Figure 2 shows a significant increase on the infected human population. Figure 3 exhibits a notable influence, indicating that an increase in α_0 corresponds to a noticeable rise in the reservoir within the human community. Therefore, interventions that reduce parasite growth rates contribute to minimizing disease in the human population.

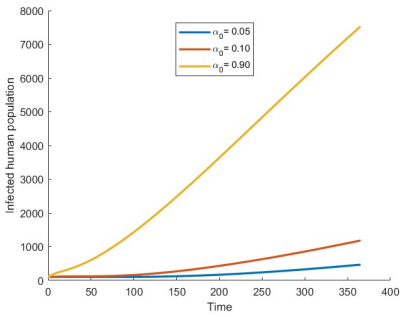

Fig. 2 Effect of α_0 on infected human population

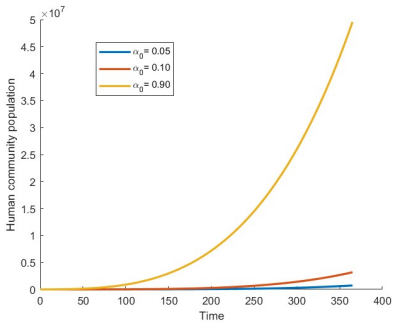

Fig. 3 Effect of α_0 on human community population

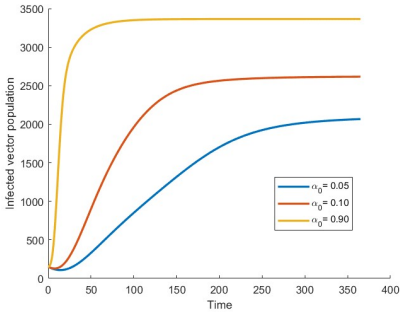

Fig. 4 Effect of α_0 on infected vector population

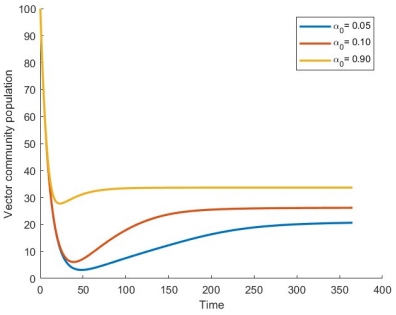

Fig. 5 Effect of α_0 on vector community population

Figure 4 shows an increase in the initial days and reaching its peak after 100 days it then become stable. In Figure 5 we notice a significant decline on the vector community population after 50 days and reach a stable state. The Figure 6-9 shows graphs of numerical solutions of model system (1) showing variation of I_H, P_H, I_V, P_V for the two different values of the immune killing effect $k_0 : k_0 = 0.045$, and $k_0 = 0.45$.

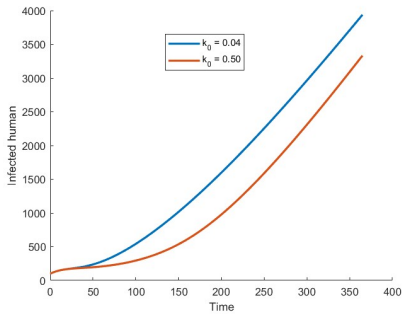

Fig. 6 Effect of k_0 on infected vector population

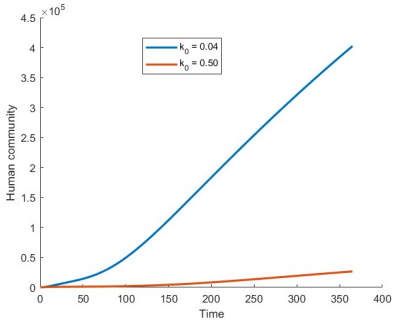

Fig. 7 Effect of k_0 on vector community population

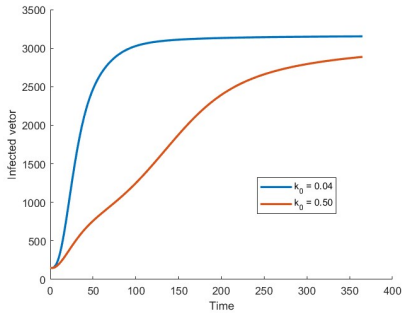

Fig. 8 Effect of k_0 on infected vector population

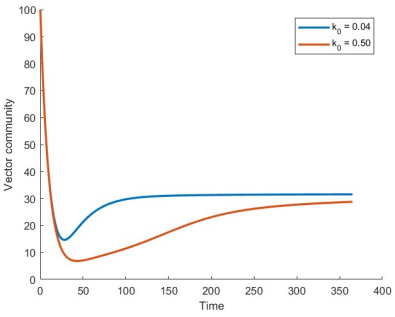

Fig. 9 Effect of k_0 on vector community population

This influence shows that the increasing killing effect of the immune system ensures a decrease in the between-host variables (I_H, P_H, I_V, and P_V). The results confirm that the within-host scale continuously influences the HAT disease and the HAT population dynamics throughout the infection.

5.2 Influence of between-host on the within-host

In this subsection, we present the solution profile, illustrating variations in the parasite population when we use different values of b and μ_V. The selected values for b: $b = 0.01, b = 0.33$, and $b = 0.50$, and μ_V: $\mu_V = 0.03, 0.10$, and $\mu_V = 0.50$. Figure 10 demonstrates that as the biting rate, b on the between-host scale increases, the parasite population shows a noticeable rise. Conversely, an increase in μ_V results in a decrease in the parasite population. Based on this observation, it can be concluded that the between-host scale influences the within-host scale.

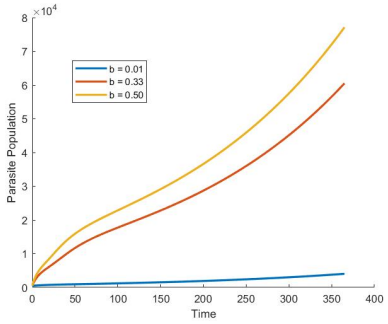

Fig. 10 Effect of biting rate on parasite population

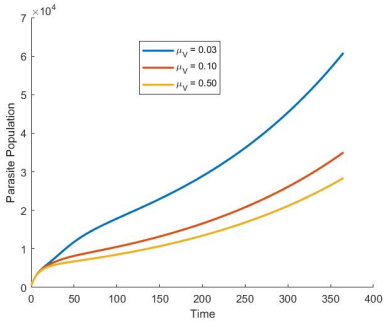

Fig. 11 Effect of μ_V on parasite population

5.3 Optimal control simulations

In this section, we present the numerical solutions of the embedded multiscale model (1) to examine the dynamics of HAT disease both with and without control measures. The constants are defined as $A_1 = 1, A_2 = 2, A_3 = 2, b_1 = 2$, and $b_2 = 10$. Upon implementing the two control measures, it is observed that the populations of infected humans, parasites, the human community, susceptible vectors, infected vectors, and vector communities decrease while the susceptible human population increases. This trend is evident in Figures 12 to 19. The population numbers decrease rapidly with the two control interventions compared to the results without optimal control.

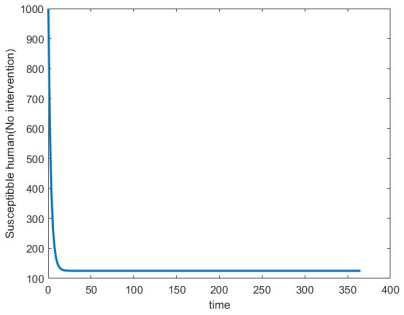

Fig. 12 Susceptible human population dynamics without control

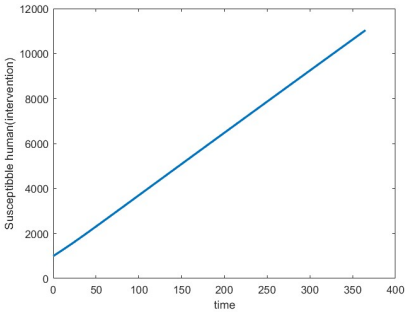

Fig. 13 Susceptible human population dynamics with control

The results from Figures 12 to 19 indicate that applying optimal controls u_1 and u_2 yields preferable outcomes compared to scenarios without optimal control measures. The control strategy ensuring the reduction of the variable is shown in Figure 20 and

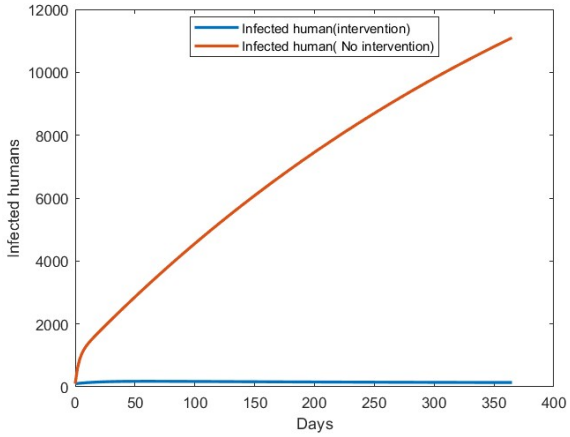

Fig. 14 Infected human population disease dynamics with and without control.

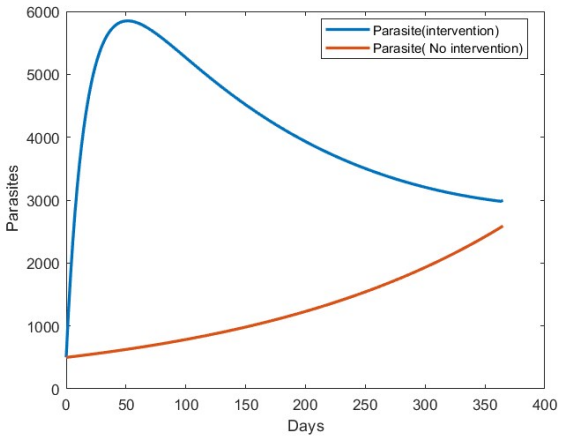

Fig. 15 Parasite population dynamics with and without control.

Figure 21. As a result of these results, the optimal control strategy outlined in Figure 20 and Figure 21 appears to reduce HAT disease numbers within a short time frame.

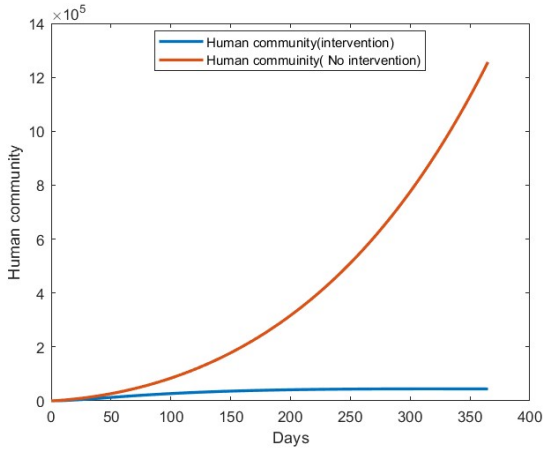

Fig. 16 Human reservoir population dynamics with and without control.

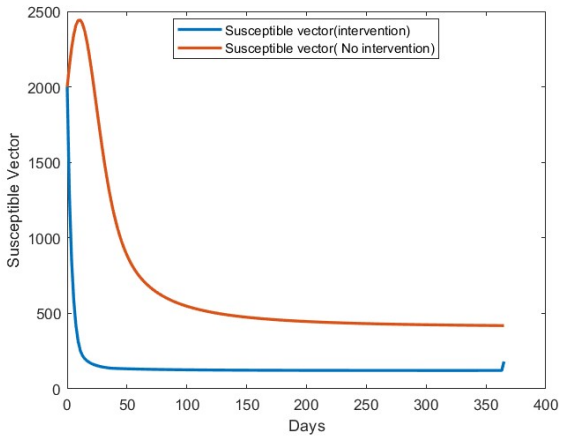

Fig. 17 Susceptible vector population dynamics with and without control.

6 Conclusions

This study focuses on developing an embedded multiscale model (1) to study HAT transmission dynamics. As presented herein, the model encompasses infectiousness and disease transmission across both the between-host and within-host scales. Two equilibrium points, namely disease-free and endemic points, were identified. Through the analysis of the reproduction number R_0, both equilibria were established as locally asymptotically stable.

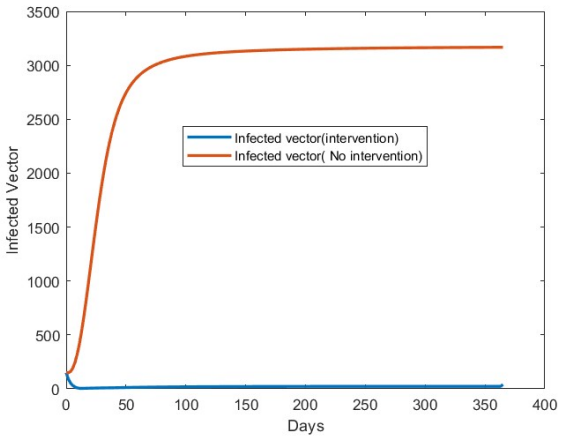

Fig. 18 Infected vector population dynamics with and without control.

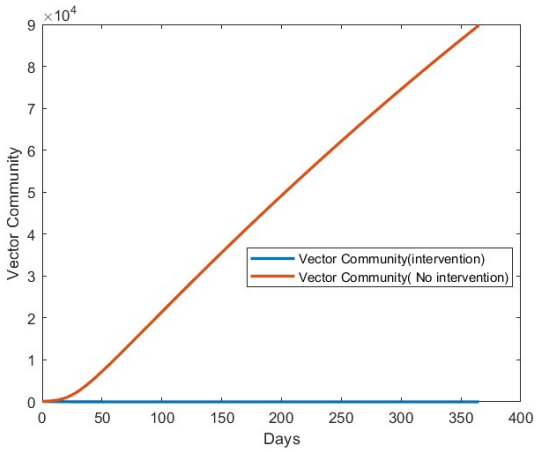

Fig. 19 Vector reservoir population dynamics

Two control functions were introduced to control the disease dynamics of the multi-scale model, effectively governing the variables S_H, I_H, p_0, P_H, I_V, and P_V. Treatment and vector traps are prescribed as control measures, and their impact on disease dynamics has been thoroughly investigated. Applying Pontryagin's maximum principle was instrumental in determining the optimal strategy for disease control.

The study successfully demonstrated the efficiency of the two control measures and their visible impact on the dynamics of different populations. Notably, the numerical solutions underscored that once infection has taken root within the host, the parasite

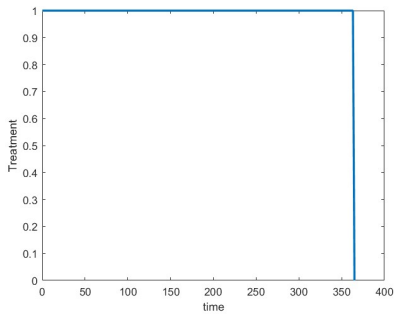

Fig. 20 Treatment profile ensuring optimal solutions

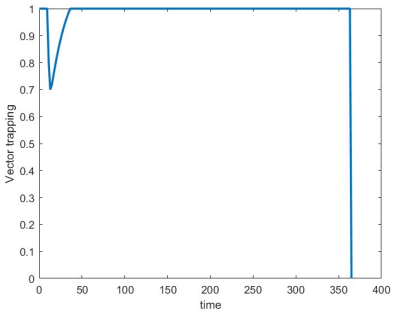

Fig. 21 Vector trapping profile ensuring optimal solutions

growth rate plays a pivotal role in sustaining the dynamics of HAT disease. Furthermore, the results highlighted that implementing two commonly utilized control measures could reduce disease prevalence, particularly in the early stages of infection.

The embedded multiscale model developed in this study contributes valuable insights into super-infection dynamics and the reciprocal influence between parasite growth at the within-host and between-host scales.

Acknowledgments

The support of the DSI-NRF Centre of Excellence in Mathematical and Statistical Sciences (CoE-MaSS) and the University of Kwazulu-Natal, School of Mathematics, Statistics and Computer Science, Pietermaritzburg Campus towards this research is hereby acknowledged. Opinions expressed and conclusions arrived at, are those of the author and are not necessarily to be attributed to the CoE.

Data availability

The datasets generated during and/or analysed during the current study are available from the corresponding author on reasonable request.

References

[1] Garira, W., Chirove, F.: A general method for multiscale modelling of vector-borne disease systems. Interface Focus **10**(1), 20190047 (2020)

[2] (WHO), W.H.O.: Trypanosomiasis, human African (sleeping sickness) (2023). https://www.who.int/news-room/fact-sheets/detail/trypanosomiasis-human-african-(sleeping-sickness) Accessed 2023-12-06

[3] Artzrouni, M., Gouteux, J.-P.: A compartmental model of sleeping sickness in central africa. Journal of Biological Systems **4**(04), 459–477 (1996)

[4] Pandey, A., Atkins, K.E., Bucheton, B., Camara, M., Aksoy, S., Galvani, A.P., Ndeffo-Mbah, M.L.: Evaluating long-term effectiveness of sleeping sickness control measures in guinea. Parasites & vectors **8**, 1–10 (2015)

[5] Stone, C.M., Chitnis, N.: Implications of heterogeneous biting exposure and animal hosts on trypanosomiasis brucei gambiense transmission and control. PLoS computational biology **11**(10), 1004514 (2015)

[6] Ndondo, A., Munganga, J., Mwambakana, J., Saad-Roy, C., Driessche, P., Walo, R.: Analysis of a model of gambiense sleeping sickness in humans and cattle. Journal of biological dynamics **10**(1), 347–365 (2016)

[7] Gervas, H.E., Opoku, N.K.-D.O., Ibrahim, S., et al.: Mathematical modelling of human african trypanosomiasis using control measures. Computational and Mathematical Methods in Medicine **2018** (2018)

[8] Meisner, J., Barnabas, R.V., Rabinowitz, P.M.: A mathematical model for evaluating the role of trypanocide treatment of cattle in the epidemiology and control of trypanosoma brucei rhodesiense and t. b. gambiense sleeping sickness in uganda. Parasite epidemiology and control **5**, 00106 (2019)

[9] Liana, Y.A., Shaban, N., Mlay, G., Phibert, A.: African trypanosomiasis dynamics: Modelling the effects of treatment, education, and vector trapping. International Journal of Mathematics and Mathematical Sciences **2020**, 1–15 (2020)

[10] Odeniran, P.O., Onifade, A.A., MacLeod, E.T., Ademola, I.O., Alderton, S., Welburn, S.C.: Mathematical modelling and control of african animal trypanosomosis with interacting populations in west africa—could biting flies be important in main taining the disease endemicity? PLoS One **15**(11), 0242435 (2020)

[11] Aliee, M., Keeling, M.J., Rock, K.S.: Modelling to explore the potential impact of asymptomatic human infections on transmission and dynamics of african sleeping sickness. PLoS computational biology **17**(9), 1009367 (2021)

[12] Frank, S.A.: A model for the sequential dominance of antigenic variants in african trypanosome infections. Proceedings of the Royal Society of London. Series B: Biological Sciences **266**(1426), 1397–1401 (1999)

[13] Gjini, E., Haydon, D., Barry, J., Cobbold, C.: Critical interplay between parasite differentiation, host immunity, and antigenic variation in trypanosome infections. The American Naturalist **176**(4), 424–439 (2010)

[14] Liu, D., Albergante, L., Newman, T., Horn, D.: Faster growth with shorter antigens can explain a vsg hierarchy during african trypanosome infections: a feint attack by parasites. Scientific Reports **8**(1), 10922 (2018)

[15] Navarrete, D.J.: Parasites, clocks, and immunity: A within-host mathematical model of human african trypanosomiasis (2019)

[16] Garira, W.: A complete categorization of multiscale models of infectious disease systems. Journal of biological dynamics **11**(1), 378–435 (2017)

[17] Gjini, E., Haydon, D.T., Barry, J., Cobbold, C.A.: Linking the antigen archive structure to pathogen fitness in african trypanosomes. Proceedings of the Royal Society B: Biological Sciences **280**(1753), 20122129 (2013)

[18] Group, W.B.: Birth rate, crude (per 1,000 people) - Sub-Saharan Africa, Congo, Dem. Rep. (2024). https://data.worldbank.org/indicator/SP.DYN.CBRT.IN?locations=ZG-CD) Accessed 2024-08-17

[19] Makhuvha, M.-M.H. M.: Studying the effect of parasite switching in optimal control analysis of sleeping sickness. Letters in Biomathematics **10**(1), 207–233 (2023)

[20] Rock, K.S., Torr, S.J., Lumbala, C., Keeling, M.J.: Predicting the impact of intervention strategies for sleeping sickness in two high-endemicity health zones of the democratic republic of congo. PLoS neglected tropical diseases **11**(1), 0005162 (2017)

[21] Kajunguri, D., Hargrove, J.W., Ouifki, R., Mugisha, J., Coleman, P.G., Welburn, S.C.: Modelling the use of insecticide-treated cattle to control tsetse and trypanosoma brucei rhodesiense in a multi-host population. Bulletin of Mathematical biology **76**(3), 673–696 (2014)

[22] Sowole, S.O., Sangare, D., Ibrahim, A.A., Paul, I.A.: On the existence, uniqueness, stability of solution and numerical simulations of a mathematical model for measles disease. Int. J. Adv. Math **4**, 84–111 (2019)

[23] Castillo-Chavez, C., Blower, S., Driessche, P., Kirschner, D., Yakubu, A.-A.: Mathematical Approaches for Emerging and Reemerging Infectious Diseases: Models, Methods, and Theory vol. 126, (2002)

[24] Bejarano, I.-M.E. D., Gómez-Hernández, E.A.: A stability test for non linear systems of ordinary differential equations based on the gershgorin circles. Contemporary Engineering Sciences **11**(91), 4541–4548 (2018)

Chapter 5

Discussion and conclusion

The thesis endeavors to formulate deterministic mathematical models with the aim of comprehending disease transmission across various scales, spanning from within-host dynamics to between-host dynamics. The foundational premise for understanding the interconnection of dynamics, ranging from within-host to person-to-person, necessitates single-scale models delineating disease progression at the individual level and extending to interpersonal transmission.

In Chapter 1, we provided a brief introduction to sleeping sickness, encompassing transmission dynamics, available interventions, causes, and disease stages. This chapter included an exposition of the parasite's life cycle and immune system responses, referencing relevant studies as foundational components for our research. The problem statement, aims, objectives, and a list of pertinent publications were elucidated. Methodologically, definitions and various mathematical analysis concepts were expounded upon in Chapter 2, 3, and 4.

In Chapter 2, our focus was on understanding the progression of sleeping sickness within a single infected individual, incorporating the dynamics of immune response and cytokines upon parasite ingestion. We formulated, analyzed, and discussed a deterministic mathematical model using ordinary differential equations to depict sleeping sickness at the immunological scale. The model encapsulated HAT disease with immune responses, parasite stages, and cytokine dynamics, considering naive macrophages, classical macrophages, alternative activated macrophages, and cytokine dynamics. Analytical and numerical analyses were conducted, elucidating the concept of parasite switching and its impact on disease progression. The model presented three disease equilibrium points, distinguishing it from conventional analyses, which typically involve one disease-free equilibrium point and two

endemic equilibria. The results indicated that in the absence of switching, the human immune system could clear the parasite, while switching led to the emergence of new parasite types, overwhelming the body. We concluded that immune cell dynamics and cytokines should not be disregarded in mathematical models of within-host disease transmission, offering insights into how the body functions when afflicted by a parasitic disease that does not infect cells or organs. Additionally, two optimal control models for distinct therapeutic drugs were introduced, highlighting the importance of identifying disease stages for appropriate treatment selection.

After elucidating the progression of the disease within a single infected individual and emphasizing the importance of diagnosing the correct stages in Chapter 2, we applied this information in Chapter 3. The main aim of Chapter 3 was to develop a mathematical model to investigate the disease transmission of sleeping sickness across multiple hosts, incorporating disease stage-specific treatment and vector trapping. We formulated and analyzed a between-host HAT mathematical model using a set of ordinary differential equations for three different species: humans, vectors, and wild or domesticated animals. The mathematical analysis for our model was conducted both analytically and numerically. Unlike Chapter 2, our model yielded two disease equilibrium points, namely one disease-free point and one endemic point. Results suggested that certain parameters allow for forward and backward bifurcation, emphasizing the need for correct patient diagnosis and a focus on reducing the proportions of infectious vector bites to susceptible humans, thus preventing the co-existence of disease equilibrium points. Furthermore, the results highlighted the biting rate as the most sensitive parameter and emphasized the importance of increasing the vector trapping rate to reduce the disease burden. The model's results captured outputs without treatment and with intervention, displaying the optimal control profile of interventions used to minimize the sleeping sickness disease burden. Our study confirmed that effective control of HAT disease should prioritize vector trapping.

Observing the importance of analyzing both within-host dynamics in Chapter 2 and population dynamics in Chapter 3, we coupled the two models in Chapter 4. The objective was to investigate the insights gained by integrating epidemiological and immunological dynamics for sleeping sickness. We formulated and analyzed a general multiscale mathematical model using the embedded multiscale framework, incorporating the dynamics of two populations: humans and vectors, capturing the pathogen life cycle within the human host. The model explained how pathogen population dynamics at the within-host scale influence the between-host scale and vice versa. In the context of our embedded multiscale model, a key feature was the reciprocal influence of within-host parameters on between-host and between-host dynamics and vice versa. The model was analytically and numerically analyzed, capturing

the concept of super-infection at the within-host scale. The multiscale model used a system of ordinary differential equations, introducing interventions to formulate an optimal control problem exploring the effects of treatment and vector trapping. Results demonstrated the reciprocal influence of within-host parameters on between-host and between-host dynamics, as well as between-host parameters on within-host dynamics. The findings indicated that once the minimum infectious dose is consumed, infection at the within-host scale is sustained by pathogen replication, with the pathogen load increased through super-infection. Based on the comparison of multiscale results and the single scale results it is favorable to use multiscale modeling to analyse infectious diseases.

Future directions

The current study serves as a foundational framework for future research, introducing novel insights into the dynamics of sleeping sickness. Several potential avenues for further investigation that could enhance our understanding of Human African Trypanosomiasis (HAT) disease dynamics include:

- Expanding upon the current multiscale model for sleeping sickness disease dynamics, future studies could enrich the framework by incorporating additional aspects that offer a more comprehensive understanding of Human African Trypanosomiasis (HAT) disease. One key consideration is the inclusion of the pathogen load in the non-human host and vector populations. This extension would provide a more nuanced representation of the dynamics involved in the transmission cycle, offering insights into the pathogen's interactions within these crucial components of the disease ecology.

  Furthermore, an additional enhancement to the model could involve the incorporation of optimal control measures targeting both within-host and between-host dynamics. By introducing optimal control strategies, future studies could explore intervention measures that are not only effective at the individual level but also address the broader dynamics of disease transmission. This approach would align with the growing emphasis on integrated and multifaceted strategies for disease management.

- Incorporation of Temperature Dynamics: The influence of temperature on vector population dynamics is significant. Future research could extend the developed multi-scale model by incorporating the effects of climate change, providing a more nuanced understanding of the interactions between temperature variations and disease dynamics.

- Validation through Data Fitting: To assess the practical utility and accuracy of the multiscale model, it is essential to conduct empirical testing. This involves fitting real-world data to the models and assessing their ability to predict future disease outcomes, thereby enhancing the reliability and applicability of the developed framework.
- Comparison of Multiscale Models: An interesting avenue for future exploration involves a comparative analysis between nested multiscale models and embedded multiscale models. Such a comparison could offer valuable insights into the predictive capabilities and nuances of different multiscale modeling approaches in elucidating the dynamics of sleeping sickness.
- Incorporation of Cost-Effectiveness: Considering the practical constraints associated with intervention strategies, it is imperative to integrate cost-effectiveness considerations into the multiscale model. Future studies may extend the model to incorporate economic factors, focusing on specific endemic areas, to optimize resource allocation and intervention planning.
- Stochastic Model Approach: Introducing a stochastic modeling approach that incorporates randomness and variation could provide a more realistic representation of the inherent uncertainties in disease dynamics. This approach would be particularly relevant in capturing the unpredictable elements of sleeping sickness transmission.

References

[1] World Health Organization. (2013). Sustaining the drive to overcome the global impact of neglected tropical diseases: second WHO report on neglected diseases (No. WHO/HTM/NTD/2013.1). World Health Organization.

[2] World Health Organization. (2023) *Fact sheets-Trypanosomiasis, human African (sleeping sickness)*. Available from https://www.who.int/news-room/fact-sheets/detail/trypanosomiasis-human-african-(sleeping-sickness) [Accessed 13 November 2023].

[3] Steverding, D. (2008). The history of African trypanosomiasis. *Parasites & vectors*. 1(1), 1-8.

[4] Centers for Disease Control and Prevention. (2019) *Laboratory identification of parasites of public health concern*. Available from https://www.cdc.gov/dpdx/trypanosomiasisafrican/index.html [Accessed 15 November 2023].

[5] Frank, S. A. (1999). A model for the sequential dominance of antigenic variants in African trypanosome infections. *Proceedings of the Royal Society of London. Series B: Biological Sciences*. 266(1426), 1397-1401.

[6] Stijlemans, B., Guilliams, M., Raes, G., Beschin, A., Magez, S., and De Baetselier, P. (2007). African trypanosomosis: from immune escape and immunopathology to immune intervention. *Veterinary parasitology*. 148(1), 3-13.

[7] Ponte-Sucre, A. (2016). An overview of Trypanosoma brucei infections: an intense host–parasite interaction. *Frontiers in microbiology*. 7, 2126.

[8] Borst, P., and Rudenko, G. (1994). Antigenic Variation in African Trypanosomes. *Science*. 264(5167), 1872-1873.

[9] Imeri, L., and Opp, M. R. (2009). How (and why) the immune system makes us sleep. *Nature Reviews Neuroscience*. 10(3), 199-210.

[10] Baral, T. N. (2010). Immunobiology of African trypanosomes: need of alternative interventions. *BioMed Research International*. 2010.

[11] Kuriakose, S. M., Singh, R., and Uzonna, J. E. (2016). Host intracellular signaling events and pro-inflammatory cytokine production in African trypanosomiasis. *Frontiers in immunology*. 7, 181.

[12] Gjini, E., Haydon, D. T., Barry, J. D., and Cobbold, C. A. (2010). Critical interplay between parasite differentiation, host immunity, and antigenic variation in trypanosome infections. *The American Naturalist*. 176(4), 424-439.

[13] Liu, D., Albergante, L., Newman, T. J., and Horn, D. (2018). Faster growth with shorter antigens can explain a VSG hierarchy during African trypanosome infections: a feint attack by parasites. Scientific Reports, 8(1), 10922.

[14] Navarrete, D. J. (2019). PARASITES, CLOCKS, AND IMMUNITY: A Within-Host Mathematical Model of Human African Trypanosomiasis.

[15] Makhuvha, M., and Mambili-Mamboundou, H. (2023). Studying the Effect of Parasite Switching in Optimal Control Analysis of Sleeping Sickness. *Letters in Biomathematics*. 10(1), 207-233.

[16] Zhang, J. M., and An, J. (2007). Cytokines, inflammation and pain. *International anesthesiology clinics*. 45(2), 27.

[17] Gyapong, J., and Boatin, B. (Eds.). (2016). Neglected tropical diseases-sub-Saharan Africa (p. 13). Springer International Publishing.

[18] Brun, R., Blum, J., Chappuis, F., and Burri, C. (2010). Human african trypanosomiasis. *The Lancet*. 375(9709), 148-159.

[19] Aksoy, S., Buscher, P., Lehane, M., Solano, P., and Van Den Abbeele, J. (2017). Human African trypanosomiasis control: achievements and challenges. *PLoS neglected tropical diseases*. 11(4), e0005454.

[20] Tong, J., Valverde, O., Mahoudeau, C., Yun, O., and Chappuis, F. (2011). Challenges of controlling sleeping sickness in areas of violent conflict: experience in the Democratic Republic of Congo. *Conflict and health*. 5(1), 1-8.

[21] Robays, J., Bilengue, M. M. C., Stuyft, P. V. D., and Boelaert, M. (2004). The effectiveness of active population screening and treatment for sleeping sickness control in

the Democratic Republic of Congo. *Tropical Medicine & International Health*. 9(5), 542-550.

[22] Rock, K. S., Torr, S. J., Lumbala, C., and Keeling, M. J. (2017). Predicting the impact of intervention strategies for sleeping sickness in two high-endemicity health zones of the Democratic Republic of Congo. *PLoS neglected tropical diseases*. 11(1), e0005162.

[23] Castaño, M. S., Aliee, M., Mwamba Miaka, E., Keeling, M. J., Chitnis, N., and Rock, K. S. (2020). Screening strategies for a sustainable endpoint for gambiense sleeping sickness. *The Journal of Infectious Diseases*. 221(Supplement_5), S539-S545.

[24] Kumar, A., and Srivastava, P. K. (2023). Role of optimal screening and treatment on infectious diseases dynamics in presence of self-protection of susceptible. *Differential Equations and Dynamical Systems*. 31(1), 135-163.

[25] Rock, K. S., Torr, S. J., Lumbala, C., and Keeling, M. J. (2015). Quantitative evaluation of the strategy to eliminate human African trypanosomiasis in the Democratic Republic of Congo. *Parasites & vectors*. 8, 1-13.

[26] Bottieau, E., and Clerinx, J. (2019). Human African trypanosomiasis: progress and stagnation. *Infectious Disease Clinics*. 33(1), 61-77.

[27] Kroubi, M., Karembe, H., and Betbeder, D. (2011). Drug delivery systems in the treatment of African trypanosomiasis infections. *Expert Opinion on Drug Delivery*. 8(6), 735-747.

[28] Dumas, M., and Bouteille, B. (2000). Treatment of human African trypanosomiasis. *Bulletin of the World Health Organization*. 78, 1474-1474.

[29] Pohlig, G., Bernhard, S. C., Blum, J., Burri, C., Mpanya, A., Lubaki, J. P. F., ... and Olson, C. A. (2016). Efficacy and safety of pafuramidine versus pentamidine maleate for treatment of first stage sleeping sickness in a randomized, comparator-controlled, international phase 3 clinical trial. *PLoS neglected tropical diseases*. 10(2), e0004363.

[30] Doran, J. W., Thompson, R. N., Yates, C. A., and Bowness, R. (2023). Mathematical methods for scaling from within-host to population-scale in infectious disease systems. *Epidemics*. 100724.

[31] Brauer, F. (2017). Mathematical epidemiology: Past, present, and future. *Infectious Disease Modelling*. 2(2), 113-127.

[32] White, P. J., and Enright, M. C. (2010). Mathematical models in infectious disease epidemiology. *Infectious Diseases*. 70.

[33] Ferguson, N. E., Steele, L., Crawford, C. Y., Huebner, N. L., Fonseka, J. C., Bonander, J. C., and Kuehnert, M. J. (2003). Bioterrorism web site resources for infectious disease clinicians and epidemiologists. *Clinical infectious diseases*. 36(11), 1458-1473.

[34] Ferguson, N. M., Donnelly, C. A., and Anderson, R. M. (2001). Transmission intensity and impact of control policies on the foot and mouth epidemic in Great Britain. *Nature*. 413(6855), 542-548.

[35] Ferguson, N. M., Donnelly, C. A., and Anderson, R. M. (2001). The foot-and-mouth epidemic in Great Britain: pattern of spread and impact of interventions. *Science*. 292(5519), 1155-1160.

[36] Donnelly, C. A., Fisher, M. C., Fraser, C., Ghani, A. C., Riley, S., Ferguson, N. M., and Anderson, R. M. (2004). Epidemiological and genetic analysis of severe acute respiratory syndrome. The Lancet infectious diseases, 4(11), 672-683.

[37] Riley, S., Fraser, C., Donnelly, C. A., Ghani, A. C., Abu-Raddad, L. J., Hedley, A. J., and Anderson, R. M. (2003). Transmission dynamics of the etiological agent of SARS in Hong Kong: impact of public health interventions. *Science*. 300(5627), 1961-1966.

[38] Garira, W. (2017). A complete categorization of multiscale models of infectious disease systems. *Journal of biological dynamics*. 11(1), pp.378-435.

[39] Ross, R. (1911). The prevention of malaria. *John Murray*.

[40] Macdonald, G. (1957). The epidemiology and control of malaria. *The Epidemiology and Control of Malaria*.

[41] Smith, R. J. (2008). Could low-efficacy malaria vaccines increase secondary infections in endemic areas?. *Mathematical Modeling of Biological Systems*. Volume II: Epidemiology, Evolution and Ecology, Immunology, Neural Systems and the Brain, and Innovative Mathematical Methods. 3-9.

[42] Teboh-Ewungkem, M. I., Ngwa, G. A., and Ngonghala, C. N. (2013). Models and proposals for malaria: a review. *Mathematical Population Studies*. 20(2), 57-81.

[43] Rogers, D. J. (1988). A general model for the African trypanosomiases. *Parasitology*. 97(1), 193-212.

[44] Artzrouni, M., and Gouteux, J. P. (1996). A compartmental model of sleeping sickness in central Africa. Journal of Biological Systems, 4(04), 459-477.

[45] Chalvet-Monfray, K., Artzrouni, M., Gouteux, J. P., Auger, P., and Sabatier, P. (1998). A two-patch model of Gambian sleeping sickness: application to vector control strategies in a village and plantations. *Acta biotheoretica*. 46, 207-222.

[46] Welburn, S. C., Fèvre, E. M., Coleman, P. G., Odiit, M., and Maudlin, I. (2001). Sleeping sickness: a tale of two diseases. *Trends in parasitology*. 17(1), 19-24.

[47] Hargrove, J. W., Ouifki, R., Kajunguri, D., Vale, G. A., and Torr, S. J. (2012). Modeling the control of trypanosomiasis using trypanocides or insecticide-treated livestock. PLoS neglected tropical diseases, 6(5), e1615.

[48] Gjini, E., Haydon, D. T., Barry, J. D., and Cobbold, C. A. (2010). Critical interplay between parasite differentiation, host immunity, and antigenic variation in trypanosome infections. *The American Naturalist*. 176(4), 424-439.

[49] Liu, D., Albergante, L., Newman, T. J., and Horn, D. (2018). Faster growth with shorter antigens can explain a VSG hierarchy during African trypanosome infections: a feint attack by parasites. Scientific Reports, 8(1), 10922.

[50] Navarrete, D. J. (2019). PARASITES, CLOCKS, AND IMMUNITY: A Within-Host Mathematical Model of Human African Trypanosomiasis.(Doctoral dissertation)

[51] Kajunguri, D. (2013). Modelling the control of tsetse and African trypanosomiasis through application of insecticides on cattle in Southeastern Uganda (Doctoral dissertation, Stellenbosch: Stellenbosch University).

[52] Pandey, A., Atkins, K. E., Bucheton, B., Camara, M., Aksoy, S., Galvani, A. P., and Ndeffo-Mbah, M. L. (2015). Evaluating long-term effectiveness of sleeping sickness control measures in Guinea. *Parasites & vectors*. 8, 1-10.

[53] Samia, Y., Kealey, A., and Smith?, R. J. (2016). A mathematical model of a theoretical sleeping sickness vaccine. *Mathematical Population Studies*. 23(2), 95-122.

[54] Gervas, H. E., Opoku, N. K. D. O., and Ibrahim, S. (2018). Mathematical modelling of human African trypanosomiasis using control measures. *Computational and Mathematical Methods in Medicine*. 2018.

[55] Meisner, J., Barnabas, R. V., and Rabinowitz, P. M. (2019). A mathematical model for evaluating the role of trypanocide treatment of cattle in the epidemiology and control of Trypanosoma brucei rhodesiense and T. b. gambiense sleeping sickness in Uganda. *Parasite epidemiology and control*. 5, e00106.

[56] Shaier, S., and Burke, M. (2019). A Mathematical Model for the Effect of Domestic Animals on Human African Trypanosomiasis (Sleeping Sickness). The Kennesaw Journal of Undergraduate Research, 6(1), 1.

[57] Aliee, M., Keeling, M. J., and Rock, K. S. (2021). Modelling to explore the potential impact of asymptomatic human infections on transmission and dynamics of African sleeping sickness. *PLoS computational biology*. 17(9), e1009367.

[58] Dushoff, J. (1996). Incorporating immunological ideas in epidemiological models. Journal of theoretical biology, 180(3), 181-187.

[59] Vickers, D. M., and Osgood, N. D. (2007). A unified framework of immunological and epidemiological dynamics for the spread of viral infections in a simple network-based population. *Theoretical Biology and Medical Modelling*. 4(1), 1-13.

[60] Feng, Z., Velasco-Hernandez, J., Tapia-Santos, B., and Leite, M. C. A. (2012). A model for coupling within-host and between-host dynamics in an infectious disease. *Nonlinear Dynamics*, 68, 401-411.

[61] Cen, X., Feng, Z., and Zhao, Y. (2014). Emerging disease dynamics in a model coupling within-host and between-host systems. *Journal of theoretical biology*. 361, 141-151.

[62] Souza, M. O. (2014). Multiscale analysis for a vector-borne epidemic model. *Journal of mathematical biology*, 68, 1269-1293.

[63] Garira, W., Mathebula, D., and Netshikweta, R. (2014). A mathematical modelling framework for linked within-host and between-host dynamics for infections with free-living pathogens in the environment. *Mathematical biosciences*. 256, 58-78.

[64] Netshikweta, R., and Garira, W. (2017). A multiscale model for the world's first parasitic disease targeted for eradication: guinea worm disease. *Computational and Mathematical Methods in Medicine*. 2017.

[65] Wang, X., and Wang, J. (2017). Disease dynamics in a coupled cholera model linking within-host and between-host interactions. *Journal of biological dynamics*. 11(sup1), 238-262.

[66] Garira, W., and Mathebula, D. (2019). A coupled multiscale model to guide malaria control and elimination. *Journal of theoretical biology*. 475, 34-59.

[67] Garira, W., and Chirove, F. (2020). A general method for multiscale modelling of vector-borne disease systems. *Interface Focus*. 10(1), 20190047.

[68] Garira, W., and Mathebula, D. (2020). Development and application of multiscale models of acute viral infections in intervention research. *Mathematical Methods in the Applied Sciences*. 43(6), 3280-3306.

[69] Netshikweta, R. (2021). Multiscale Modelling of Environmentally Transmitted Infectious Diseases (Doctoral dissertation).

[70] Sharomi, O., and Malik, T. (2017). Optimal control in epidemiology. *Annals of Operations Research*. 251, 55-71.

[71] Lenhart, S., and Workman, J. T. (2007). Optimal control applied to biological models. CRC press.

[72] Neilan, R. M., and Lenhart, S. (2010). An Introduction to Optimal Control with an Application in Disease Modeling. *In Modeling paradigms and analysis of disease trasmission models*. 67-81.

[73] Miller Neilan, R. L., Schaefer, E., Gaff, H., Fister, K. R., and Lenhart, S. (2010). Modeling optimal intervention strategies for cholera. *Bulletin of mathematical biology*. 72, 2004-2018.

[74] Modnak, C. (2013). Optimal control modeling and simulation, with application to cholera dynamics. Old Dominion University.

[75] Adams, B. M., Banks, H. T., Davidian, M., Kwon, H. D., Tran, H. T., Wynne, S. N., and Rosenberg, E. S. (2005). HIV dynamics: modeling, data analysis, and optimal treatment protocols. *Journal of Computational and Applied Mathematics*. 184(1), 10-49.

[76] Adams, B. M., Banks, H. T., Kwon, H. D., and Tran, H. T. (2004). Dynamic multidrug therapies for HIV: Optimal and STI control approaches. North Carolina State University. *Center for Research in Scientific Computation*.

[77] Jung, E., Lenhart, S., and Feng, Z. (2002). Optimal control of treatments in a two-strain tuberculosis model. *Discrete and Continuous Dynamical Systems Series B*. 2(4), 473-482.

[78] Okosun, K. O., Ouifki, R., and Marcus, N. (2011). Optimal control analysis of a malaria disease transmission model that includes treatment and vaccination with waning immunity. *Biosystems*. 106(2-3), 136-145.

[79] Son, H. J. (2018). Analysis and Optimal control of deterministic Vector-Borne diseases model (Doctoral dissertation, Auburn University).

[80] Apollinaire, N. M., Rebecca, W. O., and Yengo Vala-ki-sisa, M. (2016). Optimal Control of a Model of Gambiense Sleeping Sickness in Humans and Cattle. *American Journal of Applied Mathematics*. 4(5), 204-216.

[81] Gervas, H. E., and HUGO, A. K. (2021). Modelling african trypanosomiasis in human with optimal control and cost-effectiveness analysis. *Journal of applied mathematics & informatics*. 39(5-6), 895-918.

[82] Liana, Y. A., Shaban, N., and Mlay, G. (2021). Modeling Optimal Control of African Trypanosomiasis Disease with Cost-Effective Strategies. *Journal of Biological Systems* 29(04), 823-848.

[83] Thieme H.R. (1948). Mathematics in population biology. *Princeton University Press*. John Wiley and sons.

[84] Morris, Q. (2010). Analysis of co-epidemic model. *SIAM Undergrad*. Res. Online, 4, pp.121-133.

[85] Van den Driessche, P. and Watmough, J. (2002). Reproduction numbers and subthreshold endemic equilibria for compartmental models of disease transmission. *Mathematical biosciences*. 180(1-2), pp.29-48.

[86] Chavez, C.C., Feng, Z. and Huang, W. (2002). *"On the computation of R0 and its role on global stability "* in *Mathematical Approaches for Emerging and Re-emerging Infection Diseases Part 1: An Introduction to models, Methods and Theory*; Blower, S., Driessche, P., and Kirschner, D. Eds., vol 125 of The IMA Volumes in Mathematics and Its Applications. Springer-Verlag, Berlin, pp.31-65.

[87] Manda, E.C., and Chirove, F. (2019). In-host mathematical models for Hepatitis B virus infection prognosis: incorporating pharmacokinetics of immune-based therapies. PhD thesis.

[88] Nagurney, A., and Zhang, D. (1996). *Stability Analysis* in: *Projected Dynamical Systems and Variational Inequalities with Applications*. International Series in Operations Research & Management Science, vol 2. Springer, Boston, MA.

[89] Stuart, A., and Humphries, A. R. (1998). *Dynamical systems and numerical analysis*, Vol. 2. Cambridge University Press.

[90] Brauer, F., Castillo-Chavez, C., and Castillo-Chavez, C. (2012).*Mathematical models in population biology and epidemiology*, Vol. 2, No. 40. New York: springer.

[91] Mahardika, R. and Sumanto, Y.D. (2019). Routh-hurwitz criterion and bifurcation method for stability analysis of tuberculosis transmission model. *Journal of Physics: Conference Series*. 1217: No. 1, p. 012056. IOP Publishing.

[92] Bejarano D.A.O., Ibargüen-Mondragón E., and Gómez-Hernández E.A. (2018). A stability test for non linear systems of ordinary differential equations based on the Gershgorin circles. *Contemporary Engineering Sciences*. 11(91): 4541-4548.

[93] Castillo-Chavez C., Blower S., Van den Driessche P., Kirschner D., and Yakubu, A.A. (2002). Mathematical approaches for emerging and reemerging infectious diseases: models, methods, and theory. *Springer Science & Business Media*. (Vol. 126)